Molecular control of dendritic cell development and function

Colleen M. Lau

Submitted in partial fulfillment of the
requirements for the degree of
Doctor of Philosophy
under the Executive Committee
of the Graduate School of Arts and Sciences

COLUMBIA UNIVERSITY

2015

ABSTRACT

Molecular control of dendritic cell development and function

Colleen M. Lau

Dendritic cells (DCs) comprise a distinct lineage of potent antigen-presenting mononuclear phagocytes that serve as both mediators of innate immune responses and key facilitators of the adaptive immune response. DCs play both immunogenic and tolerogenic roles through their dual ability to elicit pathogen-specific T cell immunity as well as induce regulatory T cell (T_{reg}) responses to promote tolerance in the steady state. The aim of the work presented here is to examine the normal regulatory mechanisms of DC development and function, starting with the dissection of mechanisms behind an aberrantly activated developmental pathway, followed by the exploration of new mechanisms governed by two candidate transcription factors. The first chapter of the thesis focuses on the growth factor receptor Flt3, an essential regulator of normal DC development in both mice and humans, and concurrently one of the most commonly mutated proteins found in acute myeloid leukemia (AML). We investigated the effect of its most common activating mutation in AML, the Flt3 internal tandem duplication (Flt3-ITD), and found that this mutation caused a significant cell-intrinsic expansion of all DC populations. This effect was associated with an expansion of T_{regs} and the ability to dampen self-reactivity, with an inability to control autoimmunity in the absence of $T_{regs.}$ Thus, we describe a potential mechanism by which leukemia can modulate T cell responses and support T_{reg} expansion indirectly through DCs, which may compromise immunosurveillance and promote leukemogenesis. The subsequent chapters explore the basic molecular mechanisms of DC development by using Flt3 expression as a guide to uncover new candidates involved in the DC transcriptional program. We show that Myc family transcription factor, Mycl1, is largely dispensable for DC development and function, contrary to recent published findings that propose a role in proliferation and T cell priming. On the other hand, we find that conditional deletion of our second candidate gene, an Ets family transcription factor, has diverse effects on DC development, monocyte homeostasis, and cytokine production. Overall, our studies highlight an unexpected molecular link between DC development and leukemogenesis, and elucidate novel mechanisms controlling DC differentiation and function.

TABLE OF CONTENTS

LIST OF TABLES AND FIGURES

CHAPTER II FIGURES

CHAPTER III FIGURES

ACKNOWLEDGEMENTS

First and foremost, I would like to thank Boris Reizis for his mentorship and constant support throughout the course of my graduate career and this thesis work. I would also like to thank Kang Liu, Ulf Klein, Michael Shen, Thomas Ludwig, and Steven Reiner for their time, patience, and guidance as committee members. I would like to acknowledge our collaborators Damian Turner from the lab of Donna Farber, Simone Nish from the lab of Steven Reiner, Brandon Hogstad and Aleksey Chudnovskiy from the lab of Miriam Merad, and Nir Yogev from the lab of Ari Waisman. I would like to thank the Integrated Program, Med into Grad Program, and Zaia Sivo for financial and administrative support, as well as personal encouragement. Finally, I am very grateful to all former and current members of the Reizis Lab for their technical help, advice, discussion, and their contributions in facilitating a pleasant work environment.

DEDICATIONS

I dedicate this work to my parents, who have always been the driving force behind my big endeavors.

GENERAL INTRODUCTION

The Immune System

The human body has developed intricate defense mechanisms that protect the organism from any pathogenic assault that it encounters. Replenishment of these immune cells relies on the hematopoietic stem cell (HSC), a pluripotent cell that has the ability to give rise to all cells within the hematopoietic system, while still maintaining its own populations through the process of self-renewal. By using a tightly orchestrated combination of intrinsic programs and environmental communication, the HSC gives rise to highly proliferative progeny committed to distinct lineages. These progenitors ultimately undergo a series of differentiation events that produces erythrocytes for oxygen transport, platelets for blood clotting, and all the leukocytes that make up the immune system. These leukocytes can broadly be categorized based on their roles within the two arms of the immune response: innate immunity and adaptive immunity.

Innate Immunity

The innate immune response is a quick, nonspecific, broad-spectrum reaction that comprises several layers of defense, the first being physical barriers (like the skin), secretion of antimicrobial molecules, and circulating plasma proteins called complement proteins that enhance microbial recognition. Hematopoietic cell types that carry out the initiating attacks include phagocytes like monocytes, macrophages and granulocytes (neutrophils, eosiniophils, and basophils), as well as lymphocytes called natural killer cells (NK cells). Innate immune cells express a number of invariant pattern recognition receptors (PRRs) that recognize general microbial components called pathogen-associated molecular patterns (PAMPS), such as liposaccharides on bacterial cell wall or double-stranded RNA from viruses[1]. Recognition by these receptors induces phagocytosis and subsequent killing (in the case of macrophages and granulocytes), or initiates cytokine signaling that facilitates recruitment of other immune cells[1]. NK cells express additional receptors that help them distinguish between healthy self and “altered” self by sensing low levels of major histocompatibility complex I (MHC I) or cellular and metabolic stress signals[2]. Activated signaling leads to local release of cytotoxic substances that penetrate cell membranes of target cells and induce apoptosis[2].

Adaptive immunity

On the other hand, the adaptive immune response incorporates more refined and precise tactics that target specific pathogens. These responses are largely mediated by T cells and B cells, which express receptors that recognize specific antigen from a given pathogen. The diversity of T cell and B cell receptors generated by random genetic recombination (known as V(D)J recombination) provides a vast repertoire of molecules that can recognize virtually any given antigen[3]. Upon antigen-receptor recognition, T cells can mature into $CD4^+$ helper T cells that secrete cytokines to help tailor and orchestrate the response, or they can mature into $CD8^+$ cytotoxic T cells that target and kill infected cells[4]. Meanwhile, B cells mature into plasma cells to generate and secrete antigen-specific antibodies that enhance pathogen recognition and targeting[4]. Recognition induces selective expansion of these antigen-specific clones and enables robust elimination of the pathogen. More importantly, after clearance, a reservoir of these antigen-specific lymphocytes remains and provides for immunological memory, a key phenomenon that allows more efficient pathogenic clearance upon re-encounter. Building up this memory is the underlying principle behind vaccine therapy[5]. But to initiate and mount these tactical responses requires prior "education" of what these pathogens are, which is a crucial task taken on by a rare population of phagocytic innate immune cells called dendritic cells.

Dendritic cells

Dendritic cells (DCs) were first described by Paul Langerhans in 1868 as novel neurons with dendritic morphology in the skin[6]. Over a century later, work by Ralph Steinman and Zanvil Cohn identified DCs from lymphoid organs as a unique cell type with long cytoplasmic projections[7] capable of potent stimulation of T cells[8]. The cascade of research that ensued solidified the central role of DCs in bridging the innate and adaptive immune responses. Ultimately, this research paved the way for Ralph Steinman to receive a Nobel Prize in Physiology or Medicine in 2011.

With their stellate morphology and long cytoplasmic processes, DCs are specialized at sensing and patrolling tissue environments for foreign intrusions. Similar to other phagocytic innate immune cells, DCs are enriched in a plethora of PRRs so that they are equipped to detect a wide variety of pathogens. These include membrane-bound PRRs like Toll-like receptors (TLRs) and C-type lectin receptors (CLRs),

as well as cytoplasmic PRRs like NOD-like receptors (NLRs)[9]. Collectively, expression of the receptors allows DCs to recognize both extracellular and intracellular components of gram-negative and -positive bacteria, viruses, fungi, and parasites. Unlike other phagocytic cells, the immediate goal of some DCs is not necessarily to take in and kill pathogens. Rather, their primary goal is to alert the adaptive arm of the immune system, by processing remnants of the pathogen and presenting this antigen to naïve T cells. For this, DCs have acquired unique features and capabilities that duly warrant their designation as professional antigen-presenting cells.

DC development

Years of DC research have established the DC lineage as a unique branch of hematopoiesis, however the exact tracing from earliest progenitor to mature DC still remains controversial. DC origins, like most hematopoietic cells, start with HSCs in the bone marrow[10]. Adoptive transfer of common myeloid progenitors (CMPs) and common lymphoid progenitors (CLPs) suggests that DCs can have either myeloid or lymphoid origin[11]. However, more recent fate-mapping studies have shown that only a minority of DCs seems to be derived from lymphoid progenitors[12], suggesting that the majority is actually of myeloid origin. In line with this, the macrophage-dendritic cell progenitor (MDP) has been proposed to be the first descendent of the CMP with the potential to give rise to DCs, as well as macrophages and monocytes[13]. However, recent clonogenic studies have questioned the DC potential of the MDP[14]. Downstream of the MDP is the common dendritic cell progenitor (CDP), the first DC-restricted progenitor capable of generating all DCs in both lymphoid and nonlymphoid tissue. At this stage, lineage bifurcation occurs to generate the two main types of DCs: conventional dendritic cells (cDCs) and plasmacytoid DCs (pDCs). cDC differentiation occurs via intermediate circulating precursor cells called pre-DCs, which seed peripheral tissues to finally differentiate into cDCs. Meanwhile, pDCs continue and complete their development in the bone marrow.

Conventional dendritic cells

The superior ability for antigen presentation by DCs is mostly attributed to cDCs. Of all murine tissue cDCs, splenic cDCs have been the most studied and well characterized. Splenic DCs can be

readily identified by high expression of β integrin CD11c and histocompatibility complex MHC class II[9]. They are broadly subcategorized into two groups: $CD11b^+$ ($CD8^-$) cDCs and $CD8^+$ ($CD11b^-$) cDCs. $CD11b^+$ cDCs are highly proficient at presenting exogenous antigen on MHC class II molecules and activating naïve $CD4^+$ T cells[15]. Within the spleen, $CD11b^+$ cDCs are mostly found in the marginal zone[15], an anatomical transit area for blood to enter the main lymphoid regions and consequently a prime location to patrol the blood for foreign antigen[16]. On the other hand, $CD8^+$ cDCs have acquired a specialized mechanism called cross-presentation that allows them to present exogenous antigen on MHC class I molecules and activate naïve $CD8^+$ T cells[17]. Within the spleen, $CD8^+$ cDCs are mainly found in the T cell zones[15]. Thus, with their broad expression of sensors, strategic placement, and their collective ability to present intracellular and extracellular antigen to any naïve T cell, cDCs are uniquely adept at mounting an adaptive immune response.

Work in recent years has revealed the significant phenotypic and functional heterogeneity that exists within these cDC subsets. $CD11b^+$ cDCs consist of two subsets that are developmentally, functionally, and phenotypically distinct. More than half of $CD11b^+$ cDCs are cDCs that rely on Notch2 receptor signaling for late development. These cDCs are required for optimal priming of $CD4^+$ helper T cells, and morphologically and genetically exhibit typical cDC qualities[18]. The remainder of $CD11b^+$ cDCs develops independently of Notch2. These cells appear more monocytic in origin, morphology and expression profile, and are more adept at cytokine secretion[18]. In parallel with $CD11b^+$ cDCs, $CD8^+$ cDCs also consist of two divergent groups. Canonical $CD8^+$ cDCs, which also express C-type lectin receptor DEC205, are dependent on transcription factor Batf3, secrete IL-12, and possess the unique cross-presenting abilities that are usually attributed to the $CD8^+$ subset[17,19]. On the other hand, a smaller but significant portion of $CD8^+$ cDCs develops independently of Batf3. The function of these non-canonical $CD8^+$ cDCs still remains elusive, as these cells lack the ability to both cross-present and secrete IL-12[20]. Conveniently, these subsets can be readily distinguished by expression of chemokine receptor CX_3CR1. Specifically, Notch2- and Batf3-dependent subsets express low/negative levels of CX_3CR1, while Notch2- and Batf3- independent subsets express high levels of CX_3CR1[18,20]. These splenic cDC populations are summarized in Table 1.

cDC subtype	Alternative names	Molecular regulation	Functional features	Cell surface markers
$CD8^+$	Canonical	Batf3-dependent	Can cross-presentation; can secrete IL-12	$DEC205^+$, $CD86^+$, CX_3CR1^-
	Non-canonical	Batf3-independent	Cannot cross-present; does not secrete IL-12; can stimulate CD4 T cells	$DEC205^-$, $CD86^-$, CX_3CR1^{hi}
$CD11b^+$	$Esam^{hi}$	Notch2-dependent	Antigen presentation to CD4 T cells	$Esam^{hi}$, CX_3CR1^{lo}
	$Esam^{lo}$	Notch2-independent	Cytokine secretion	$Esam^{lo}$, CX_3CR1^{hi}

Table 1. Summary of conventional dendritic cell subtypes within the spleen.

Analogous cDC subsets seem to exist in nonlymphoid tissues, although DC subsets in these tissues have generally been less characterized. In the intestine, skin, and lung, the functional counterparts of canonical $CD8^+$ cDCs are $CD103^+$ ($CD11b^-$) cDCs. Similar to their lymphoid-resident equivalent, $CD103^+$ cDCs are dependent on Batf3 and are capable of cross-presentation[21-24]. Conservation of the $CD11b^+$ subset remains less discernable, since these cells display more heterogeneity between tissues and are sometimes hard to separate from tissue macrophages or monocyte-derived DCs[25]. Despite this, the small intestine appears to display the most similarity to splenic $CD11b^+$ cDC subsets, as $CD11b^+$ $CD103^+$ cDCs are also Notch2-dependent and influence T cell differentiation, while $CD11b^+$ $CD103^-$ cDCs are Notch2-independent and monocyte-derived[18,26].

Plasmacytoid dendritic cells

Although derived from common origin, pDCs are morphologically and functionally distinct from their cDC siblings. Unlike the branched and dendritic shape of cDCs, pDCs exhibit a smaller, rounder, more lymphoid morphology, thus appropriating their name as “plasmacytoid” due to their resemblance to plasma cells. pDCs are developmentally dependent on transcription factor E2-2[27], and phenotypically express lower levels of CD11c and MHC class II, along with B220, mPDCA-1 (Bst2), and Siglec H[9]. While they are capable of antigen presentation in their activated state, antigen presentation does not seem to be their prime function. Instead, pDCs are known for their unrivaled ability to secrete type I interferons, primarily mediated by nucleotide sensing through TLR7/TLR9 and adaptor protein MyD88[28]. Thus, pDCs become especially critical in anti-viral responses. Secretion of interferons and other cytokines help

promote the activation of various immune cells involved in both the innate and adaptive immune responses. Therefore, along with cDCs, pDCs are also important players in bridging the innate and adaptive immune responses.

The work presented here aims to explore various aspects of dendritic cell development, function, and differentiation by studying established molecular factors and exploring new ones. Chapter 1 focuses on growth factor receptor Flt3, a key component of DC development and homeostasis. This study investigates the conditions in which Flt3 signaling is aberrantly activated and the consequences that this signaling may incur on immunity. Chapter 2 and 3 focuses more on the steady-state, exploring potentially new transcriptional regulators of DC development and function and focusing on two candidates: Mycl1 and Etv6.

CHAPTER I

THE ROLE OF ACTIVATING FLT3 MUTATIONS IN DENDRITIC CELL HOMEOSTASIS AND T CELL RESPONSES

INTRODUCTION

Flt3 signaling plays a key role throughout DC development within normal hematopoiesis. But among human malignancies, aberrant Flt3 signaling is notoriously associated with tumorigenesis. Mutations in the receptor are frequently and selectively found in acute myeloid leukemia (AML), the most common being the Flt3 internal tandem duplication (Flt3-ITD). This mutation leads to constitutive activity of the Flt3 signal cascade, promoting cell-intrinsic survival and proliferation in the early hematopoietic progenitors that actively express Flt3. Many have reported on the role of Flt3-ITD in early hematopoietic progenitors, yet no studies have explored its effect on DC development and homeostasis. In this chapter, we connect the normal role of Flt3 in DC development with its pathologic role in leukemia. Here we report that even a single allele of Flt3-ITD dramatically increased overall DC cell numbers and their progenitors in a cell-intrinsic manner. Expression of Flt3-ITD promoted a skewing towards a PD-L1 expressing DC population that lacks many hallmarks of the canonical cross-presenting DC, as well as caused a downregulation of Flt3 that reduced DC responsiveness to exogenous Flt3 ligand. Along with this, this mutation cell-extrinsically expanded the T cell population, with a bias towards more T_{regs}. We further showed that Flt3-ITD dampened the T cell expansion in the graft-versus-host response, and provided evidence that the reduced response to self-reactivity was dependent on T_{regs}. We propose that Flt3-ITD may play an early tumor-extrinsic role in leukemogenesis by altering the immunosurveillance mechanisms via dendritic cells.

BACKGROUND

Flt3 in normal hematopoiesis

Flt3 structure

Fms-like tyrosine kinase 3 (Flt3) belongs to the RTK subclass III family, all of which play important roles in cell proliferation, differentiation and survival within hematopoiesis. These other receptors include c-Kit, macrophage colony-stimulating factor receptor (M-CSFR), and platelet derived growth factor receptors (PDGFRs)[29]. Human FLT3 shows about 85% amino acid sequence homology with murine Flt3[29]. The receptor is a transmembrane protein that comprises five extracellular immunoglobulin-like domains, a transmembrane domain, an intracellular juxtamembrane domain, and two intracellular tyrosine kinase domains[30]. The juxtamembrane domain serves as an autoinhibitory mechanism, binding onto the kinase domain until key residues are phosphorylated upon activation to release its inhibition[31]. Activation occurs upon ligand binding, which causes dimerization of the normally monomeric receptors[32]. Autophosphorylation of the cytoplasmic domain follows, which provides docking sites for downstream effectors[33].

Flt3 ligand

The ligand for Flt3 was cloned shortly after the cloning of Flt3 and was appropriately named Flt3 ligand (Flt3L)[34,35]. Expression of Flt3L is widespread in both murine and human tissues. These tissues consist of hematopoietic organs like bone marrow, thymus, blood and spleen, as well as non-hematopoietic tissues like heart, gonads, lungs, kidneys, intestines, muscle, liver, and placenta[29,35,36]. Three protein isoforms have been identified in mice: the first is a transmembrane isoform with a proteolytic cleavage site that produces a soluble protein; the second is a membrane-bound isoform that lacks the proteolytic cleavage site, but is anchored to the membrane through a string of hydrophobic residues; the third isoform is a soluble protein made up mainly of the extracellular domain[37]. In humans, the transmembrane isoform is most abundant, while in mice, the membrane-bound isoform is the most common variant[37]. All isoforms, however, seem to be biologically active[37]. The important role of Flt3L in

hematopoiesis is apparent in mice that lack the gene. Specifically, severe reductions in numbers are found in myeloid and B cell progenitor populations, splenic NK cells, and dendritic cells, concomitant with an overall decrease in cellularity[38].

Flt3 signal transduction

Wild-type Flt3 mainly signals through two major pathways: the PI3K/AKT pathway and the Ras/MAPK pathway. The former is a key regulator of cell survival and metabolism, while the latter provides mitogenic signaling that promotes cell proliferation[39]. The earliest studies looking at potential downstream effectors were performed before the cloning of Flt3L, and thus required the use of chimeric receptors to artificially induce activation. Nevertheless, the work established an association with the murine Flt3 cytoplasmic domains and major players within the pathways, including PI3K itself and adaptor protein Grb2 (associated with the Ras/MAPK pathway), among others[29,40,41]. Studies conducted after the discovery of Flt3L overall agree with the involvement of these two pathways. For example, interaction studies looking at FLT3L-induced activation of human FLT3 also show binding of GRB2, as well as transient activation of MAPK[42]. In addition, FLT3L activation also induces phosphorylation of GAB proteins, which are known to interact with both GRB2 and PI3K[39,43]. It should be noted that signaling might differ between species. In particular, murine catalytic domains of Flt3 have been shown to interact directly with PI3K, while human FLT3 seems to interact indirectly with PI3K through a complex of proteins[40,41,44]. Furthermore, different cell types may employ these signaling pathways for specific functions. For example, within the DC lineage, mTOR of the PI3K pathway has been shown to be an important signaling molecule downstream of Flt3L-induced DC development[45].

Activation of the JAK/STAT pathway has also been proposed to occur downstream of endogenous Flt3 signaling independently of Jak kinases and Src family kinases[46]. Specifically, Flt3L-induced signaling results in phosphorylation of Stat5a in a murine cell line stably transfected with wild-type human FLT3[47]. Furthermore, murine myeloid progenitors deficient in Stat5a show defects in proliferation when cultured in a mix of growth factors that include Flt3L, but show minimal changes without Flt3L[47]. Another group has reported similar induction in the human AML cell line THP-1, which expressed wild-type FLT3, although no data was shown[48]. However, the role of Stat5 signaling on ligand-

induced FLT3 signaling remains controversial, as several groups using similar and different cell lines have shown that Stat5/STAT5 phosphorylation is unique to mutated forms of FLT3 that lead to constitutive activation[49-54].

Flt3 expression in the hematopoietic system

While Flt3L is expressed in an array of hematopoietic and non-hematopoietic cells, Flt3 expression is more restricted and therefore becomes the limiting factor for signaling. The receptor is mainly restricted to the hematopoietic system in both mice and human, though RNA has also been detected in placenta, gonads, and neural tissue in mice[55-57]. While Flt3 was originally identified in a compartment enriched in HSCs, murine Flt3 expression within the hematopoietic system seems to correlate more with the loss of self-renewal[58]. Accordingly, Flt3 receptor is highly expressed in a number of early hematopoietic progenitors and does not seem to be expressed on HSCs, although more recent findings suggest that it may be expressed intracellularly in HSCs[59]. This is in contrast to humans, where surface FLT3 is expressed in both early progenitors and the $CD34^+$ HSC compartment, and expression of the receptor correlates with multi-lineage engraftment in xenograft models[60,61]. Flt3 is mainly expressed on the surface of progenitors that are not fated to the megakaryocyte-erythroid lineage, which includes lymphoid-primed multipotent progenitors, common lymphoid progenitors (CLPs), proB cells, early thymic T cell progenitors, common myeloid progenitors, and a small subset of early granulocyte-monocyte progenitors (pre-GMPs)[62-64]. In line with this, mice deficient in Flt3L show reductions in CLPs, B cell precursors, NK cells, slight reductions in bulk myeloid progenitors, and reductions in pre-GMPs/GMPs[38,64,65], while mice deficient in Flt3 show reductions in the pro-B cell compartment[66].

Upon entry into circulation from the bone marrow, almost all hematopoietic cells lose the expression of Flt3[67]. The main exceptions are DCs and their precursors pre-DCs, making DCs the only mature hematopoietic cell to actively express the receptor[62]. More importantly, signaling through Flt3 plays a functional and significant role all throughout DC development and DC homeostasis[67]. Mice deficient in Flt3 show impairment in DC development, although those lacking Flt3L show more pronounced deficiencies[38,68]. Accordingly, *in vivo* administration of Flt3L increases DC numbers in both

mice and human, while *in vitro*, it is sufficient to drive DC development from whole bone marrow cultures[69,70].

Tolerogenic role of Flt3 signaling

Given the pivotal role of DCs in generating T cell responses, many researchers have used Flt3L as an adjuvant to increase DC production thereby improving protective T cell responses. This has been effective in overcoming models of peripheral tolerance, mounting tumor immunity, and protection against pathogens[71-73]. In this context, Flt3 signaling can be considered highly immunogenic, and is usually associated with DCs that have been activated and matured. However, in the steady state, DCs remain in a relatively immature state but still present self-antigen to induce tolerance by way of T cell deletion, T cell anergy, or regulatory T cells (T_{regs}). These T_{regs} are T cells that suppress the effector activity of conventional $CD4^+$ and $CD8^+$ T cells[74-78]. In fact, Flt3 signaling increases the levels of T_{regs} in the periphery and overall can generate a tolerogenic environment in different non-steady state conditions, including chronic ileitis, T cell mediated colitis, atherosclerosis, autoimmune diabetes, and graft-versus-host disease[79-83]. In this context, Flt3 signaling can be considered tolerogenic.

The simultaneous increase in both DCs and T_{regs} upon Flt3L administration suggests that there is regulatory link between the two populations mediated by Flt3 signaling. Indeed, Flt3L administration leads to increased numbers of both DCs and T_{regs}, while Flt3L deficiency leads to decreased numbers of both[80]. The increase in T_{regs} has mainly been attributed to the simple increase in DC numbers, but Flt3L-induced DC expansion activates specific signaling pathways and skews DC subsets, which may also affect T_{reg} regulation[45]. Conversely, depletion of T_{regs} leads to an expansion of DCs, revealing a feedback control mechanism by T_{regs} to control DC numbers[84]. This DC expansion is dependent on Flt3, which further supports the crucial role of Flt3 in the DC-T_{reg} feedback loop.

Flt3 in acute myeloid leukemia

Soon after mouse models showed the *in vivo* role of Flt3 in hematopoiesis, mutations within *FLT3* were identified in patients with acute myeloid leukemia (AML), a disease that results from aberrant clonal expansion of immature white blood cells that fills the bone marrow and ultimately leads to hematopoietic

failure[85]. Discovery of these mutations in the context of human disease solidified the important role of Flt3 signaling in hematopoiesis. Since then, it has been reported that approximately 30% of all AML patients harbor some form of *FLT3* mutation, making it one of the most common genetic lesions encountered in AML[86]. Unfortunately, the clinical significance of these mutations is unfavorable for the patient. In addition to typically presenting with a large disease burden, the prognosis for patients harboring the mutation is mostly adverse[86]. While exact results vary between study groups, patients harboring FLT3 mutations generally show lower remission rates, increased relapse rates, and decreased overall survival compared to those that do not harbor the mutations[87-89].

Most patients succumb to the disease because there are very limited treatments available for AML. The current standard care of combination chemotherapy (cytarabine and anthracycline) was developed nearly 40 years ago and stem cell transplant, with all of its risks, is the only curable option[90]. Therefore, the field is in dire need of new forms of treatment. Given the prominence of FLT3 mutations, FLT3 seems like a prime candidate for molecular targeting. Unfortunately, early FLT3 tyrosine kinase inhibitors (TKIs) such as lestaurtinib and midostaurin, while promising in pre-clinical testing, failed to provide substantial and sustained responses in early clinical trials[91]. Consequently, this led many to question whether or not FLT3 mutations were simply passenger mutations. However, new and more-specific FLT3 TKIs like quizartinib have shown good promise in early clinical trials, and there is now evidence that the leukemia confers a selective pressure to maintain FLT3 mutations in relapsed AML[91,92]. Together, these results affirm that FLT3 mutations are indeed driver mutations and that FLT3 TKIs may be promising treatments for AML.

The most prevalent mutation among *FLT3* AML mutations is the FLT3 internal tandem duplication (FLT3-ITD). The mutation is always found in-frame and can range from 3 to 400 base pairs long[93]. A majority of the FLT3-ITD mutations occur in the juxtamembrane domain, while about 30% of the mutations occur in the tyrosine kinase domain[94]. Point mutations that lead to single amino acid changes within the activation loop of the tyrosine kinase domain also occur, but these are less common[86]. Nonetheless, activating FLT3 mutations lead to ligand-independent dimerization, autophosphorylation of the cytoplasmic domain, and subsequent activation of the pathway. It is believed that the elongation of the juxtamembrane domain found in FLT3-ITD mutations results in conformational changes that

aberrantly release inhibition of the kinase domain, as well as promotes dimerization[31,51]. These conformational changes have also been proposed to expose key residues in the juxtamembrane domain that serve as aberrant docking sites for STAT5[53]. Mice that harbor the mutation acquire a monocytic myeloproliferative neoplasm which may be fatal, depending on mouse model, but rarely develop AML without cooperating mutations[95-99].

Cancer immunosurveillance and the role of DCs in the tumor microenvironment

The concept of cancer immunosurveillance, a process in which the immune system can detect and eliminate transformed cells before malignancy, was originally proposed 50-100 years ago[100]. Despite this, only recently has the immune system been appreciated as a significant contributor to cancer development in not only preventing tumorigenesis but also sculpting it in a way that inadvertently enhances tumor growth, also known as cancer immunoediting[101,102]. Several cell types and mechanisms from both the innate and adaptive immune systems have been proposed to contribute. From the innate immune system, $CD8^+$ cDCs have been shown to contribute to the rejection of immunogenic sarcomas through their secretion of type I interferon[103], and depletion of NK cells by antibody treatment has been shown to enhance tumor susceptibility to carcinogen-induced tumors[104]. From the adaptive immune system, Rag1- or Rag2-deficient mice, which lack T cells, B cells and natural killer T cells, also have enhanced susceptibility to carcinogen-induced tumors[105]. Rag2-deficient mice that additionally lack lymphocytes of the innate immune system show even higher tumor incidence[106]. Furthermore, the importance of the cytotoxic molecule perforin, which is expressed by cytotoxic lymphocytes like T cells and NK cells, has been demonstrated, as perforin-deficient mice display increased incidence of spontaneous lymphomas[107].

Several mechanisms involving DCs specifically have been proposed in solid tumors that ultimately promote an immunosuppressive environment. Many tumors subvert immunosurveillance by impairing the activity of immunogenic antigen-presenting DCs. For example, production of VEGF by a number of human cell lines has been shown to inhibit DC maturation from human HSCs, while other tumors have been shown to secrete factors that limit their migration to lymphoid organs[108,109]. In other cases, DCs have been shown to have an active role in generating an immunosuppressive environment.

In ovarian cancer, for instance, cDCs that express inhibitory receptor PD-1 and its ligand PD-L1 accumulate in the tumor model and is associated with suppression of T cell activity, and pDCs have been proposed to promote immunosuppression by the recruitment of T_{regs} in human samples[110,111].

Impairment of immunosurveillance mechanisms involving DCs has also been proposed in AML[112]. AML-derived DCs have been shown to be present in abnormal quantities and show functional impairment in their allostimulation of $CD4^+$ T cells and cytokine secretion[113]. In addition, these DCs have also been proposed to induce T cell anergy *in vitro*[114]. Similar to solid tumors, AML-derived DCs have been shown to upregulate PD-L1 compared to healthy donors[115]. However, the general mechanisms of immune evasion in AML is relatively understudied compared to the many reports on solid tumors like melanoma[116]. Thus, our understanding of how DCs specifically contribute to the failure of immunosurveillance during AML is severely lacking.

Given the unfavorable prognosis of FLT3-ITD^+ AML patients compared to FLT3-ITD^- AML patients, we considered additional leukemogenic mechanisms that may confer an advantage over other non-FLT3-mutated leukemias beyond cell-intrinsic transformation. Since Flt3 plays a key role in the immune system, especially during DC development, we hypothesized that constitutively active Flt3 signaling may affect immunosurveillance mechanisms in a way that is conducive for leukemic survival. To this end, we explored the effect of the Flt3-ITD mutation in DCs and T cells and have unveiled early alterations in homeostasis and response mechanisms that may promote leukemogenesis.

RESULTS

Flt3-ITD expands fully differentiated DCs and early DC progenitors

To analyze the role of Flt3-ITD in the DC compartment, we utilized a mouse model in which a human internal tandem duplication sequence was knocked into the endogenous *Flt3* murine locus[95]. Flow cytometric analysis of the DC compartment in multiple lymphoid organs in young adult mice showed significant expansion of both cDCs and pDCs (Figure 1.1) in heterozygous *Flt3*$^{ITD/+}$ tissues, in both primary and peripheral lymphoid tissues, except in the thymus. This is in stark contrast to other hematopoietic lineages where more subtle changes occurred in the periphery. In particular, the only significant change seen in the periphery was a slight reduction in mature B cells (Figure 1.2B). In the bone marrow, these changes were more apparent in both the B cell compartment and monocyte compartment, which showed an increase in numbers (Figure 1.2A). Despite this, the DC compartment collectively was noticeably more affected than other mature hematopoietic lineages, as DCs showed the greatest fold change in frequencies in both bone marrow (BM) and spleen (Figure 1.3). cDCs showed up to a 4-fold increase compared to wild-type (WT), whereas monocytes at most showed a little less than a 2-fold increase. Analysis of nonlymphoid tissues such as the small intestine showed a similarly robust expansion of cDC populations (Figure 1.4).

When we analyzed the DC compartment in homozygous *Flt3*$^{ITD/ITD}$ mice, all tissues showed an even greater increase in these DC populations (Figure 1.1). However, unlike heterozygous *Flt3*$^{ITD/+}$ mice, other hematopoietic lineages were severely affected. Specifically, mice showed a dramatic increase in the monocyte compartment and compromised B cell production in the BM and the periphery (Figure 1.2), which is in agreement with what has been described previously[95].

Cx3cr1^{GFP} reporter mice have been useful tools to detect early DC progenitors, as MDPs, CDPs, and pre-DCs all express CX_3CR1[13,117]. To look at DC progenitors more precisely, we generated *Cx3cr1*$^{GFP/+}$ *Flt3*$^{ITD/+}$ and analyzed BM and spleen by flow cytometry using the gating strategy shown in Figure 1.5A-B. While MDPs did not show a significant increase, both CDPs and pre-DCs in the BM and spleen showed an expansion in absolute numbers (Figure 1.5C). Other lineage negative progenitors, including c-Kit^{hi} Flt3^{-} (P1) and c-Kit$^{hi/lo}$ Flt3^{+} CX_3CR1^{+} CD115^{-} (P2) were unaffected (Figure 1.5D).

Progenitors that were c-Kit$^{hi/lo}$ Flt3^{+} CX_3CR1^{-} CD115^{-} (P3) showed a decrease in numbers, which most likely consist of common lymphoid progenitors (Figure 1.5D).

Together, these data show that Flt3-ITD preferentially expands both mature and early DC populations, while having more moderate effects on other mature hematopoietic cells.

Expansion of DC populations is cell-intrinsic

To test whether this DC expansion was cell-intrinsic, we generated competitive bone marrow chimeras and tracked donor contribution with the CD45 congenic marker, which marks all leukocytes. WT competitive (CD45.1^{+}) and either *Flt3*$^{+/+}$, *Flt3*$^{ITD/+}$, or *Flt3*$^{ITD/ITD}$ donor (CD45.2^{+}) bone marrow were injected into lethally irradiated F_1 B6x129 recipients (CD45.1^{+}/CD45.2^{+}) at a 1:1 ratio. 14 weeks post transfer, BM, spleen, skin-draining lymph nodes, and thymi were analyzed (Figure 1.6, data not shown). Data were analyzed by quantifying cell type contribution out of respective total donor population within each tissue, as represented in Figure 1.6A. In all tissues, expansion of cDCs occurred only in donor *Flt3*$^{ITD/+}$ and *Flt3*$^{ITD/ITD}$ CD45.2^{+} cells (Figure 1.6A-B). pDCs showed a similar expansion in heterozygous donor *Flt3*$^{ITD/+}$ cells, but this expansion was not consistent among tissues in chimeras harboring *Flt3*$^{ITD/ITD}$ cells (Figure 1.6C), likely due to the proportional expansion of other lineages. Analysis of early DC progenitors in the bone marrow also exhibited expanded populations only in *Flt3*$^{ITD/+}$ expressing bone marrow (Figure 1.7A). As DC progenitors are identified by their expression of Flt3, DC progenitors in homozygotes were difficult to identify due to downregulation of the surface Flt3 receptor (Figure 1.7B; 1.8C-D). However, alternative gating without the use of Flt3 suggests that CDPs are expanded in a cell-extrinsic manner as well (Figure 1.7B-C). These data indicate that the expansion of DC populations by *Flt3*$^{ITD/+}$ mutation is cell-intrinsic.

Flt3-ITD causes downregulation of surface Flt3 receptor on DCs and abrogates exogenous Flt3 signaling

Downregulation of the Flt3 receptor in *Flt3*^{ITD} BM have been described before[118,119], however Flt3 expression specifically on DCs has not been explored. Therefore we analyzed Flt3 cell surface expression by flow cytometry in peripheral DCs and CDPs in the BM. Analysis of surface Flt3 expression in competitive chimeras (described above) showed that Flt3 expression is significantly downregulated in *Flt3*$^{ITD/ITD}$-expressing cDCs, pDCs, and CDPs, but not in the WT competitor (Figure 1.8). Moderate cell-

extrinsic downregulation of Flt3 in WT CDPs was also seen (Figure 1.8D). Interestingly, heterozygous *Flt3*$^{ITD/+}$ cells showed differential Flt3 downregulation among DC populations. Specifically, no downregulation was seen in heterozygous cDCs, while partial downregulation was seen in heterozygous pDCs and CDPs (Figure 1.8B,D).

In order to test how this downregulation of Flt3 expression affects Flt3L-induced DC development, we cultured whole bone marrow cells from *Flt3*$^{+/+}$, *Flt3*$^{ITD/+}$ and *Flt3*$^{ITD/ITD}$ mice with murine Flt3L in variable concentrations and measured DC output. Without exogenous Flt3L, neither *Flt3*$^{ITD/+}$ nor *Flt3*$^{ITD/ITD}$ was sufficient to drive DC development *in vitro* (Figure 1.9A). In the presence of Flt3L, only *Flt3*$^{+/+}$ and *Flt3*$^{ITD/+}$, but not *Flt3*$^{ITD/ITD}$, generated robust populations of both cDCs and pDCs. Notably, *Flt3*$^{ITD/+}$ cultures generated pDCs in a dose dependent manner. These data suggest that Flt3-ITD downregulates Flt3 surface expression on DCs and renders them insensitive to exogenous Flt3L signaling.

Flt3-ITD skews cDC subsets

In vitro Flt3L cultures of *Flt3*$^{ITD/+}$ indicated that there was developmental bias towards generating more CD8$^+$-like cDCs (Figure 1.9B-C). While this bias was not apparent *in vivo,* we decided to perform whole genome expression analysis on *ex vivo* splenic *Flt3*$^{ITD/+}$ CD8$^+$ cDCs to investigate whether or not *Flt3*$^{ITD/+}$ affected the genetic repertoire of the DCs. Consistent with what was seen *in vitro*, whole genome analysis indicated that CD8$^+$ cDCs were most affected by the ITD mutation, as more genes showed differential expression compared to those found in CD11b$^+$ cDCs or pDCs (Figure 1.10). Interestingly, *Flt3*$^{ITD/+}$ CD8$^+$ cDCs showed a genetic signature that was very similar to that of non-canonical CD8$^+$ cDCs, as many of the genes upregulated in non-canonical CD8$^+$ cDCs were upregulated in *Flt3*$^{ITD/+}$ CD8$^+$ cDCs[20] (data not shown). To this end, we analyzed the effect of Flt3-ITD on specific subgroups using the *Cx3cr1*$^{GFP/+}$ reporter mice, which readily distinguishes CD11b$^+$ and CD8$^+$ cDC subsets by GFP expression as shown in Figure 1.11A. While all subgroups were increased in *Flt3*$^{ITD/+}$ spleens (Figure 1.11B), there was a greater representation of CX_3CR1^+ subgroups within both CD8$^+$ and CD11b$^+$ cDCs, especially within the CD8$^+$ cDC compartment (Figure 1.11A,C). In contrast, Flt3L administration to *Cx3cr1*$^{GFP/GFP}$ mice showed a significant bias towards GFP$^-$ canonical CD8$^+$ cDCs (Figure 1.11D,E), suggesting that the

population of cDCs generated by constitutive Flt3 signaling from *Flt3*$^{ITD/+}$ expression was not the same as those yielded by Flt3L-induced signaling.

Microarray analysis also indicated that inhibitory ligand PD-L1 was one of several cell-surface markers that was upregulated in *Flt3*$^{ITD/+}$ CD8^{+} cDCs (data not shown). Consequently, we analyzed the cell surface expression of PD-L1 on our *Flt3*$^{ITD/+}$ mice and noticed that there was a greater proportion of PD-L1^{+} CD86^{-} CD8^{+} cDCs (Figure 1.12A). Analysis of these same sub-populations in *Cx3cr1*^{GFP} reporter mice showed that these PD-L1^{+} CD8^{+} cDCs uniformly expressed GFP (Figure 1.12B), indicating that our PD-L1^{+} CD8^{+} cDC subset represented these non-canonical CD8^{+} cDCs.

Non-canonical CD8^{+} cDC have been reported to be developmentally independent of transcription Batf3[20]. Consistent with this, *Batf3*$^{-/-}$ mice show a specific depletion of canonical CD86^{+} PD-L1^{-} CD8^{+} cDC, leaving only residual non-canonical PD-L1^{+} CD8^{+} cDCs behind (Figure 1.13A). Furthermore, *Batf3*$^{-/-}$ *Flt3*$^{ITD/+}$ mice show a selective expansion of the non-canonical PD-L1^{+} CD8^{+} cDCs (Figure 1.13A), which were also negative for DEC205 (Figure 1.13B). Of note, in older mice we see a variable accumulation of CD86^{+} PD-L1^{+} population in *Batf3*$^{-/-}$ *Flt3*$^{ITD/+}$ mice (data not shown). Further characterization of this population is still under investigation.

To test the functional consequence of this CD8^{+} subset expansion, we infected mice with *Listeria monocytogenes*, which has been shown to use canonical CD8^{+} cDCs as an entry-point for bacterial spreading[120]. *Flt3*$^{ITD/+}$ mice showed increased bacterial load, as expected given the expansion of canonical CD8^{+} cDCs (Figure 1.14). Meanwhile, *Batf3*$^{-/-}$ *Flt3*$^{ITD/+}$ mice were resistant to *Listeria* infection, similar to *Batf3*$^{-/-}$ *Flt3*$^{+/+}$ mice, despite the increase in absolute cell numbers in CD8^{+} cDCs, suggesting that non-canonical CD8^{+} cDCs cannot compensate for the canonical CD8^{+} cDC capabilities. This data provides a functional correlate for the specific pattern of DC subset expansion by Flt3-ITD.

Flt3-ITD expands T cells in a cell-extrinsic manner

Flow cytometric analysis of T cell numbers in the steady state of naïve mice showed virtually no change in conventional T cell (T_{conv}) numbers (Figure 1.15A) but showed a dose-dependent expansion of regulatory T cells (T_{regs}) in BM (Figure 1.15B). Analysis of T cell populations in mixed chimeras showed an expansion of both T_{conv} cells and T_{regs} strictly in the WT competitor and host T cells, but not in the

Flt3^{ITD}-expressing T cells (Figure 1.16A,B; data not shown). Interestingly, this cell-extrinsic expansion was mainly found in chimeras reconstituted with heterozygous *Flt3*$^{ITD/+}$ cells, and was most affected within the chimeric bone marrow.

To test how *Flt3*$^{ITD/+}$ DCs affect antigenic stimulation of T cells, we set up allogeneic mixed leukocyte reactions by incubating various doses of CD11c^{+} enriched splenocytes with magnetically sorted bulk T cells from *FoxP3*$^{GFP/+}$ reporter mice, which allowed us to identify T_{regs} using GFP expression. At all doses, *Flt3*$^{ITD/+}$ DCs induced a greater number of CD4^{+} T_{conv} cells, CD8^{+} T_{conv} cells, and T_{regs} (Figure 1.17A). In addition, all T cell populations showed a greater proportion of proliferated cells, as measured by Cell Trace Violet dye (Figure 1.17C). These results suggest that expression of Flt3-ITD on DCs generally enhances antigen-driven T cell proliferation.

We also tested the effect of Flt3-ITD on lymphopenia-induced proliferation of T cells by adoptive transfer of bulk T cells into *Rag1*-deficient mice, which lack B or T cells. Presence of the Flt3-ITD resulted in higher numbers of both T_{conv} cells and T_{regs} (Figure 1.18A) that had either remained or undergone homeostatic proliferation as measured by Cell Trace Violet dye (T cells that had completely diluted out the dye and therefore represent microbiota-induced spontaneous proliferation were excluded). Interestingly, there was no significant difference in the proportion of proliferative T_{conv} cells (Figure 1.18B) despite the increased number of cells. Additionally, no significant difference was seen in cells that underwent spontaneous proliferation (data not shown). These data suggest that Flt3-ITD also enhances the survival of T cells reconstituted in a lymphopenic environment.

Flt3-ITD increases T_{reg} proportions in the T cell compartment and dampens aGVHD response

Closer analysis of competitive chimeras showed that while all T_{conv} cells and T_{regs} increased in a cell-extrinsic manner, these populations did not increase equally. Specifically, mice harboring *Flt3*$^{ITD/+}$ bone marrow led to an increased percentage of WT T_{regs} out of total WT competitor T cells (Figure 1.16C). Similarly, the mixed leukocyte reactions incubated with the *Flt3*$^{ITD/+}$ CD11c-enriched population resulted in a greater proportion of T_{regs} out of total responder T cells (Figure 1.17B). To analyze how *Flt3*$^{ITD/+}$ affects T_{reg} homeostasis specifically, we crossed *Flt3*$^{ITD/+}$ mice with *FoxP3*$^{DTR\text{-}GFP}$, which allows both detection as well as specific depletion of T_{regs} by administration of diptheria toxin (DT)[84]. Before

depletion, we did see a greater proportion of T_{regs} in spleen and peripheral blood in the steady state in these reporter mice (Figure 1.19A,C), likely due to the more sensitive readout by GFP. After DT administration, *Flt3*$^{ITD/+}$ facilitated a more robust reconstitution of peripheral blood T_{regs} than in *Flt3*$^{+/+}$ at all time points tested (Figure 1.19A), and maintained a greater proportion of T_{regs} in the spleen and thymus even after T_{reg} depletion (Figure 1.19B). Thus, *Flt3*$^{ITD/+}$ facilitates the presence of more T_{regs} in the periphery.

Flt3L treatment has been shown to ameliorate the acute graft-versus-host (aGVH) response in mice[83]. Therefore, we tested whether Flt3-ITD may have similar tolerogenic effects by setting up a parent to-F_1 transplant as a model for aGVH-mediated self-reactivity. Cells from spleen and lymph nodes of WT B6 (CD45.2$^+$) were injected into non-irradiated B6xFVB F_1 hosts (CD45.1$^+$/CD45.2$^+$) that were *Flt3*$^{+/+}$ or *Flt3*$^{ITD/+}$, and graft response was measured by expansion of graft T cells (CD45.1$^-$) one week after transplant. Hosts harboring the Flt3-ITD allele displayed a reduced frequency and number of graft T cells compared to the control (Figure 1.20A,B), indicating that Flt3-ITD hosts were able to reduce the burden of self-reactive T cells *in vivo.* Meanwhile, host T cells exhibited an increased proportion of host T_{regs} (Figure 1.20C). Given the expansion of PD-L1 expressing cDCs (Figure 1.12A), we tested whether this dampening of aGVH response was dependent on PD-L1 or the PD-1 pathway by treating recipients with α-PD-L1 and α-PD-1 blocking antibodies. As seen in Figure 1.21, while the blockage of PD-1 enhanced the aGVHD response (1.21B), the dampening effect of *Flt3*$^{ITD/+}$ on graft T cell expansion still remained (1.21A,B), indicating that this tolerogenic effect is not dependent on the PD-L1/PD-1 pathway.

Finally, to test whether this dampening effect of self-reactive T cells was dependent on T_{regs}, we crossed *Flt3*$^{ITD/+}$ mice with *FoxP3*^{sf} (scurfy) mice that lack functional T_{regs} and develop lethal T cell-mediated autoimmunity. If Flt3-ITD directly impaired self-reactive effector T cell responses, one would expect that the autoimmunity in *Flt3*$^{ITD/+}$ *FoxP3*^{sf} mice would be ameliorated. Contrary to this notion, we found that these mice succumbed to the disease significantly sooner than *Flt3*$^{+/+}$ *FoxP3*^{sf} littermates (Figure 1.22). Collectively, these results suggest that Flt3-ITD mutation causes a preferential expansion of T_{reg} cells, which is accompanied by dampened T cell responses against self-antigens.

DISCUSSION

Connecting the roles of Flt3 signaling in leukemogenesis and the immune system

Activating FLT3 mutations are one of the most common genetic lesions found in AML and is highly associated with poor prognoses. Hence, much attention has been focused on studying the role of Flt3 within the context of leukemogenesis. Given its prominent expression of Flt3 in undifferentiated early progenitors and its role in cell survival and proliferation, most of the leukemia-promoting characteristics have been attributed to aberrant activation and function within these early progenitors. However, the DC lineage is the only portion of normal hematopoiesis that expresses the Flt3 receptor and utilizes its signaling continuously throughout maturation, unlike most other lineages that lose expression upon differentiation. Moreover, Flt3L signaling has profound tolerogenic consequences mediated through the activity of T_{regs}. Thus, Flt3 also has a prominent role within the immune system as a crucial regulator of DC development and T_{reg} homeostasis. To this end, we explored the role of Flt3-ITD within the immune system, specifically on DC development and the effect on T cell responses. Here we provide evidence of the immunological consequences of activated Flt3-ITD signaling beyond the more established cell-intrinsic mechanisms of leukemic transformation within the early progenitor compartment.

Flt3-ITD preferentially expands DCs

Consistent with the effects of Flt3L signaling, the most striking phenotype that we observed was in DCs. One allele of Flt3-ITD was sufficient to drive DC development and promote expansion of all DC cell types even at the progenitor level, while having very moderate effects on other fully mature hematopoietic cells. This was unlikely due to increased Flt3L in the serum, as earlier reports have shown that Flt3L levels do not change significantly in *Flt3*$^{ITD/+}$ mice[96,121]. In agreement with this, we showed through competitive chimeras that this expansion was strictly cell-intrinsic and was even more pronounced in the homozygote. This is in contrast to what has been described by another group, in which heterozygote *Flt3*$^{ITD/+}$ mice exhibit severe alterations in other myeloid populations and progenitors, and the mice succumb to a fatal myeloproliferative disease[96]. Of note, this group utilizes a different mouse strain from the one used in this study. Additionally, previous data corroborates with our data, in that

hematopoiesis is largely normal in the heterozygote *Flt3*$^{ITD/+}$ mouse strain that we use[95,121]. Overall, similarly to normal Flt3L signaling, Flt3-ITD heavily promotes dendritic cell development.

Flt3-ITD downregulates the surface receptor and impairs Flt3L-induced signaling

As seen in myeloid progenitors[121], Flt3-ITD also caused the downregulation of Flt3 receptor expression and desensitized DCs to exogenous Flt3L signaling, suggesting that Flt3-ITD activity acts independently of exogenous Flt3L. As seen in our *in vitro* cultures, Flt3-ITD signaling does not entirely recapitulate Flt3L signaling, as Flt3-ITD signaling alone was not sufficient to drive DC development, but is more than proficient at driving it *in vivo*. This may reflect the difference in signaling between the two, in which Flt3-ITD lacks some of the signaling components required to drive development *in vitro*. *In vivo*, other cytokine signaling may be present to support or synergize with Flt3-ITD-mediated DC expansion, while *in vitro* no such support exists. Furthermore, this downregulation of surface Flt3 receptor certainly may have implications on immunotherapy. For example, antibody-mediated anti-Flt3 therapies for AML may be less effective, as cell surface availability would very much limit binding to the receptor.

Flt3-ITD preferentially expands a non-canonical cDC subset

Inconsistent with the effects of Flt3L signaling, Flt3-ITD preferentially expanded the non-canonical subset of CD8$^+$ cDCs. In our hands (Figure 1.11E) as well as in the hands of others[20], Flt3L treatment has been shown to significantly promote the expansion of canonical CD8$^+$ cDCs. Surprisingly, this was not the case for Flt3-ITD-expanded cDCs, as there was a greater representation of the non-canonical subtype. These cells appear CD8$^+$-like and genetically pDC-like, but lack the many functional hallmarks that are unique to these cell types, like IL-12 production, cross-presentation, and interferon production[20]. Since non-canonical CD8$^+$ cDCs do not significantly respond to Flt3L, it is possible that Flt3-ITD may aberrantly activate proliferative pathways within these cells that are normally not activated with Flt3L signaling specifically. Stat5, for example, has been shown to be aberrantly activated in cell lines expressing Flt3-ITD, and may play a role in promoting the expansion of this normally minor cDC subset. More importantly, we have shown by *Listeria* infection that these non-canonical CD8$^+$ cDCs cannot substitute for their canonical counterparts, even when increased in cell numbers. This subset skewing may have important

implications on tumor immunity, as canonical cross-presenting $CD8^+$ cDCs have been critical in T cell-mediated cytotoxicity of tumor cells[17]. The increasing proportion of a non-cross-presenting $CD8^+$ cDC may influence the ability for the immune system to reject the leukemia. Interestingly, recent studies have described a cDC/pDC "precursor" cell that expressed both cDC and pDC human markers and is found in low numbers in healthy patient samples[122]. This study demonstrated that there was a higher accumulation of these mixed-lineage cells in FLT3-ITD^+ patient samples than in FLT3-ITD^- AML samples. While these cells are reminiscent of the cDC/pDC-like attributes of murine non-canonical $CD8^+$ cDCs, further investigation is required to see if human counterparts exist, especially in AML patients.

Flt3-ITD promotes T_{reg} homeostasis and can attenuate self-reactivity

While we have shown the Flt3-ITD cell-extrinsically expands both conventional T cells and T_{regs}, the relative proportions of T_{reg} to T_{conv} cells may ultimately matter. We have shown that Flt3-ITD does indeed favor the expansion of T_{regs} and their overall proportion among the T cell compartment in the steady state, antigen-induced T cell proliferation, and within the host compartment in aGVH response. This increased proportion was associated with an attenuated aGVH response, thus recapitulating the tolerogenic responses seen with Flt3L[83]. We provide further support that the attenuation of self-reactivity is dependent on T_{regs}, as Flt3-ITD was unable to ameliorate the fatal autoimmunity exhibited in T_{reg}-deficient scurfy mice.

Flt3-ITD - an immunomodulating mutation that promotes leukemogenesis

Together, these results cultivate the notion that Flt3-ITD may establish a tolerogenic environment through DC expansion and subsequent expansion of T_{regs}, and that this may play a role in disabling immunosurveillance mechanisms in leukemogenesis. The expansion of DCs coinciding with the expansion of T_{regs} is reminiscent of normal Flt3L signaling which has been associated with many tolerogenic conditions. The additional effects on the immune system may therefore explain the prevalence of FLT3-ITD^+ AML and its association with a higher incidence of relapse. Flt3-ITD has already been shown to have effects on normal hematopoiesis that would enhance its ability to promote leukemogenesis at the cell-intrinsic progenitor level. These include the impairment of HSC quiescence

and promotion of a myeloid-based transcriptional program at the expense of lymphopoiesis[59,119]. In this study, we propose another component downstream of the leukemic stem cell clone that is unique to Flt3-ITD – the induction of tolerance mediated by DCs and T_{regs} (Figure 1.23). For this to occur, HSCs harboring the FLT3-ITD mutation would give rise to FLT3-ITD DCs early in leukemogenesis, before the clinical manifestations of AML, as only one hit of ITD is required to affect the immune system in our murine model. DCs would likely acquire the mutation quickly, since DCs have a short half-life and are frequently replenished by progenitors[10,123]. The expansion of DCs conferred by the FLT3-ITD mutation would then lead to a favored expansion of T_{regs} that would establish an immunosuppressive environment that is permissive for leukemic growth. In agreement, the FLT3-ITD mutation has been identified in pre-leukemic and leukemic HSCs[124,125], and found in DCs harvested from FLT3-ITD$^+$ AML patients, which interestingly also show impaired cytokine secretion and an accumulation[122,126]. Furthermore, increased T_{reg} frequencies have been reported in AML patients[127]. Moreover, the tolerogenic effect of FLT3-ITD on the immune system would not only promote *de novo* AML, but may also promote the failure of graft-versus-leukemia response from allogeneic transplant, thus providing an explanation for the increased risk of relapse. Accordingly, it has been demonstrated that AML patients that harbor the FLT3-ITD mutation have higher incidence of relapse than FLT3-ITD-negative patients after receiving allogeneic transplant[128].

Overall, our studies reveal a novel immunological effect of Flt3-ITD during normal hematopoiesis that results in the expansion of DCs and the subsequent alteration of T cell homeostasis and function. This previously unappreciated feature would prompt investigations on immunosurveillance in AML development and potential complementary immunotherapy strategies to fight the disease.

MATERIALS AND METHODS

Animals

All mice were on C57BL/6 background, unless otherwise indicated. *Flt3*$^{ITD/+}$ mice[95], *Cx3cr1*$^{GFP/GFP}$ mice[117], *Batf3*$^{-/-}$ mice[17], *Rag1*$^{-/-}$ mice[129], *FoxP3*$^{DTR-GFP}$ mice[84], and *FoxP3*^{Sf} mice were purchased from Jackson Laboratories, while WT FVB/N mice were purchased from Taconic. *FoxP3*^{GFP} mice[130] were a kind gift from Dr. Kang Liu. Recipients for competitive chimeras were F_1 progeny of 129SvEv (Taconic) and B6.SJL (Taconic). For T_{reg} depletion model, homozygous *FoxP3*$^{DTR-GFP/DTR-GFP}$ females were crossed to heterozygous *Flt3*$^{ITD/+}$ males, and only male progeny were used for the study. For aGVH model, FVB/N females were crossed to *Flt3*$^{ITD/+}$ males to generate F_1 recipients. For T cell-mediated autoimmunity model, heterozygous *FoxP3*$^{sf/+}$ females were bred to heterozygous *Flt3*$^{ITD/+}$ males, and only male progeny that exhibited disease phenotypes (runting, scaly skin on ears and tails, and hunched posture) were included in the study. All animal studies were performed according to the investigator's protocol approved by the Institutional Animal Care and Use Committee of Columbia University.

Cell preparations

Spleen, thymus, and lymph nodes (inguinal, axillary, brachial, and cervical) were minced and pressed through a nylon cell strainer to yield single cell suspensions and then subjected to red blood cell (RBC) lysis before being filtered. Bone marrow was prepared by flushing femurs and tibias with phosphate buffer saline (PBS) using a 27-gauge needle before RBC lysis. For dendritic cell (DC) analysis, lymphoid organs were digested with collagenase D (1 mg/mL) and DNaseI (20μg/mL) in DMEM/10% FCS for 30-60 min at 37°C prior to generating cell suspensions and RBC lysis. Small intestine lamina propria lymphocytes were prepared as described before[131].

Flow cytometry

Cells were stained with the following fluorochrome- or biotin-conjugated antibodies from eBioscience or as indicated: anti-CD11c (N418), MHC II (M5/114.15.2), CD11b (M1/70), CD8α (53-6.7), Gr-1 (RB6-8C5), TCRβ (H57-597), CD3 (17A2), B220 (RA3-6B2), NK1.1 (PK136), Ter119 (TER-119), CD49b (DX5), CD4

(RM4-5 and GK1.5), FoxP3 (FJK-16s), CD24 (M1/69), Flt3 (A2F10), c-Kit (2B8), Sca-1 (D7), CD115 (AFS98), IL7-Rα (A7R34), CD45.1 (A20), CD45.2 (104), PD-L1 (MIH5), CD86 (GL1), DEC205 (NLDC-145; BioLegend), mPDCA-1/Bst2 (Miltenyi Biotec), Sirpα (P84, BD Biosciences). Intracellular staining of FoxP3 was performed per manufacturer's instructions (eBioscience). Cell acquisition was done on LSR II (BD Biosciences) using FACSDiva (BD Biosciences) and analysis was done on FlowJo (Tree Star).

Competitive chimeras

Bone marrow from B6-SJL (CD45.1$^+$) and *Flt3*$^{+/+}$, *Flt3*$^{ITD/+}$, *and Flt3*$^{ITD/ITD}$ (CD45.2$^+$) were prepared as described above. 129-B6.SJL F_1 recipients (CD45.1$^+$/CD45.2$^+$) were lethally irradiated with two doses of 600 cGy prior to receiving a mix of 1 x 10^6 B6.SJL bone marrow and 1 x 10^6 *Flt3*$^{+/+}$, *Flt3*$^{ITD/+}$, or *Flt3*$^{ITD/ITD}$ bone marrow cells intravenously in PBS/1% FCS. Peripheral blood was checked 4 weeks after transplant to confirm engraftment. Bone marrow, spleens, lymph nodes, and thymi were harvested and prepped for DC analysis as described above.

***In vitro* BM-derived DC cultures**

Bone marrow cells were harvested as described above. RBC-lysed cells were plated in triplicates in a 24-well plate at 2 x 10^6 per well in DMEM/10% FCS and various concentrations of recombinant murine Flt3 ligand (PeproTech) as indicated. Suspension and adherent cells were harvested after 7 days and triplicates were pooled for counting and flow cytometric analysis.

Flt3L administration

Cx3cr1$^{GFP/GFP}$ mice were injected intraperitoneally with PBS or 5 µg recombinant Flt3L-Fc (LakePharma) every 3 days (d0, d3, d6) and analyzed on day 9 after initial treatment. Spleens were harvested for flow cytometry and prepared as described above for DC analysis.

***Listeria monocytogenes* infection**

Mice were infected with 5 x 10^3 CFU of *Listeria monocytogenes* expressing OVA in PBS and injected intravenously. For bacterial titration, spleens were weighed and then pressed into nylon strainers to make

single cell suspensions in sterile PBS. Cells were lysed with equal volume of sterile water with 0.1% Triton X-100, and plated on brain heart infusion agar plates (Difco, BD Biosciences) for overnight incubation at 37°C. Colonies were counted the next day.

Lymphopenia-induced homeostatic proliferation

Spleen and lymph nodes were isolated from *FoxP3*^{GFP} reporter mice and prepared as described above. T cells were negatively selected by MACS columns per manufacturer's instructions (Miltenyi Biotec) using streptavidin microbeads and the following biotinylated antibodies: anti-CD11b, CD11c, B220, Gr-1, CD49b, and Ter119. T cells were stained with 5 μM Cell Trace Violet (Life Technologies) in PBS for 20 minutes at 37°C and washed with RPMI/10% FCS. 2 x 10^6 bulk T cells resuspended in PBS/1% FCS were injected intravenously into *Rag1*$^{-/-}$ *Flt3*$^{+/+}$ or *Rag1*$^{-/-}$ *Flt3*$^{ITD/+}$ recipients. Spleens were harvested and analyzed 5 days after transfer by flow cytometry.

Allogeneic mixed leukocyte reaction

For stimulator isolation: Splenic DCs were prepared from C57BL/6-FVB/N F_1 progeny by positive selection using biotinylated anti-CD11c, streptavidin microbeads, and MACS columns, per manufacturer's instructions (Miltenyi Biotec). For responder T cell isolation: T cells from *FoxP3*$^{GFP/GFP}$ (C57BL/6) spleen and lymph nodes were negatively selected by MACS columns per manufacturer's instructions (Miltenyi Biotec) using streptavidin microbeads and the following biotinylated antibodies: anti-CD11b, CD11c, B220, Gr-1, CD49b, and Ter119. T cells were stained with 5 μM Cell Trace Violet (Life Technologies) in PBS for 20 minutes at 37°C and washed with RPMI/10% FCS. 5 x 10^4 bulk T cells were plated on a 96-well plate in RPMI/10% FCS with various amounts of CD11c-enriched stimulator cells, as indicated, and incubated for 4 days at 37°C and 5% CO_2.

T_{reg} depletion

FoxP3$^{DTR-GFP/y}$ *Flt3*$^{+/+}$ and *FoxP3*$^{DTR-GFP/y}$ *Flt3*$^{ITD/+}$ mice were injected intraperitoneally with diptheria toxin (Sigma) resuspended in PBS at 50 μg/kg each day for 2 days. Blood was retrieved and analyzed for

presence of GFP^+ T_{regs} on day 0 (initial treatment), 2, 10, 14, 21, and 28, and mice that showed no depletion were excluded from analysis. End-point analysis of spleen and thymus occurred on day 28.

Acute graft-versus-host model

Spleen and lymph nodes were isolated from WT C57BL/6 ($H\text{-}2^b$; CD45.2) mice and single cell suspensions were subject to red blood cell lysis and filtered. 30×10^6 cells of pooled cells were injected intravenously into nonirradiated C57BL/6-FVB/N F_1 recipients ($H\text{-}2^b/H\text{-}2^q$; CD45.2/CD45.1). Spleens were harvested and analyzed 1 week later. For antibody blockade studies, 200 μg of control IgG, anti-mPD-L1 (10F.9G2) or anti-mPD-1 (RMP1-14) were intraperitoneally injected same day prior to graft transfer on day 0, 2 and 5, and finally analyzed on day 7 or 8. Antibodies were a kind gift from Nir Yogev and Ari Waisman.

Statistical analysis

Statistical significance was estimated with unpaired, two-tailed Student's T test. For survival curves, statistical significance was measured with log-rank (Mantel-Cox) test.

CHAPTER I FIGURES

Figure 1.1. Expansion of mature DC populations in *Flt3*^{ITD} mice.

(A) Representative staining prolifes for cDCs (left) and pDCs (right) in bone marrow (BM), spleen (SPL), lymph nodes (LN), and thymus (THY) of naïve *Flt3*$^{+/+}$, *Flt3*$^{ITD/+}$, or *Flt3*$^{ITD/ITD}$ mice. Numbers indicate frequency of DCs within the gated population. In LN, CD11c^{hi} MHCII^{+} cDCs represent resident cDCs, while CD11c^{lo} MHCII^{hi} represent migratory cDCs.

(B) Frequencies (top row) and absolute cell numbers (bottom row) of cDCs (mean ± SD, n = 5; 9.5-12.5 wks old)

(C) Frequencies (top row) and absolute cell numbers (bottom row) of pDCs (mean ± SD, n = 5; 9.5-12.5 wks old)

Statistically significant differences are indicated as: * $p < 0.05$; ** $p < 0.01$; *** $p < 0.001$

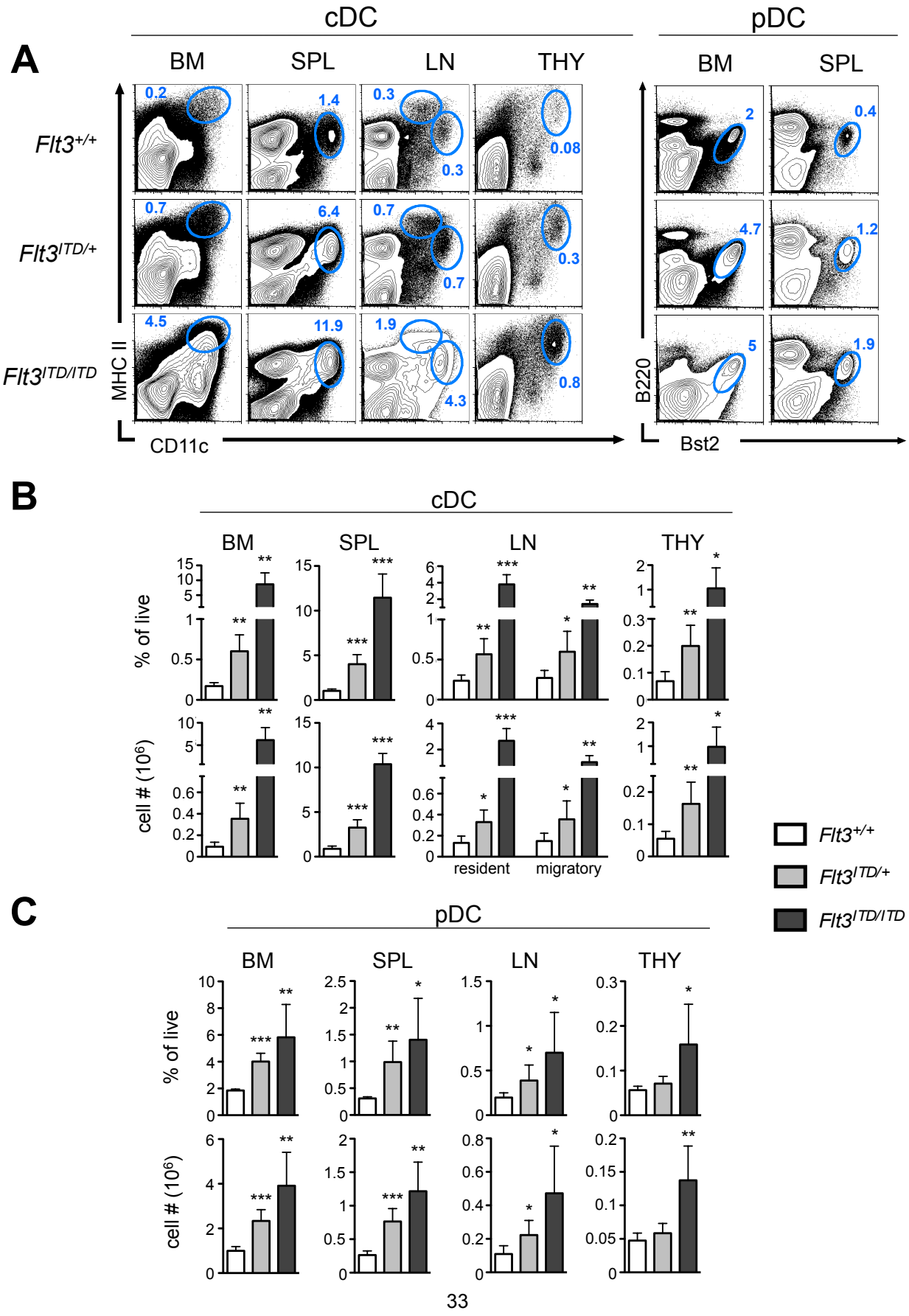
A
cDC
pDC
BM
SPL
LN
THY
BM
SPL
Flt3+/+
Flt3ITD/+
Flt3ITD/ITD
0.2
1.4
0.3
0.3
0.08
0.7
6.4
0.7
0.7
0.3
4.5
11.9
1.9
4.3
0.8
2
0.4
4.7
1.2
5
1.9
MHC II
CD11c
B220
Bst2
B
cDC
BM
SPL
LN
THY
% of live
cell # (10^6)
resident
migratory
C
pDC
BM
SPL
LN
THY
% of live
cell # (10^6)
Flt3+/+
Flt3ITD/+
Flt3ITD/ITD

Figure 1.2. Flt3$^{ITD/+}$ shows minimal effect on other mature myeloid populations, while Flt3$^{ITD/ITD}$ reveals myeloid skewing.

(A-B) Frequencies (top row) and absolute numbers (bottom row) of myeloid cells and B-cells in bone marrow (A) and spleen (B) of naïve *Flt3*$^{+/+}$, *Flt3*$^{ITD/+}$, or *Flt3*$^{ITD/ITD}$ mice. (mean ± SD, n = 5; 9.5-12.5 wks old)

Lineages were defined as follows: granulocytes (Gr-1^{hi} CD11b^{+} SSC^{hi} FSC^{hi}), monocytes (Gr-1$^{int/-}$ CD11b^{+} MHCII^{-} FSC^{lo} SSC^{lo}), macrophages (Gr-1$^{int/-}$ CD11b^{+} MHCII^{-} SSC^{hi} FSC^{int}), immature B-cells (B220^{lo} MHCII^{lo} Bst2^{-}), mature B cells (B220^{hi} MHCII^{hi} Bst2^{-}).

Statistically significant differences are indicated as: * $p < 0.05$; ** $p < 0.01$; *** $p < 0.001$

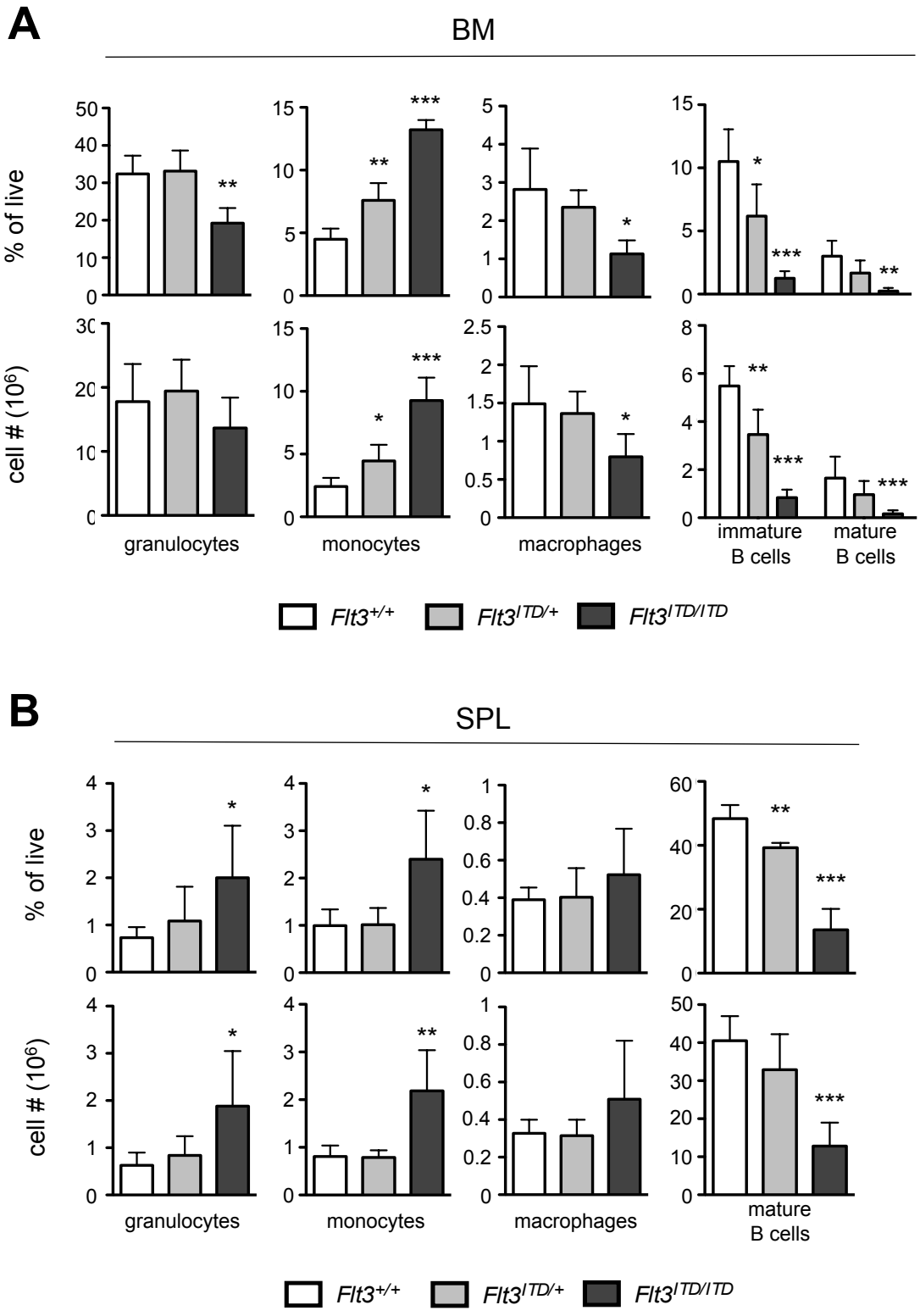
A
BM
% of live
cell # (10^6)
granulocytes
monocytes
macrophages
immature B cells
mature B cells
Flt3+/+
Flt3ITD/+
Flt3ITD/ITD
B
SPL
% of live
cell # (10^6)
granulocytes
monocytes
macrophages
mature B cells
Flt3+/+
Flt3ITD/+
Flt3ITD/ITD

Figure 1.3. Flt3-ITD shows a selective expansion in DC populations.

Fold change between *Flt3*$^{+/+}$ and *Flt3*$^{ITD/+}$ cell types in BM and SPL of naïve mice. To calculate fold change, individual *Flt3*$^{ITD/+}$ cell frequencies were normalized to the *Flt3*$^{+/+}$ mean frequency for each tissue cell type. Dotted line delineates fold change of 1. (mean ± SD, n = 5; 9.5-12.5 wks old). Lineages were defined as follows: granulocytes (Gr-1^{hi} CD11b^{+} SSC^{hi} FSC^{hi}), monocytes (Gr-1$^{int/-}$ CD11b^{+} MHCII^{-} FSC^{lo} SSC^{lo}), macrophages (Gr-1$^{int/-}$ CD11b^{+} MHCII^{-} SSC^{hi} FSC^{int}), immature B-cells (B220^{lo} MHCII^{lo} Bst2^{-}), mature B-cells (B220^{hi} MHCII^{hi} Bst2^{-}).

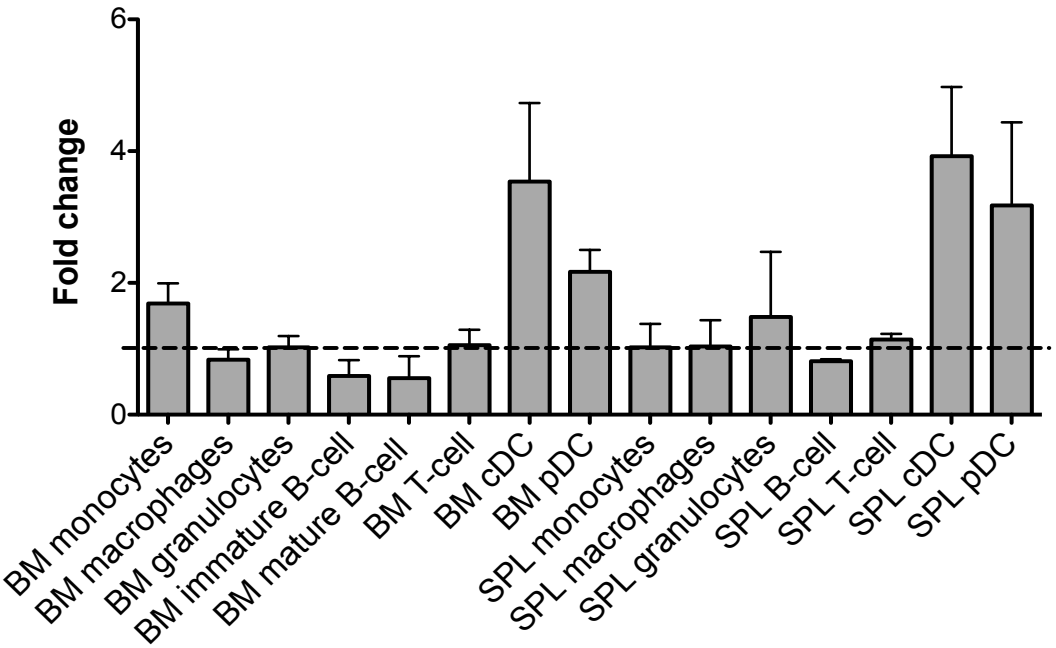
Fold change
6
4
2
0
BM monocytes
BM macrophages
BM granulocytes
BM immature B-cell
BM mature B-cell
BM T-cell
BM cDC
BM pDC
SPL monocytes
SPL macrophages
SPL granulocytes
SPL B-cell
SPL T-cell
SPL cDC
SPL pDC

Figure 1.4. Flt3-ITD expands DCs in non-lymphoid tissues.

Flow cytometric analysis of lamina propria lymphocytes isolated from naïve *Flt3*$^{+/+}$ or *Flt3*$^{ITD/+}$ small intestine. Numbers indicate percent of cells within gated population. Representative of two independent experiments. (7 wks old)

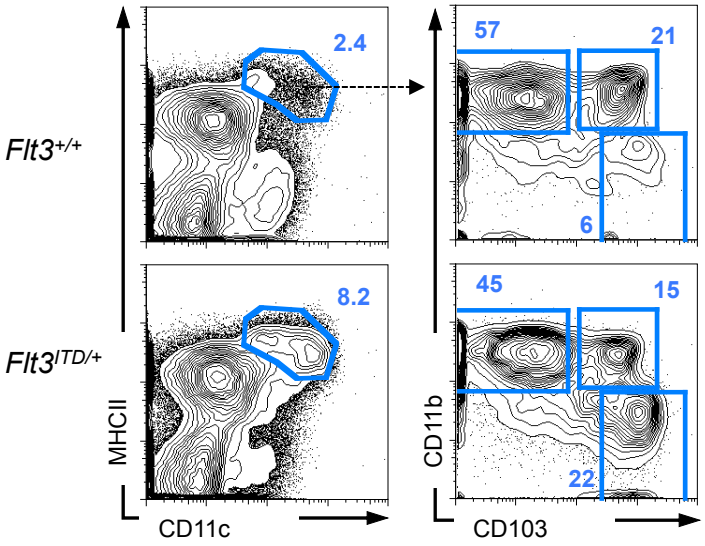
Flt3+/+
Flt3ITD/+
2.4
8.2
57
21
6
45
15
22
MHCII
CD11c
CD11b
CD103

Figure 1.5. Flt3-ITD expands DC progenitors.

(A) Representative gating strategy for macrophage/DC progenitor (MDP), common DC progenitor (CDP), and non-DC progenitor populations in *Cx3cr1*$^{GFP/+}$ bone marrow.

(B) Representative gating strategy for pre-DCs in *Cx3cr1*$^{GFP/+}$ bone marrow. Similar gating strategy was used for spleen.

(C) Absolute numbers of MDPs, CDPs, and pre-DCs, as defined in (A) and (B) in bone marrow (BM) and spleen (SPL) (mean ± SD, n = 5; 6-9 wks old).

(D) Absolute numbers of non-DC progenitors as defined in (A) in bone marrow (mean ± SD, n = 5; 6-9 wks old).

Statistically significant differences are indicated as: * $p < 0.05$; ** $p < 0.01$; *** $p < 0.001$

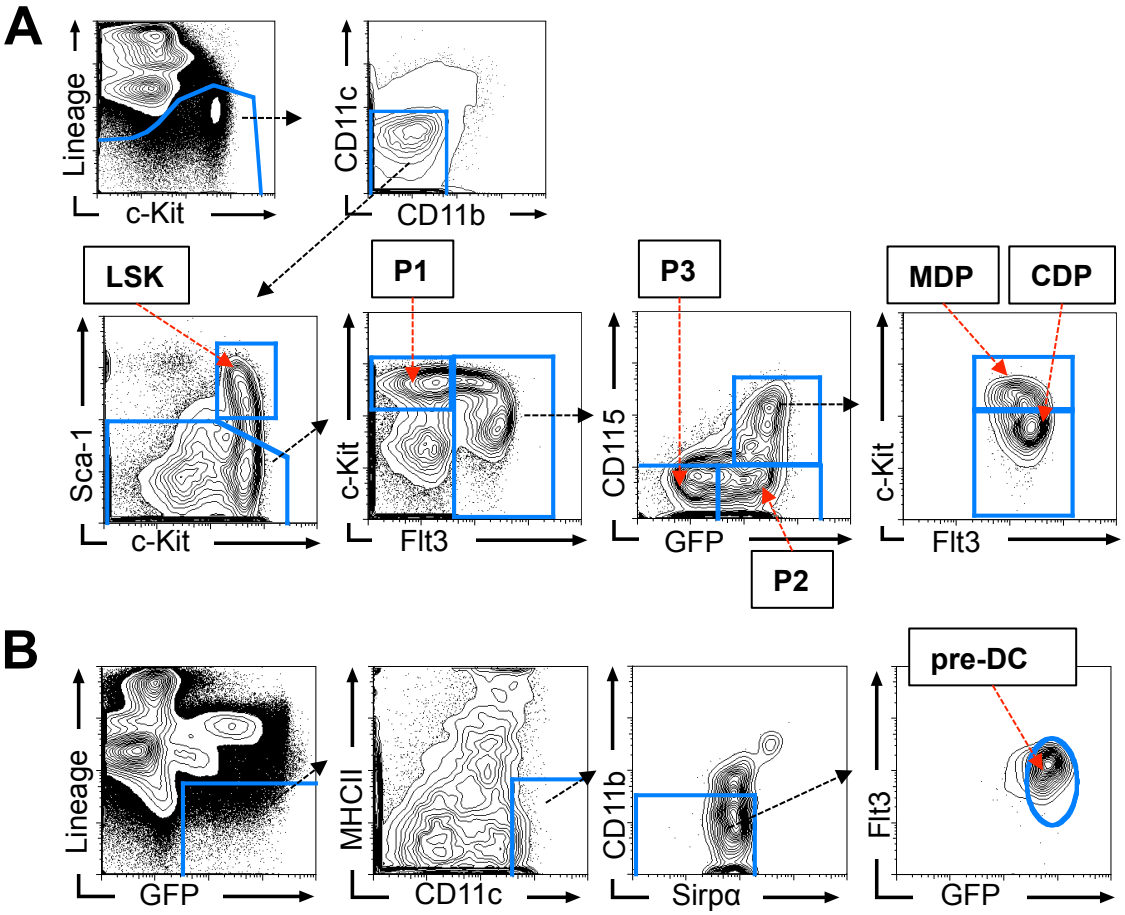
A
Lineage
c-Kit
CD11c
CD11b
LSK
P1
P3
MDP
CDP
Sca-1
c-Kit
c-Kit
Flt3
CD115
GFP
P2
c-Kit
Flt3
B
Lineage
GFP
MHCII
CD11c
CD11b
Sirpα
pre-DC
Flt3
GFP

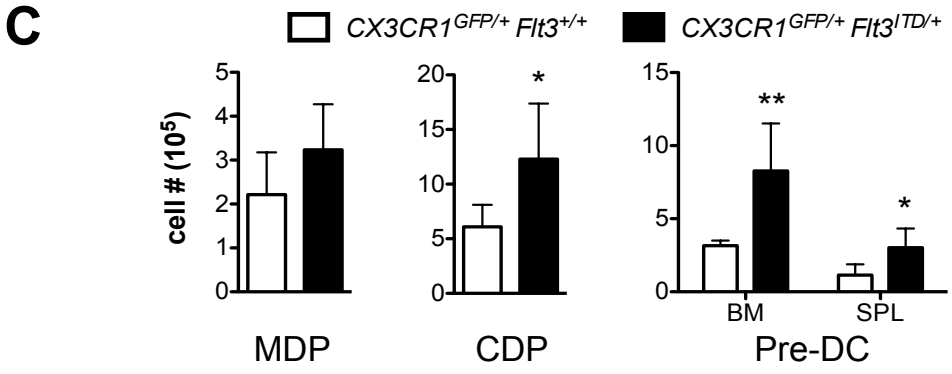
C
CX3CR1GFP/+ Flt3+/+
CX3CR1GFP/+ Flt3ITD/+
cell # (10^5)
MDP
CDP
BM
SPL
Pre-DC

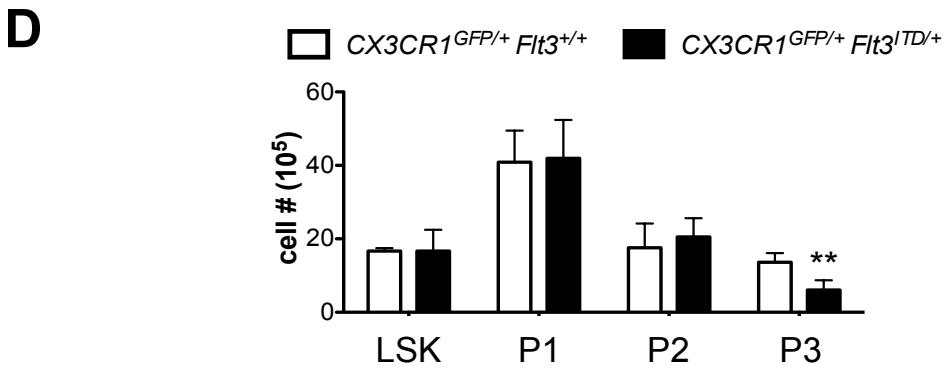
D
CX3CR1GFP/+ Flt3+/+
CX3CR1GFP/+ Flt3ITD/+
cell # (10^5)
LSK
P1
P2
P3

Figure 1.6. Flt3-ITD expands DCs in a cell-intrinsic manner.

Lethally irradiated recipients ($CD45.1^+/CD45.2^+$) were reconstituted with a 1:1 ratio of $CD45.1^+$ WT competitor and $CD45.2^+$ *Flt3*$^{+/+}$, *Flt3*$^{ITD/+}$, or *Flt3*$^{ITD/ITD}$ donor bone marrow. Bone marrow (BM), spleen (SPL), and lymph nodes (LN) were analyzed 14 weeks after transfer by flow cytometry.

(A) Representative staining profiles of cDC contribution from total $CD45.1^+$ WT competitor and $CD45.2^+$ donor cells within SPL. Numbers on the plots show percent of cells within the gated population.

(B) Percent of cDCs out of total WT competitor $CD45.1^+$ cells (white bars) or donor $CD45.2^+$ cells (blue bars) as defined in (A) (mean ± SD, n = 4-5).

(C) Percent of pDCs out of total WT competitor $CD45.1^+$ cells or donor $CD45.2^+$ cells. pDCs were defined as $B220^+$ $CD11c^{lo}$ $MHCII^{lo/-}$ $CD11b^-$ (mean ± SD, n = 4-5).

Statistically significant differences are indicated as: * $p < 0.05$; ** $p < 0.01$; *** $p < 0.001$

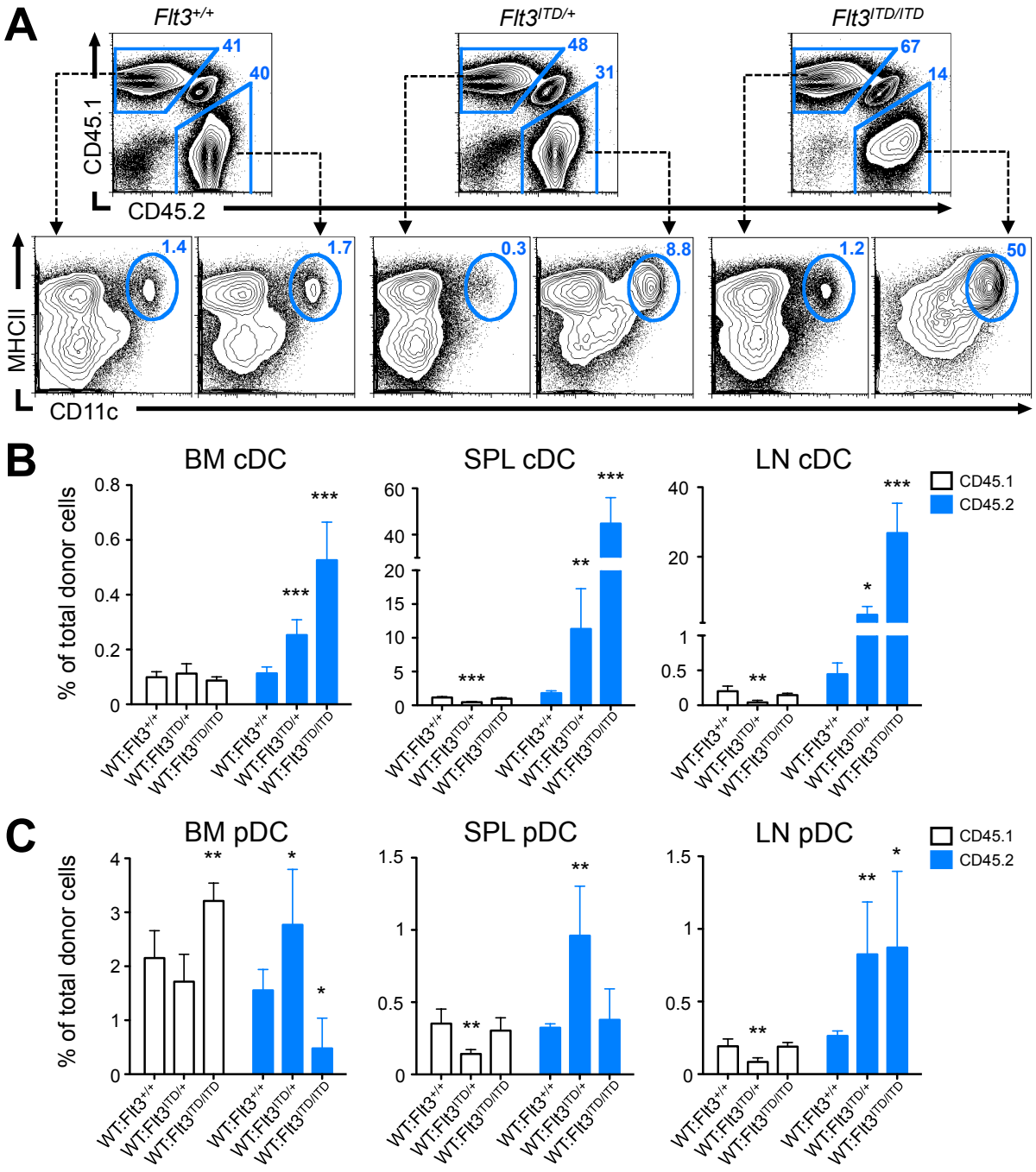
A
Flt3+/+
Flt3ITD/+
Flt3ITD/ITD
41
40
48
31
67
14
CD45.1
CD45.2
1.4
1.7
0.3
8.8
1.2
50
MHCII
CD11c
B
BM cDC
SPL cDC
LN cDC
% of total donor cells
CD45.1
CD45.2
WT:Flt3+/+
WT:Flt3ITD/+
WT:Flt3ITD/ITD
C
BM pDC
SPL pDC
LN pDC

Figure 1.7. Flt3-ITD expands DC progenitors in a cell-intrinsic manner.

Lethally irradiated recipients (CD45.1$^+$/CD45.2$^+$) were reconstituted with a 1:1 ratio of CD45.1$^+$ WT competitor and CD45.2$^+$ *Flt3*$^{+/+}$, *Flt3*$^{ITD/+}$, or *Flt3*$^{ITD/ITD}$ donor bone marrow. Bone marrow (BM) and spleen (SPL) were analyzed 14 weeks after transfer by flow cytometry.

(A) Percent of CDPs and pre-DCs out of total WT competitor CD45.1$^+$ cells (white bars) or donor CD45.2$^+$ cells (blue bars)(mean ± SD, n = 4-5). CDPs were defined as as Lin$^-$ (B220, CD3, NK1.1, CD11b, Gr-1, Ter119, CD11c) Sca-1$^-$ c-Kit^{lo} Flt3$^+$ CD115$^+$; and pre-DCs as Lin$^-$ (B220, CD3, NK1.1, CD11b, Gr-1, Ter119) CD11c$^+$ MHCII$^-$ Flt3$^+$ Sirpα$^-$.

(B) Representative staining profiles of the alternative gating for CDP. Left column of plots are pre-gated on Lin$^-$ (B220, CD3, NK1.1, CD11b, Gr-1, Ter119, CD11c) Sca-1$^-$ IL7R$^-$. Wild-type competitor cells were defined as CD45.1$^+$, while CD45.2$^+$ donor *Flt3*$^{+/+}$, *Flt3*$^{ITD/+}$, or *Flt3*$^{ITD/ITD}$ cells were defined as CD45.1$^-$.

(C) Percent of alternatively-defined CDPs out of total WT competitor CD45.1$^+$ cells or donor CD45.2$^+$ (CD45.1$^-$) cells as shown in (B)(mean ± SD, n = 4-5).

Statistically significant differences are indicated as: * $p < 0.05$; ** $p < 0.01$; *** $p < 0.001$

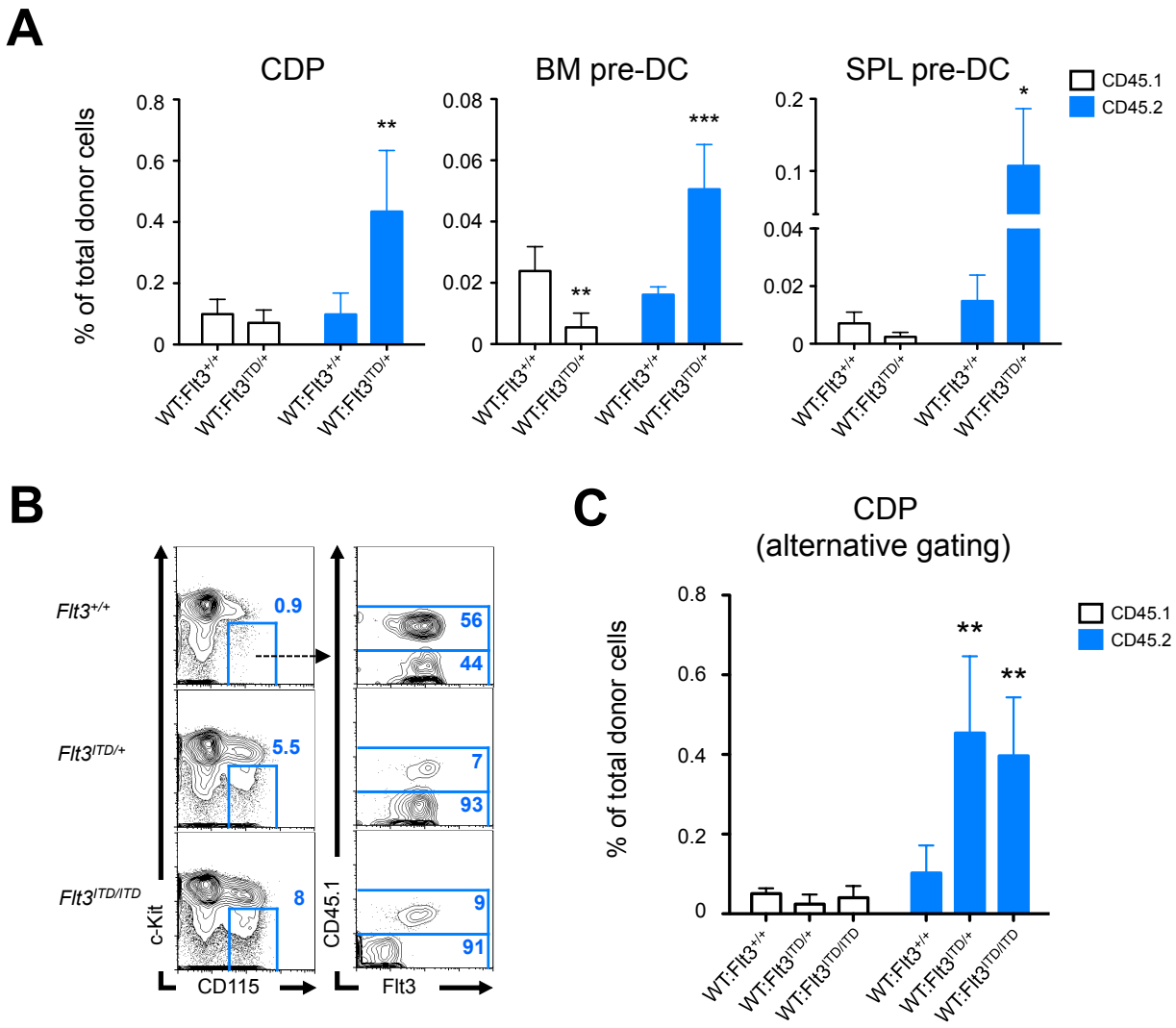
A
CDP
BM pre-DC
SPL pre-DC
% of total donor cells
CD45.1
CD45.2
WT:Flt3+/+
WT:Flt3ITD/+
WT:Flt3ITD/ITD
B
Flt3+/+
Flt3ITD/+
Flt3ITD/ITD
c-Kit
CD115
CD45.1
Flt3
0.9
56
44
5.5
7
93
8
9
91
C
CDP
(alternative gating)

Figure 1.8. Flt3-ITD causes downregulation of surface Flt3.

Lethally irradiated recipients (CD45.1$^+$/CD45.2$^+$) were reconstituted with a 1:1 ratio of CD45.1$^+$ WT competitor and CD45.2$^+$ *Flt3*$^{+/+}$, *Flt3*$^{ITD/+}$, or *Flt3*$^{ITD/ITD}$ donor bone marrow. Bone marrow (BM) and spleen (SPL) were analyzed 14 weeks after transfer by flow cytometry.

(A) Representative histograms of Flt3 expression on splenic cDCs and pDCs on WT CD45.1$^+$ competitor and CD45.2$^+$ donor cells (*Flt3*$^{+/+}$, *Flt3*$^{ITD/+}$, or *Flt3*$^{ITD/ITD}$). Dotted line shows mean fluorescent intensity (MFI) of Flt3 expression in WT cells.

(B) MFI of Flt3 expression from CD45.1$^+$ WT competitor and CD45.2$^+$ donor splenic cDCs (left) and pDCs (right) (mean ± SD, n = 4-5).

(C) Representative histograms of Flt3 expression on competitor and donor CDPs using an alternative gating. CDPs were defined as Lin$^-$ (B220, CD3, NK1.1, CD11b, Gr-1, Ter119, CD11c) Sca-1$^-$ IL7R$^-$ c-Kit^{lo} CD115$^+$.

(D) MFI of Flt3 expression from CD45.1$^+$ WT competitor and CD45.2$^+$ donor CDPs (mean ± SD, n = 4-5).

Statistically significant differences are indicated as: * $p < 0.05$; ** $p < 0.01$; *** $p < 0.001$

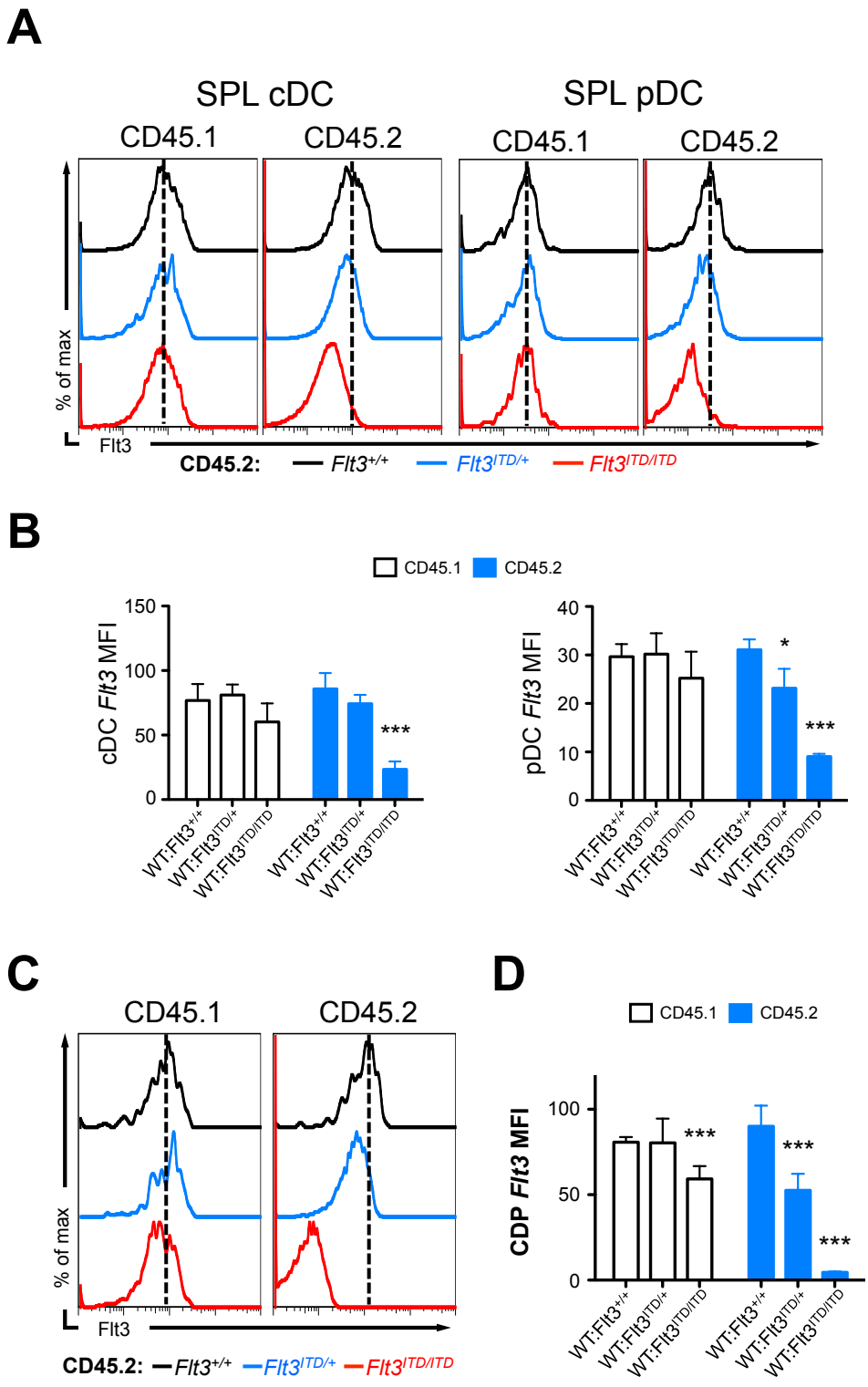
A
SPL cDC
SPL pDC
CD45.1
CD45.2
CD45.1
CD45.2
% of max
Flt3
CD45.2: Flt3+/+ Flt3ITD/+ Flt3ITD/ITD
B
CD45.1
CD45.2
cDC Flt3 MFI
150
100
50
0
***
pDC Flt3 MFI
40
30
20
10
0
*
***
WT:Flt3+/+
WT:Flt3ITD/+
WT:Flt3ITD/ITD
C
CD45.1
CD45.2
% of max
Flt3
CD45.2: Flt3+/+ Flt3ITD/+ Flt3ITD/ITD
D
CD45.1
CD45.2
CDP Flt3 MFI
100
50
0
***
***
***

Figure 1.9. Downregulation of Flt3 by Flt3-ITD abrogates Flt3L signaling and increases the proportion of CD8$^+$-like cDCs *in vitro.*

Whole bone marrow from naïve *Flt3*$^{+/+}$, *Flt3*$^{ITD/+}$, or *Flt3*$^{ITD/ITD}$ mice was cultured with indicated doses of recombinant murine Flt3L for 7 days.

(A) Bar graphs depict absolute cell numbers cDCs (defined as CD11c$^+$ MHCII$^+$) and pDCs (defined as B220$^+$ Bst2$^+$ CD11b$^-$) shown as mean ± SD from 4 independent experiments.

(B) Representative staining profiles of cDC subsets pre-gated on CD11c$^+$ MHCII$^+$. Numbers indicate fraction of cells within gated population.

(C) Ratio of CD24$^+$ (CD8-like) cDCs to CD11b$^+$ cDCs shown as mean ± SD from 4 independent experiments.

Statistically significant differences are indicated as: * $p < 0.05$; ** $p < 0.01$; *** $p < 0.001$

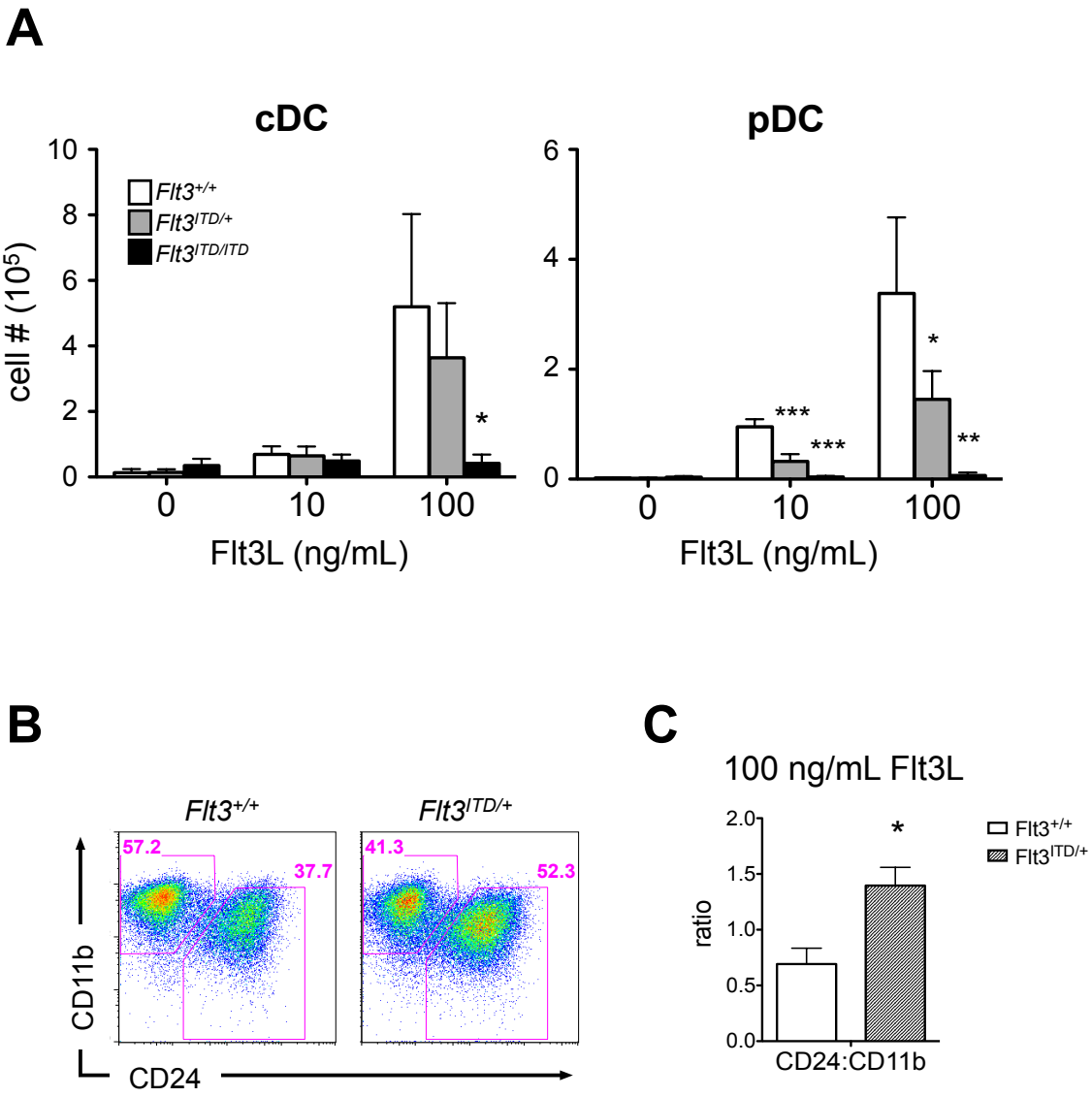
A
cDC
pDC
cell # (10^5)
Flt3+/+
Flt3ITD/+
Flt3ITD/ITD
Flt3L (ng/mL)
B
Flt3+/+
Flt3ITD/+
57.2
37.7
41.3
52.3
CD11b
CD24
C
100 ng/mL Flt3L
ratio
CD24:CD11b

Figure 1.10. Flt3-ITD mostly affects the CD8$^+$ cDC compartment.

Splenic DC populations from naïve B6xFVB *Flt3*$^{+/+}$ or *Flt3*$^{ITD/+}$ littermates were enriched from total splenocytes by MACS depletion and sorted for RNA extraction. RNA was prepared for hybridization onto Affymetrix GenChip Mouse Gene 1.0 ST Array and analyzed for differential gene expression using the NIA Array online software tool (ref. 169). Shown are scatter plots of log intensity comparing gene expression between *Flt3*$^{+/+}$ and *Flt3*$^{ITD/+}$ DCs. Red dots signify overexpressed genes and green dots signify underexpressed genes upon expression of Flt3-ITD that have more than a two-fold change in expression. Cell populations were defined as follows - CD11b$^+$ cDCs: CD11c$^+$ MHCII$^+$ Bst2$^-$ CD11b$^+$ CD8α$^-$; CD8$^+$ cDCs: CD11c$^+$ MHCII$^+$ Bst2$^-$ CD11b$^-$ CD8α$^+$; pDCs: Bst2$^+$ B220$^+$ CD11b$^-$. False discovery rate was set at <0.05.

CD11b⁺ cDC

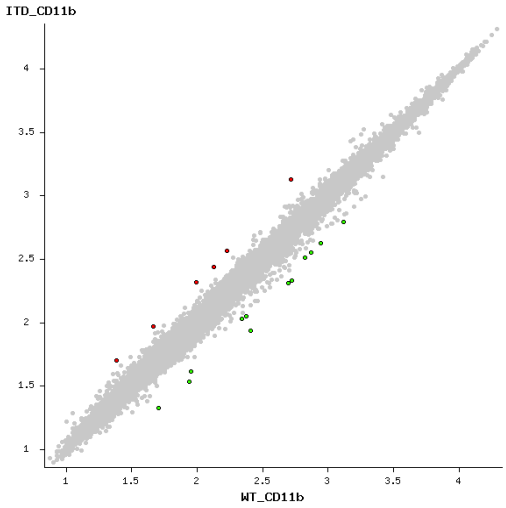

CD8⁺ cDC

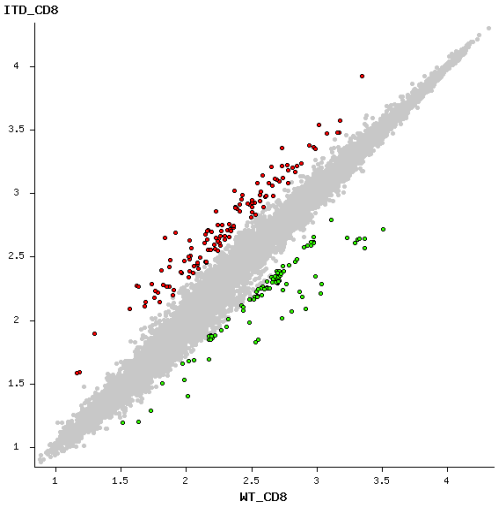

pDC

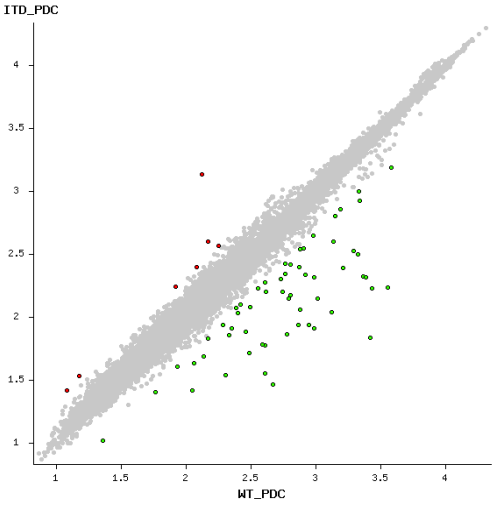

Figure 1.11. Flt3-ITD promotes the expansion of the non-canonical CD8$^+$ cDC subset.

(A) Representative staining profiles of CD8$^+$ and CD11b$^+$ cDCs from *Cx3cr1*$^{GFP/+}$ *Flt3*$^{+/+}$ or *Cx3cr1*$^{GFP/+}$ *Flt3*$^{ITD/+}$ spleen. CD8$^+$ and CD11b$^+$ cDCs are pre-gated on CD11c^{hi} MHCII$^+$ cells. Numbers show percent of cells within gated population. Histograms show divided subsets of CD8$^+$ and CD11b$^+$ cDCs differentiated by GFP expression level. Numbers on histogram show proportion of corresponding subset among total CD8$^+$ or CD11b$^+$ cDCs.

(B) Frequencies of cDC subsets within CD8$^+$ and CD11b$^+$ cDC populations as shown in (A) (mean ± SD, n = 5; 6-9 wks old)

(C) Fold change in cell frequencies of *Cx3cr1*$^{GFP/+}$ *Flt3*$^{ITD/+}$ over *Cx3cr1*$^{GFP/+}$ *Flt3*$^{+/+}$ for each cDC subset (mean ± SD, n = 5; 6-9 wks old). To calculate fold change, individual *Flt3*$^{ITD/+}$ cell frequencies were normalized to the *Flt3*$^{+/+}$ average frequency for each subset. Dotted line delineates fold change of 1.

(D) *Cx3cr1*$^{GFP/GFP}$ mice were injected i.p. with 3 doses of PBS or 5 µg recombinant Flt3L-Fc every 3 days. Shown are frequencies of cDC subsets within CD8$^+$ and CD11b$^+$ cDC populations (n = 2-3; 11 wks old)

(E) Fold change in cell frequencies of Flt3L-treated over PBS-treated for each cDC subset as described in (D) (mean ± SD, n = 2-3; 11 wks old). To calculate fold change, individual Flt3L-treated cell frequencies were normalized to the PBS-treated average frequency for each subset. Dotted line delineates fold change of 1.

Statistically significant differences are indicated as: * $p < 0.05$; ** $p < 0.01$; *** $p < 0.001$

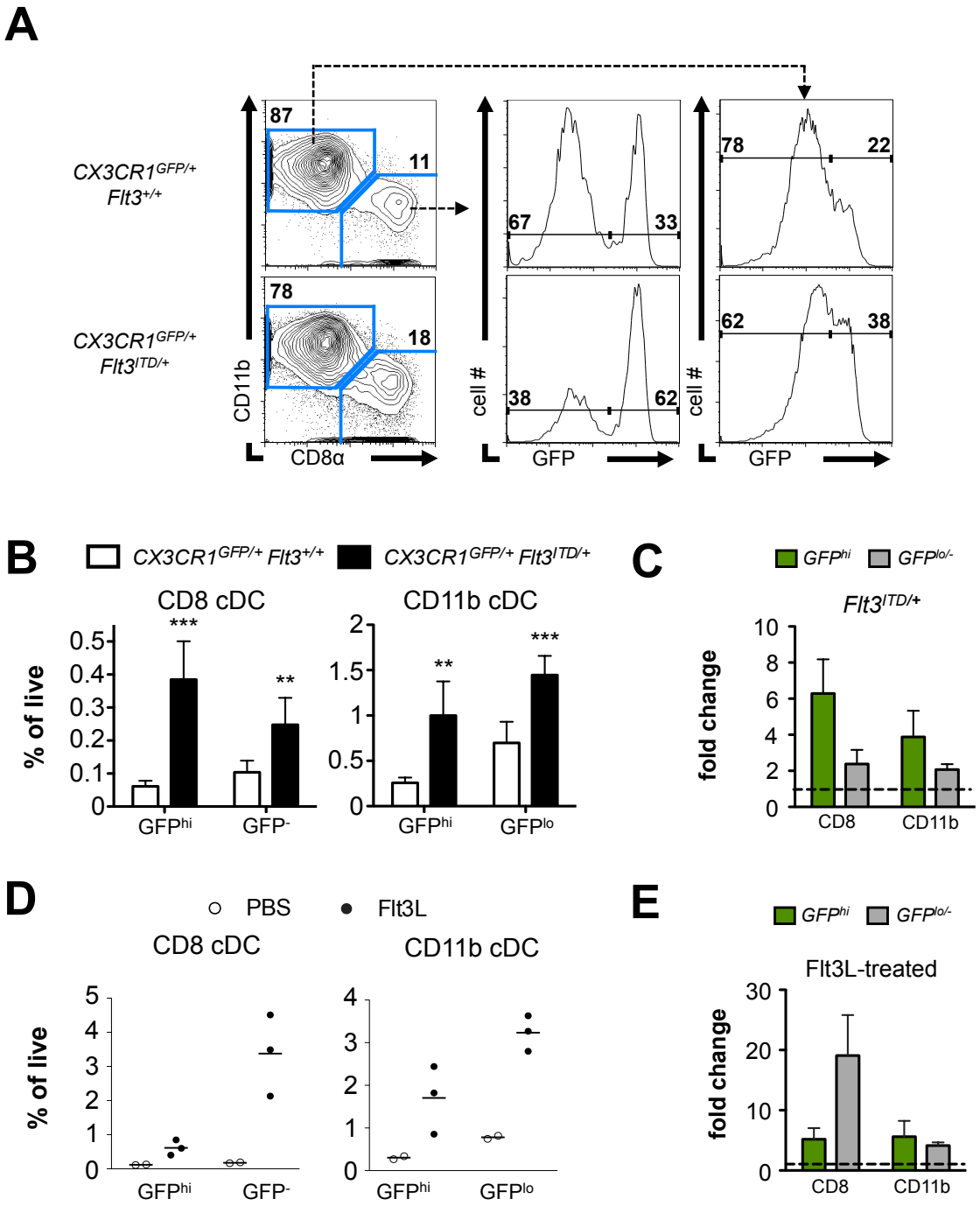
A
CX3CR1GFP/+ Flt3+/+
CX3CR1GFP/+ Flt3ITD/+
87
11
78
18
CD11b
CD8α
67
33
38
62
cell #
GFP
78
22
62
38
B
CX3CR1GFP/+ Flt3+/+
CX3CR1GFP/+ Flt3ITD/+
CD8 cDC
CD11b cDC
% of live
***
**
GFPhi
GFP-
GFPlo
C
GFPhi
GFPlo/-
Flt3ITD/+
fold change
CD8
CD11b
D
PBS
Flt3L
CD8 cDC
CD11b cDC
% of live
GFPhi
GFP-
GFPlo
E
GFPhi
GFPlo/-
Flt3L-treated
fold change
CD8
CD11b

Figure 1.12. The non-canonical $CD8^+$ cDC subset expresses PD-L1.

(A) Ratio of $PDL1^+$ to $CD86^+$ subsets among $CD8^+$ cDCs in naïve *Flt3*$^{+/+}$ or *Flt3*$^{ITD/+}$ spleen (mean ± SD, n = 4-5; 9-14 wks old).

(B) Representative staining profile of CD86 and PD-L1 expression among $CD8^+$ cDC subsets from *Cx3cr1*$^{GFP/GFP}$ splenocytes. Green population represents non-canonical GFP^{hi} $CD8^+$ cDCs, while black population represents canonical GFP^- $CD8^+$ cDCs.

Statistically significant differences are indicated as: * $p < 0.05$; ** $p < 0.01$; *** $p < 0.001$

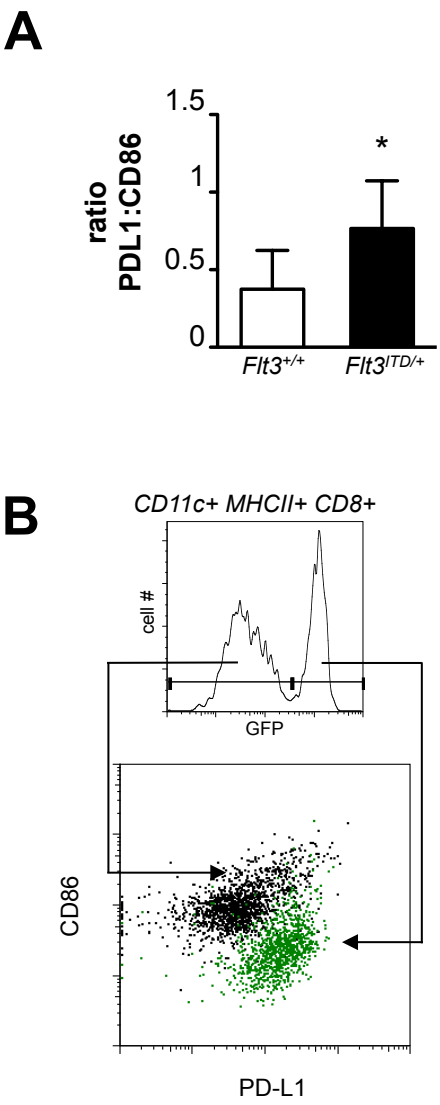
A
1.5
1
0.5
0
ratio
PDL1:CD86
*
Flt3+/+
Flt3ITD/+
B
CD11c+ MHCII+ CD8+
cell #
GFP
CD86
PD-L1

Figure 1.13. Flt3-ITD specifically expands the non-canonical CD8^{+} cDC subset in Batf3-deficient mice.

(A) Representative staining profiles (left) and bar graph of absolute cell numbers (right) of *Flt3*$^{+/+}$ or *Flt3*$^{ITD/+}$ CD8^{+} cDC populations in spleen on *Batf3*$^{+/+}$ or *Batf3*$^{-/-}$ background (n = 5; 5-9 wks old). Numbers in plots show percent of gated population.

(B) Representative staining profiles gated from CD11C^{hi} MHCII^{+} CD8^{+} in WT, *Batf3*$^{-/-}$ *Flt3*$^{+/+}$ and *Batf3*$^{-/-}$ *Flt3*$^{ITD/+}$ spleen. Numbers indicate percent of cells within gated population.

Statistically significant differences are indicated as: * $p < 0.05$; ** $p < 0.01$; *** $p < 0.001$

A

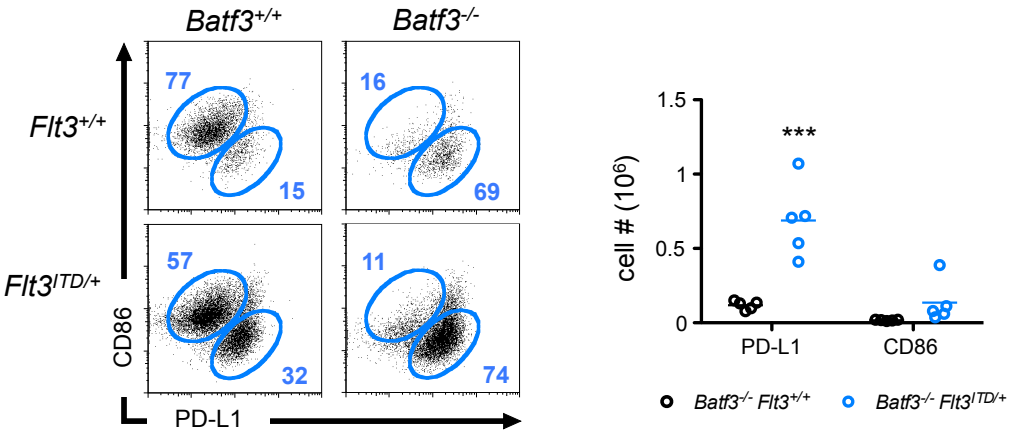
Batf3+/+
Batf3-/-
Flt3+/+
Flt3ITD/+
77
15
16
69
57
32
11
74
CD86
PD-L1
1.5
1
0.5
0
cell # (10^6)
***
PD-L1
CD86
Batf3-/- Flt3+/+
Batf3-/- Flt3ITD/+

B

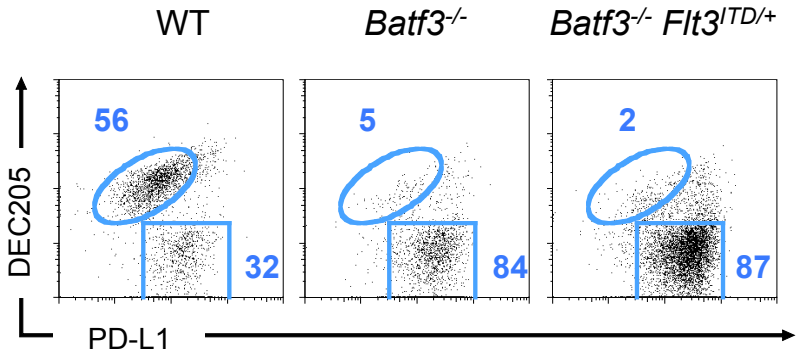
WT
Batf3-/-
Batf3-/- Flt3ITD/+
56
32
5
84
2
87
DEC205
PD-L1

Figure 1.14. Flt3-ITD increases susceptibility to Listeria infection, which requires canonical CD8$^+$ cDCs.

Wild-type or Batf3-deficient *Flt3*$^{+/+}$ or *Flt3*$^{ITD/+}$ mice were infected with 5 x 10^3 *Listeria monocytogenes*. Graph shows bacterial titers as colony forming units per gram of spleen 3 days post injection (n= 3-5, 9-12 wks old).

Statistically significant differences are indicated as: * $p < 0.05$; ** $p < 0.01$; *** $p < 0.001$

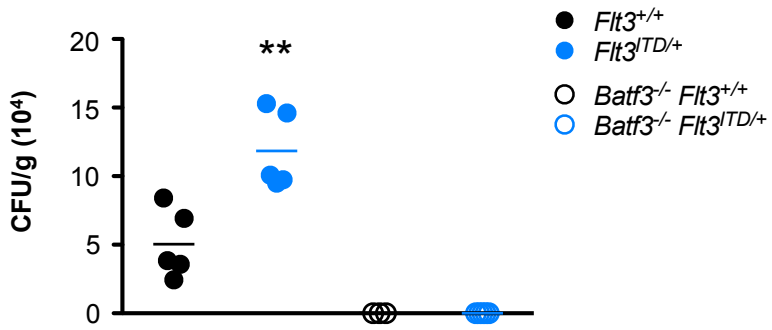
20
15
10
5
0
CFU/g (10⁴)
**
Flt3+/+
Flt3ITD/+
Batf3-/- Flt3+/+
Batf3-/- Flt3ITD/+

Figure 1.15. Flt3-ITD expands T_{regs} in the bone marrow.

The populations of TCRβ$^+$ CD4$^+$/CD8$^+$ FoxP3$^-$ conventional (T_{conv}) and TCRβ$^+$ CD4$^+$ FoxP3$^+$ regulatory (T_{reg}) T cells were analyzed in the bone marrow (BM), spleen (SPL), and lymph nodes (LN) by intracellular staining for FoxP3.

(A) Frequency (top row) and absolute numbers (bottom row) of T_{conv} cells in naïve *Flt3*$^{+/+}$, *Flt3*$^{ITD/+}$, or *Flt3*$^{ITD/ITD}$ mice (mean ± SD, n = 5; 8.5-12.5 wks old).

(B) Frequency (top row) and absolute numbers (bottom row) of T_{reg} cells in naïve *Flt3*$^{+/+}$, *Flt3*$^{ITD/+}$, or *Flt3*$^{ITD/ITD}$ mice (mean ± SD, n = 5; 8.5-12.5 wks old).

Statistically significant differences are indicated as: * $p < 0.05$; ** $p < 0.01$; *** $p < 0.001$

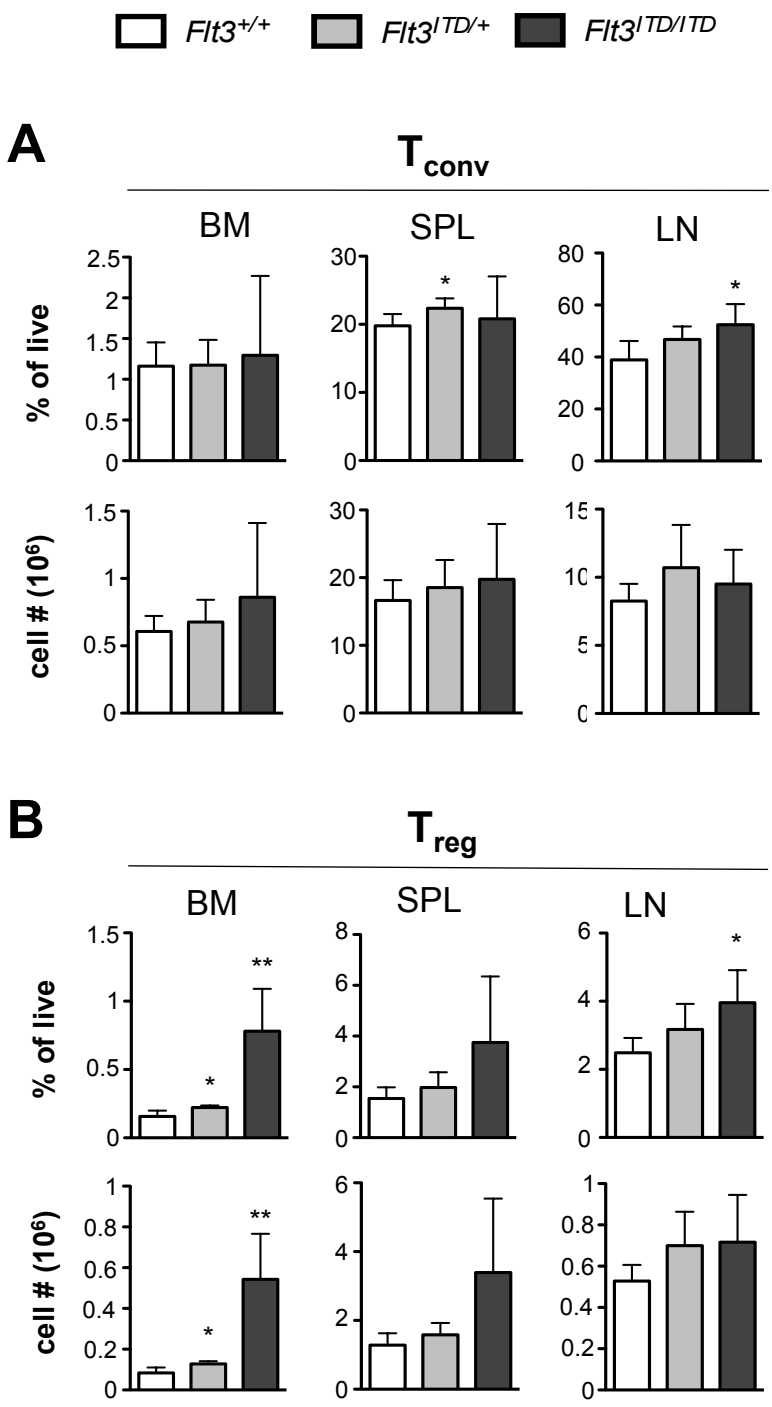
Flt3+/+
Flt3ITD/+
Flt3ITD/ITD
A
Tconv
BM
SPL
LN
% of live
cell # (10^6)
B
Treg
BM
SPL
LN
% of live
cell # (10^6)

Figure 1.16. Flt3-ITD expands T cells in a cell-intrinsic manner.

Lethally irradiated recipients (CD45.1$^+$/CD45.2$^+$) were reconstituted with a 1:1 ratio of CD45.1$^+$ WT competitor and CD45.2$^+$ *Flt3*$^{+/+}$, *Flt3*$^{ITD/+}$, or *Flt3*$^{ITD/ITD}$ donor bone marrow. Bone marrow (BM), spleen (SPL), and lymph nodes (LN) were analyzed 14 weeks after transfer by flow cytometry. The populations of TCRβ$^+$ CD4$^+$/CD8$^+$ FoxP3$^-$ conventional (T_{conv}) and TCRβ$^+$ CD4$^+$ FoxP3$^+$ regulatory (T_{reg}) T cells were analyzed by intracellular staining for FoxP3 (mean ± SD, n = 4-5)

(A) Percent of T_{conv} cells out of total WT competitor CD45.1$^+$ cells (white bars) or donor CD45.2$^+$ cells (blue bars).

(B) Percent of T_{reg} cells out of total WT competitor CD45.1$^+$ cells or donor CD45.2$^+$ cells.

(C) Proportion of of T_{reg} cells out of total WT competitor CD45.1$^+$ T cells.

Statistically significant differences are indicated as: * $p < 0.05$; ** $p < 0.01$; *** $p < 0.001$

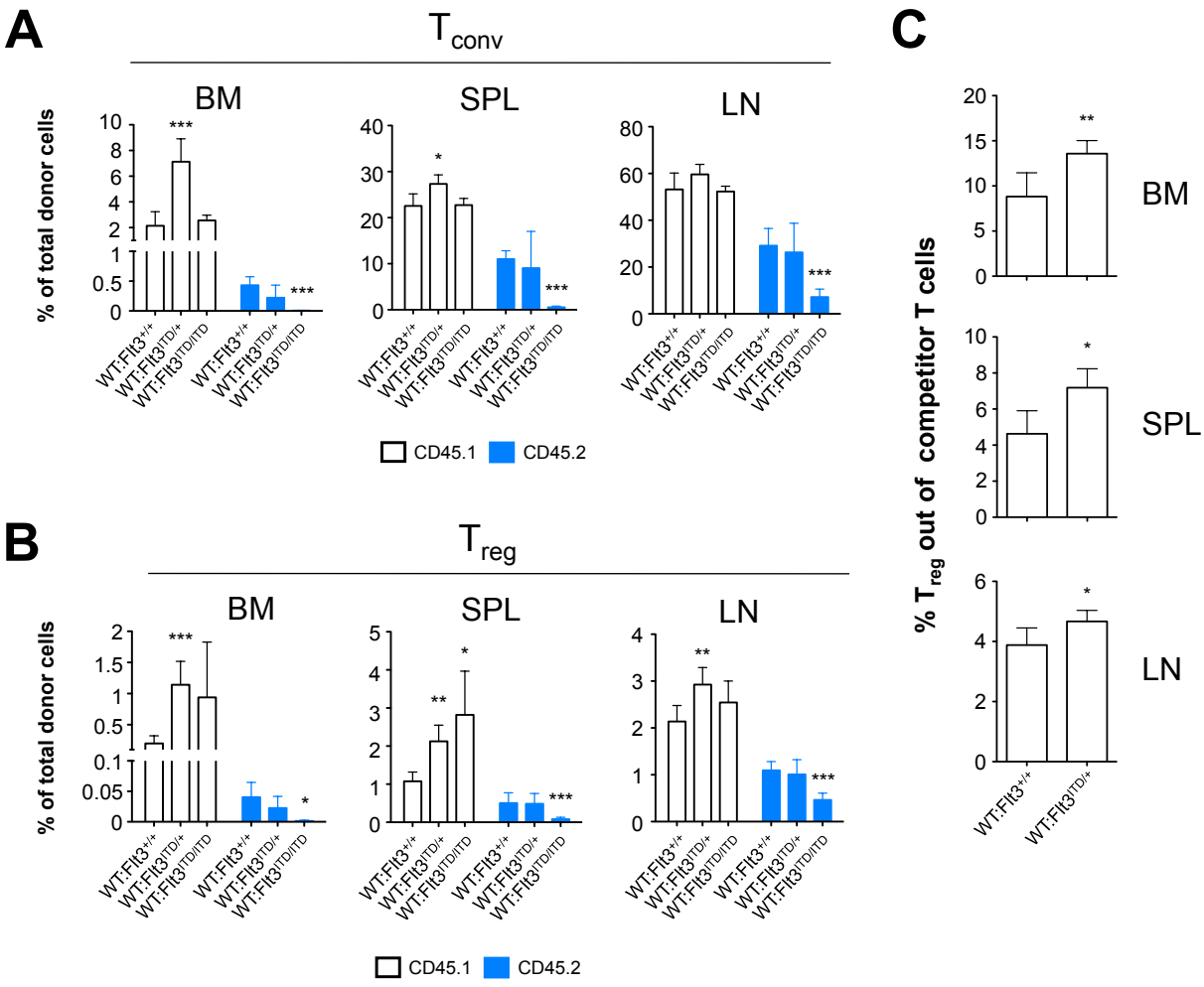
A
T conv
BM
SPL
LN
% of total donor cells
CD45.1
CD45.2
B
T reg
C
% T reg out of competitor T cells
WT:Flt3+/+
WT:Flt3ITD/+
WT:Flt3ITD/ITD

Figure 1.17. Flt3-ITD facilitates antigen-driven T cell proliferation.

Allogeneic mixed leukocyte reactions (MLRs) were performed by using either 50,000 (50k), 25,000 (25k), or 12,500 (12.5k) $CD11c^+$ enriched splenocytes as stimulators from *Flt3*$^{+/+}$ or *Flt3*$^{ITD/+}$ B6xFVB F_1 mice, and incubating them with 50,000 responder bulk T cells isolated from B6 *FoxP3*^{GFP} spleens and lymph nodes labeled with Cell Trace Violet dye (CTV) . Shown are data from 3 individual sets of stimulators with the same population of responders. T cells were defined as follows: T_{conv} - $CD45.1^-$ $TCR\beta^+$ $CD4^+/CD8^+$ GFP^-; T_{reg}- $CD45.1^-$ $TCR\beta^+$ $CD4^+$ GFP^+. Bar graphs depict mean ± SD.

(A) Absolute numbers of responder $CD4^+$ T_{conv}, $CD8^+$ T_{conv}, and T_{reg} populations.

(B) Proportion of responder T_{regs} out of total responder T cells.

(C) Representative staining profiles (left) and bar graphs (right) show proportion of proliferative T cell populations as measured by dilution of CTV in MLRs. Numbers in FACS plots represent percent of proliferating cells that have diluted out CTV.

Statistically significant differences are indicated as: * $p < 0.05$; ** $p < 0.01$; *** $p < 0.001$

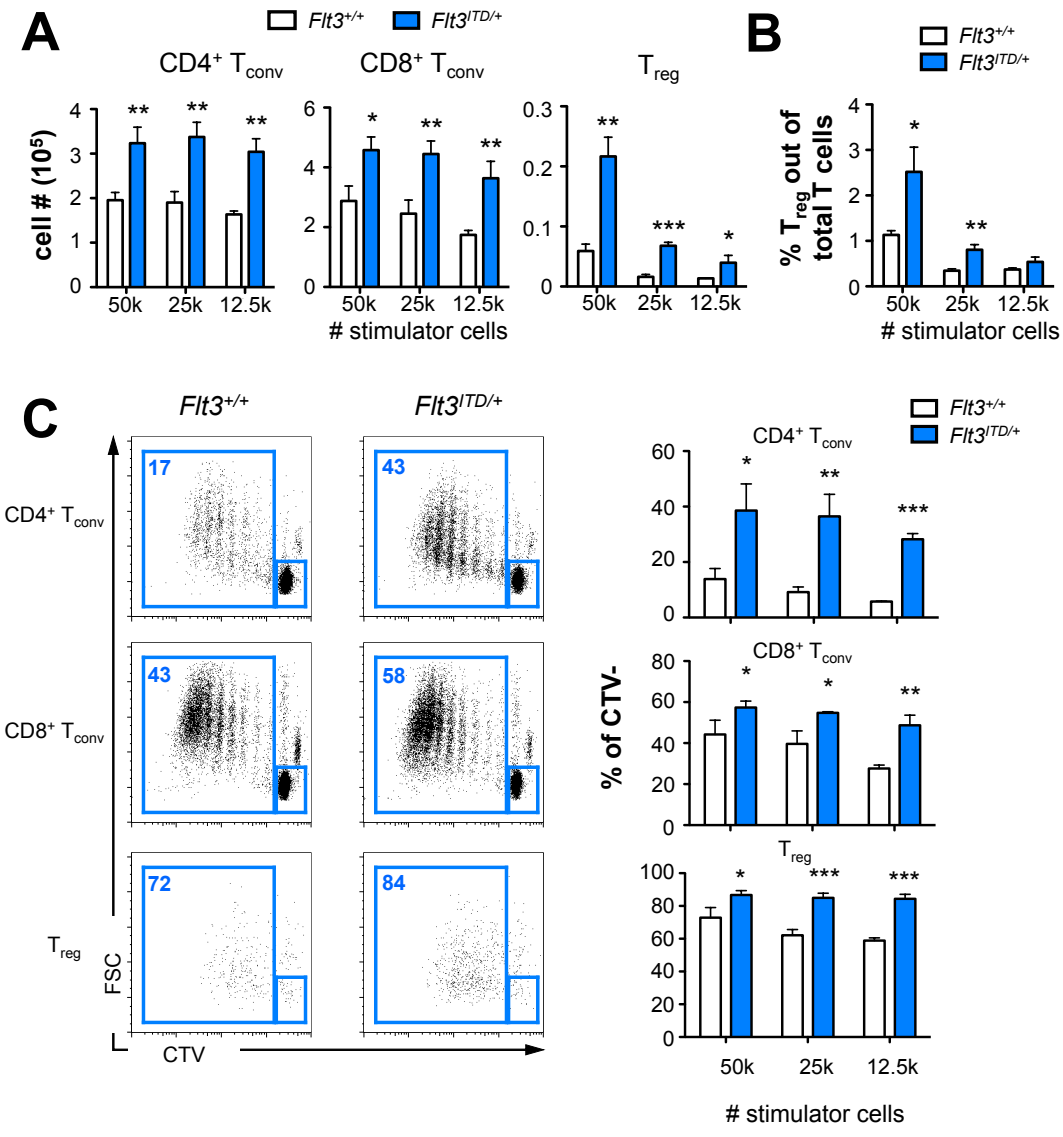
A
Flt3+/+
Flt3ITD/+
CD4+ Tconv
CD8+ Tconv
Treg
cell # (10^5)
50k
25k
12.5k
stimulator cells
B
% Treg out of total T cells
C
17
43
58
72
84
FSC
CTV
% of CTV-

Figure 1.18. Flt3-ITD facilitates homeostatic T cell proliferation.

Cell Trace Violet (CTV)-labeled T cells from *FoxP3*^{GFP} mice were transferred into Rag1-deficient *Flt3*$^{+/+}$ or *Flt3*$^{ITD/+}$ mice. Adoptively transferred T cell populations were analyzed in the spleens of recipient animals 5 days later. Data are pooled from two independent experiments. T cells were defined as follows: T_{conv} - TCRβ$^+$ CD4$^+$/CD8$^+$ GFP$^-$; T_{reg}- TCRβ$^+$ CD4$^+$ GFP$^+$.

(A) Absolute numbers of adoptively transferred CD4$^+$ T_{conv}, CD8$^+$ T_{conv}, and T_{reg} populations, excluding those that completely diluted out CTV dye due to microbiota antigen stimulation (n = 10-12; 12-17 wks old).

(B) Representative histograms of T_{conv} cell proliferation as measured by CTV dye from adoptive transfers into *Rag1*$^{-/-}$ recipients. Numbers show proportion of proliferative T cells. T cells that completely diluted out CTV dye due to microbiota antigen stimulation were excluded.

Statistically significant differences are indicated as: * $p < 0.05$; ** $p < 0.01$; *** $p < 0.001$

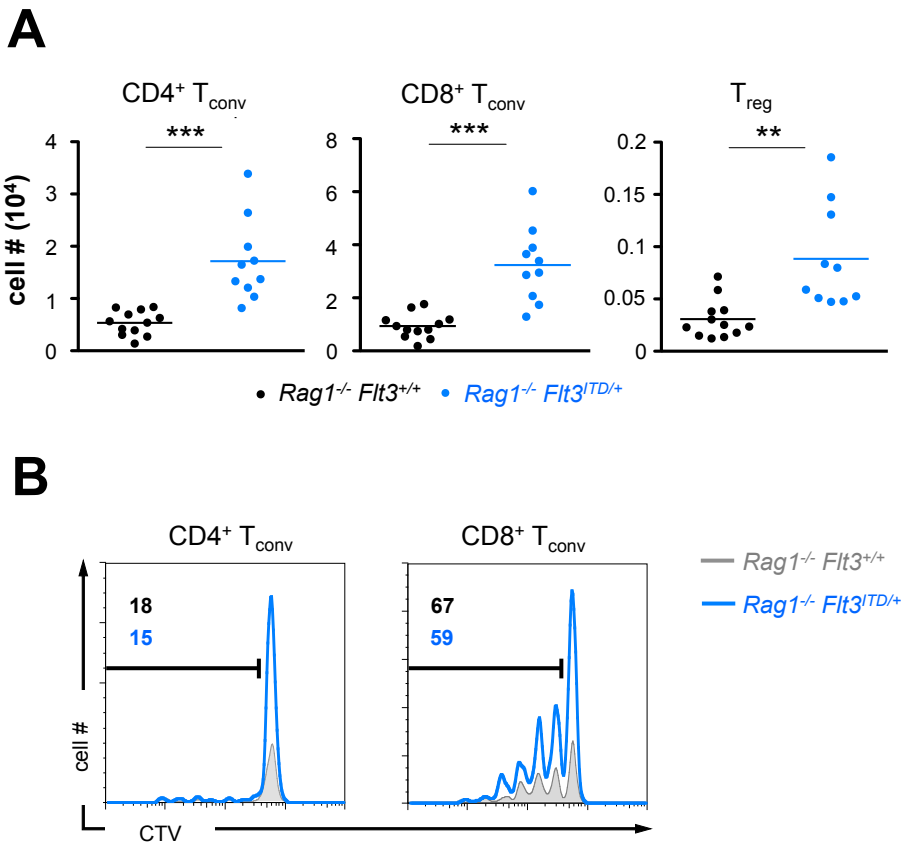
A
CD4+ Tconv
CD8+ Tconv
Treg
***
***
**
cell # (10^4)
4
3
2
1
0
8
6
4
2
0
0.2
0.15
0.1
0.05
0
Rag1-/- Flt3+/+
Rag1-/- Flt3ITD/+
B
CD4+ Tconv
CD8+ Tconv
18
15
67
59
cell #
CTV
Rag1-/- Flt3+/+
Rag1-/- Flt3ITD/+

Figure 1.19. Flt3-ITD favorably reconstitutes T_{reg} populations after T_{reg} depletion.

Flt3$^{+/+}$ or *Flt3*$^{ITD/+}$ mice carrying the *Foxp3*$^{DTR-GFP}$ allele were treated for two consecutive days with diptheria toxin (DT) to deplete T_{regs} and analyzed at different time points. T_{conv} cells were defined as TCRβ^{+} CD4^{+}/CD8^{+} GFP^{-}, while T_{regs} were defined as TCRβ^{+} CD4^{+} GFP^{+}.

(A) Time course of T_{reg} frequencies out of total lymphocytes in peripheral blood of mice after T_{reg} depletion. Red arrows indicate days in which DT treatment was performed. Blood was retrieved to monitor T_{reg} populations on day 0, 2, 10, 14, 21, and 28 (mean ± SD, n = 12-16; 7-12 wks old).

(B) End point analysis of spleen and thymus shown as percentage of T_{reg} out of mature T cells (n = 12-16; 7-12 wks old).

(C) Percentage of T_{reg} out of mature T cells in spleen and thymus prior to DT administration (n = 4; 12-20 wks old).

Statistically significant differences are indicated as: * $p < 0.05$; ** $p < 0.01$; *** $p < 0.001$

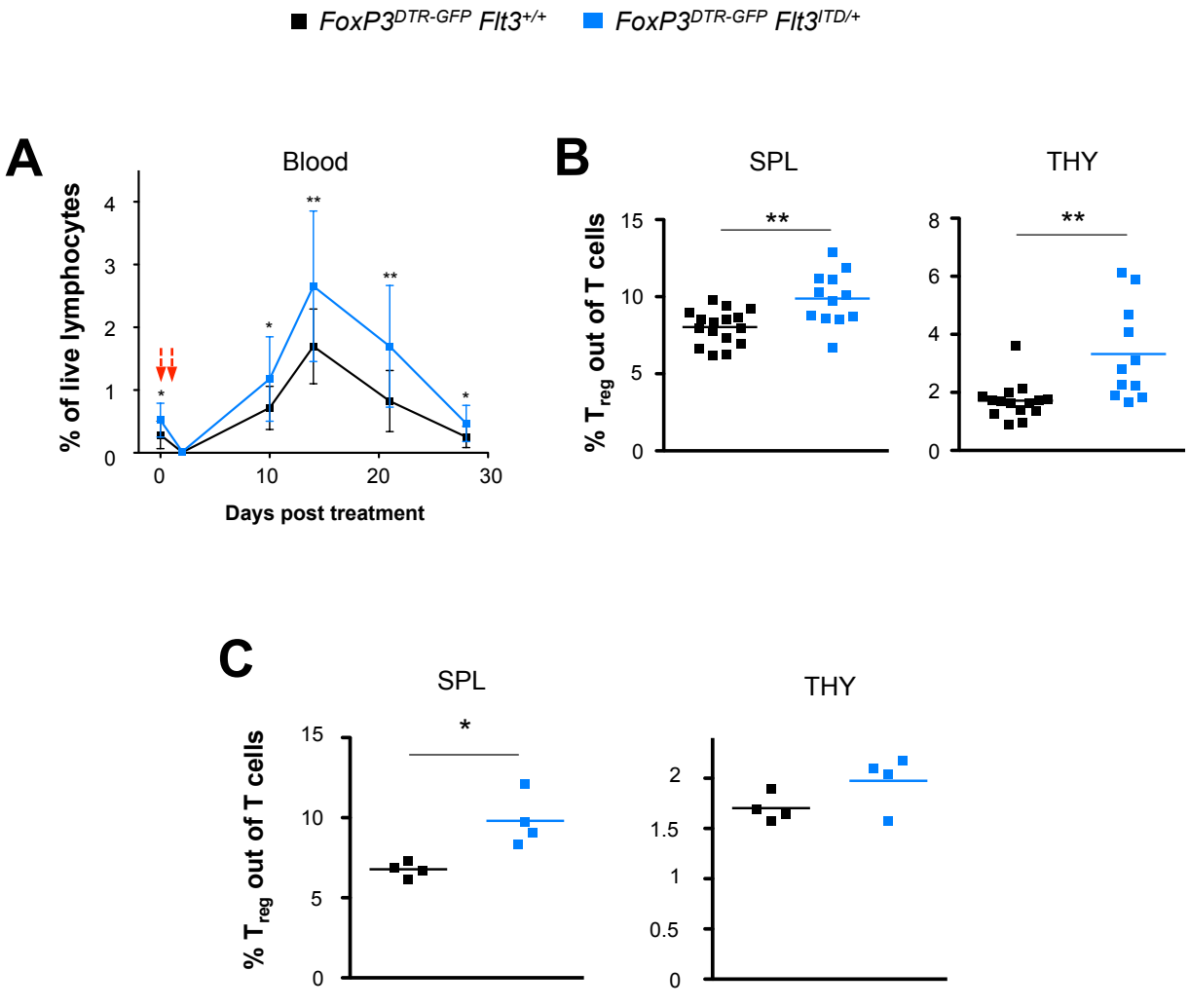
FoxP3DTR-GFP Flt3+/+
FoxP3DTR-GFP Flt3ITD/+
A
Blood
% of live lymphocytes
Days post treatment
B
SPL
THY
% Treg out of T cells
C
SPL
THY
% Treg out of T cells

Figure 1.20. Flt3-ITD dampens self-reactivity during acute graft-versus-host response.

30 x 10^6 WT B6 leukocytes from pooled spleen and lymph node cell suspensions were transferred into non-irradiated B6xFVB F_1 *Flt3*$^{+/+}$ or *Flt3*$^{ITD/+}$ recipients. Spleens were analyzed 7 days after transfer. Graft T cells were defined as CD45.1$^-$ TCRβ$^+$ CD4$^+$/CD8$^+$, while host T cells were defined as CD45.1$^+$ TCRβ$^+$ CD4$^+$/CD8$^+$.

(A) Representative staining profiles of graft T cell expansion in *Flt3*$^{+/+}$ or *Flt3*$^{ITD/+}$ recipients. Numbers indicate percent of cells within gated population.

(B) Graft T cells presented as frequency of live (left) or absolute numbers (right) in spleen (n = 10, 9 wks old).

(C) Host T_{regs} presented as percent of total host T cells (n = 8; 7-9 wks old). Data is from a separate experiment from data in (B).

Statistically significant differences are indicated as: * $p < 0.05$; ** $p < 0.01$; *** $p < 0.001$

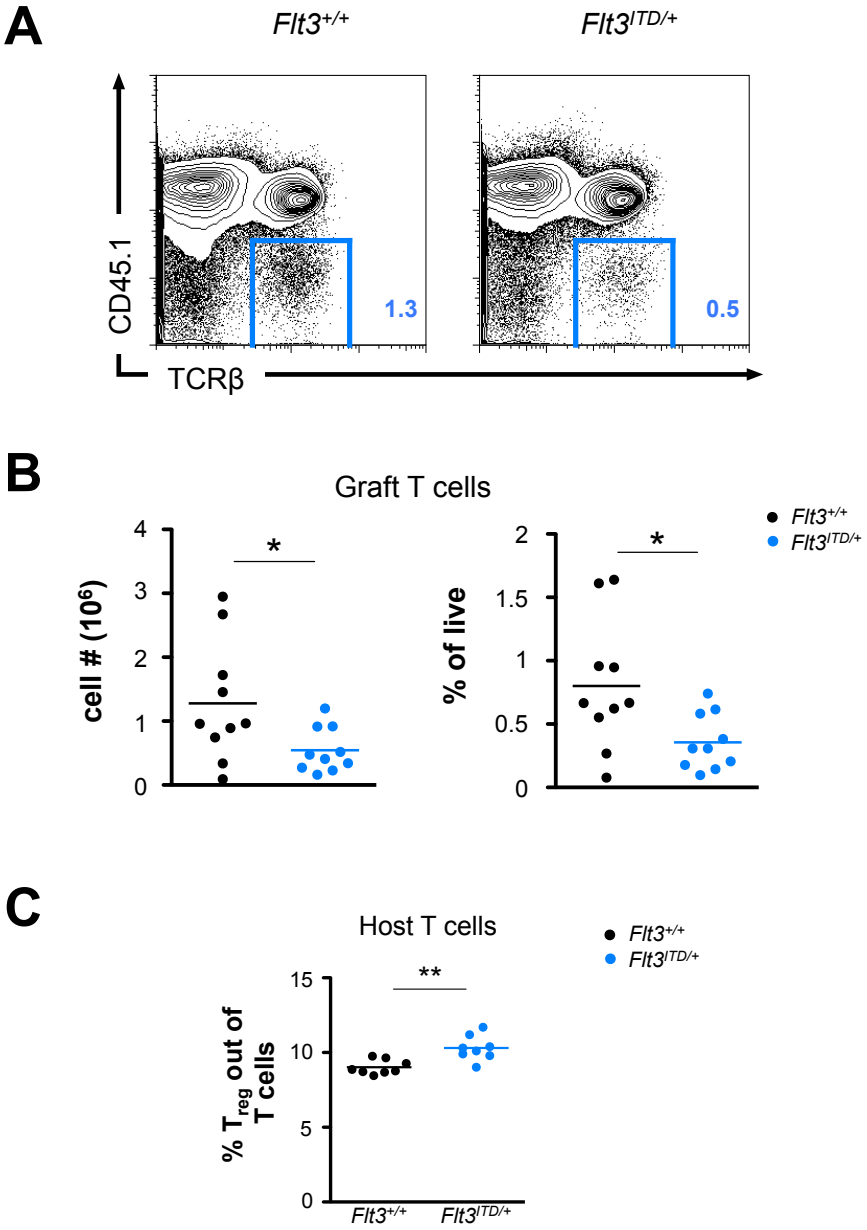
A
Flt3+/+
Flt3ITD/+
CD45.1
TCRβ
1.3
0.5
B
Graft T cells
cell # (10^6)
% of live
Flt3+/+
Flt3ITD/+
*
*
C
Host T cells
% Treg out of T cells
**
Flt3+/+
Flt3ITD/+

Figure 1.21. Flt3-ITD dampens self-reactivity during acute-graft-versus-host response in a PD-L1/PD-1 independent manner.

30 x 10^6 WT B6 leukocytes from pooled spleen and lymph node cell suspensions were transferred into non-irradiated B6xFVB F_1 *Flt3*$^{+/+}$ or *Flt3*$^{ITD/+}$ recipients. Recipients were treated immediately prior and during T cell engraftment every 2-3 days with control IgG or blocking antibodies for PD-L1 or PD-1. Spleens were analyzed 7-8 days after transfer. Graft T cells were defined as CD45.1$^-$ TCRβ$^+$ CD4$^+$/CD8$^+$.

(A) Graft T cells presented as frequency of live cells in spleen after PD-L1 blockade (n = 4-5, 7-8 wks old).

(B) Graft T cells presented as frequency of live cells in spleen after PD-1 blockade (n = 4, 12-14 wks old).

Statistically significant differences are indicated as: * $p < 0.05$; ** $p < 0.01$; *** $p < 0.001$

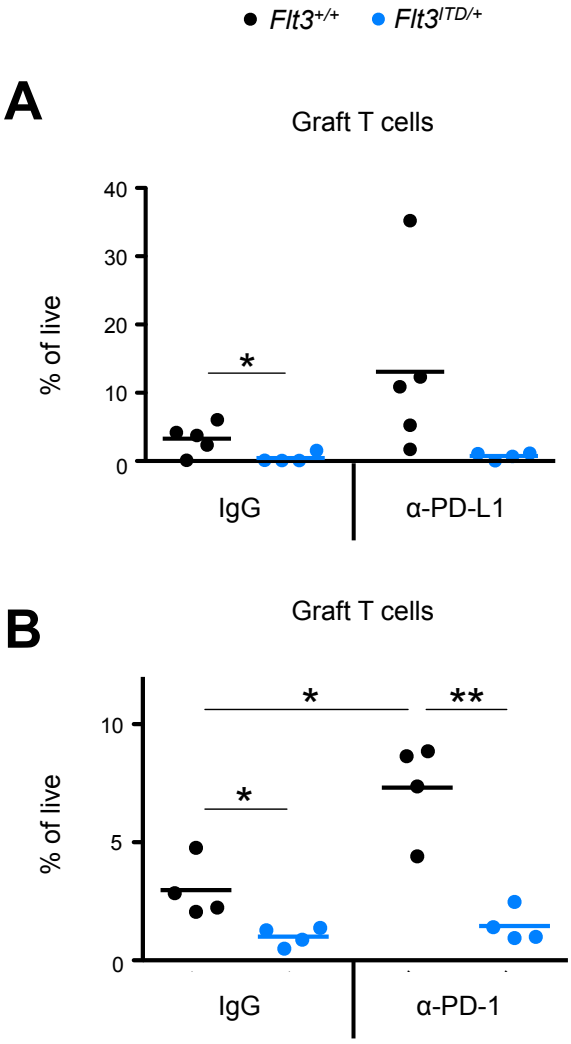
Flt3+/+
Flt3ITD/+
A
Graft T cells
% of live
40
30
20
10
0
*
IgG
α-PD-L1
B
Graft T cells
% of live
10
5
0
*
*
**
IgG
α-PD-1

Figure 1.22. Flt3-ITD cannot ameliorate self-reactivity caused by the absence of T_{regs}.

Shown is a Kaplan-Meier survival curve of T_{reg}-deficient *FoxP3*$^{sf/y}$ *Flt3*$^{+/+}$ and *FoxP3*$^{sf/y}$ *Flt3*$^{ITD/+}$ littermates. Mice that showed signs of autoimmunity (runting, scaly skin on ears and tails, and hunched posture) are presented in this graph. *Flt3*$^{+/+}$: n = 9; *Flt3*$^{ITD/+}$: n = 16.

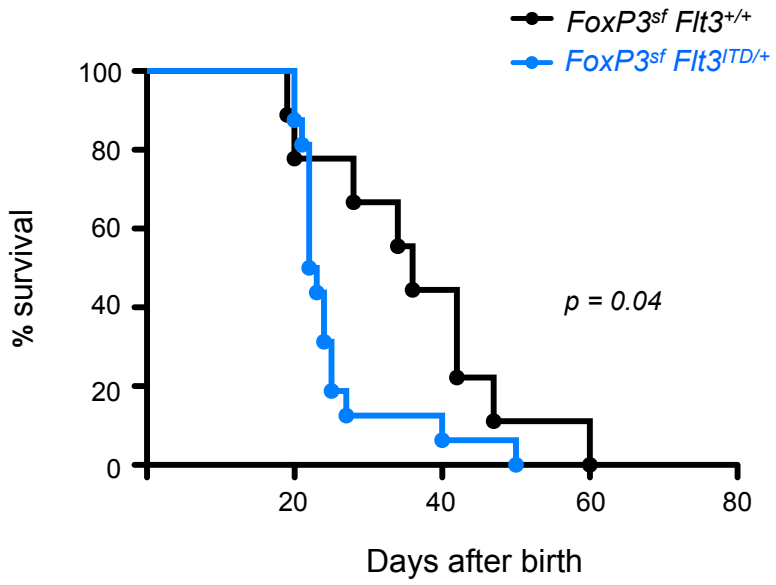
FoxP3sf Flt3+/+
FoxP3sf Flt3ITD/+
100
80
60
40
20
0
% survival
p = 0.04
20
40
60
80
Days after birth

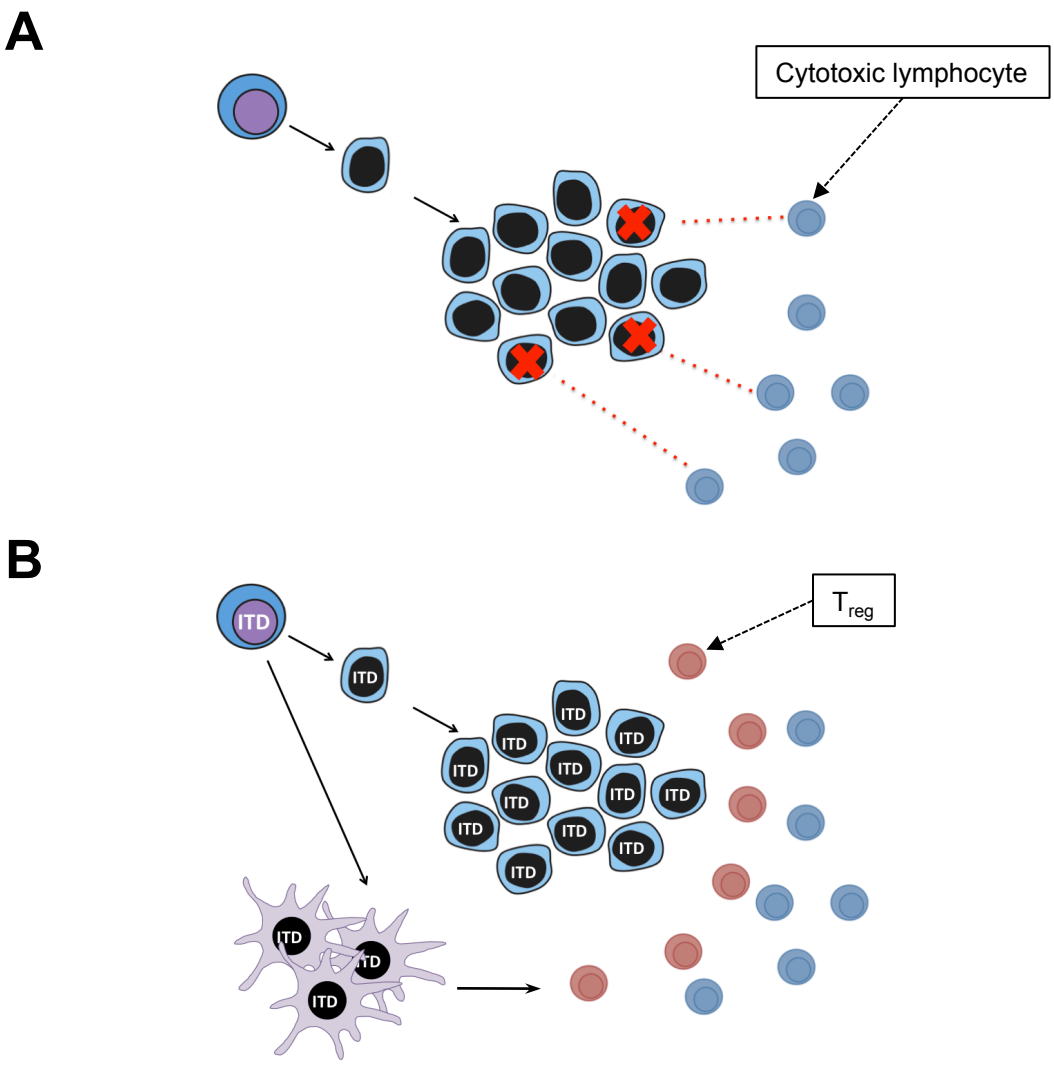

Figure 1.23. Model for the subversion of immunosurveillance during Flt3-ITD leukemogenesis.

(A) Flt3-ITD-negative leukemic clones are readily recognized and eliminated by tumor-specific cytotoxic lymphocytes.

(B) Flt3-ITD-positive leukemic clones give rise to an expanded population of DCs, which indirectly promotes the expansion of T_{regs} that can suppress lymphocyte-mediated cytotoxicity and thus allow the leukemia to survive and grow.

CHAPTER II

THE ROLE OF MYCL1 IN DENDRITIC CELL DEVELOPMENT AND FUNCTION

INTRODUCTION

In the previous chapter, we utilized the role of Flt3 as a key regulator of DC development to analyze the consequences of aberrant Flt3 activation in the context of leukemia. Here, we again utilize Flt3 to reveal novel transcriptional regulators that act in DC development and function. Given its functional importance and specific expression in DCs among mature hematopoietic cell types, we employed the Immgen database[132] to correlate the expression of Flt3 with that of other genes (Figure 2.1). Among the genes whose expression correlated with Flt3, only few encoded transcription factors. Among them was Cbfa2t3, also known as Mtg16, which has been recently characterized by our group as an important regulator of pDC/cDC cell fate decision[133]. The next two chapters will focus on two additional candidate transcription factors whose expression correlates with Flt3 in both murine and human hematopoietic cells. In this chapter, we focus on the uncharacterized Myc family transcription factor, Mycl1. While Mycl1 is highly expressed in murine DCs, absence of Mycl1 yielded no major differences in DC numbers in lymphoid and non-lymphoid tissues. In addition, we found that Mycl1-deficient DCs were fully capable of normal proliferation and T cell priming in various conditions of antigen presentation. These results, contrary to recently reported data, suggest that Mycl1 is dispensable for DC development and function.

BACKGROUND

Transcriptional regulation of DC development

While the use of cell surface markers and adoptive transfers have been essential tools to identify the DC lineage, this system is subject to technical caveats and inconsistencies that sometimes create more ambiguity than clarity. To accurately define the DC lineage requires identification of regulatory elements that functionally mediate developmental transitions, rather than just the use of sometimes arbitrary cell surface markers. Therefore, identifying key transcription factors involved in DC development will accurately clarify how DC specification occurs within hematopoiesis. Understanding these precise mechanisms *in vivo* will provide an essential guide for harnessing these systems for dendritic cell-based immunotherapy.

Regulation of early DC commitment

All of the transcription factors identified to be required for early DC fate decisions generally result in a broad reduction in all DC subtypes along with changes in other hematopoietic lineages upon genetic targeting. The first transcription factor proposed to play an important role in DC development is Ikaros, a zinc-finger transcription factor previously shown to also be an essential factor for lymphopoiesis. Expression of the dominant-negative mutant of Ikaros results in depletion of all DCs, while null mutations of Ikaros selectively depletes $CD11b^+$ cDCs and pDCs[134,135]. Ets-family member PU.1 is another transcription factor that has very well-known and broad roles in hematopoiesis. In addition to being expressed on HSCs and early myeloid and lymphoid progenitors, PU.1 is expressed on both CDPs and cDCs, and to a lesser extent pDCs[136]. Accordingly, deletion of PU.1 in adult mice results in the drastic reduction of all DC subtypes, and has been reported to control the expression of Flt3[136]. Finally, Gfi-1, which has been implicated in HSC homeostasis, T cell development and granulocyte development, has also been implicated in DC development, as mice deficient in Gfi-1 show reduced numbers of all DCs[137]. Furthermore, Gfi-1 has been shown to regulate DC development through Stat3. Consistent with this, mice deficient in Stat3 also show a depletion of the DC pool[138].

Regulation of post-commitment DC differentiation

Described below are several transcription factors that have been identified to control DC subset fate, assumingly after the CDP level. These transcription factors are categorized by the DC subsets that are most affected by their genetic manipulation:

CD11b$^+$ (or CD8$^-$) cDCs. NF-kappaB family member RelB was the first transcription factor described to affect a distinct subset of DCs. In particular, disruption of the RelB locus results in an overall reduction in thymic DCs (which was shown to be driven by non-hematopoietic cells) and a selective reduction in splenic CD8$^-$ cDCs[139,140]. Meanwhile, CD8$^+$ cDC and pDC numbers were unaffected and were still able to stimulate T cell responses and produce IFNα *ex vivo*, respectively[140,141]. The second transcription factor implicated in CD11b$^+$ cDC development is interferon-regulatory factor Irf4. Similar to phenotypes found in RelB deficiency, loss of Irf4 results in a specific reduction in splenic CD11b$^+$ CD4$^+$ cDCs with no changes in cell numbers for CD8$^+$ cDCs and pDCs[142]. Additionally, GM-CSF-derived DCs from *Irf4$^{-/-}$* bone marrow are unable to induce antigen-stimulated T cells to produce IL-2[142]. Notch signaling transcription factor RBPJ has also been implicated in regulating the CD11b$^+$ cDC subset, however RBPJ seems to promote the survival and homeostasis of CD11b$^+$ cDCs, as opposed to their development[143].

CD8$^+$ cDCs. Despite being expressed in both CD8$^+$ and CD11b$^+$ cDCs, deletion of *Batf3* leads to a depletion specifically in the CD8$^+$ cDC subset, and not in precursor DC populations like pre-DCs[17,21]. Consequently, mice that lack Batf3 show a pronounced inability to cross-present to CD8$^+$ T cells[17]. Interestingly, the residual population of CD8$^+$ cDCs that remains in these mice consists solely of the non-canonical CD8$^+$ cDCs that lack several features of the canonical counterparts[20]. Two other proteins, inhibitory helix-loop-helix transcription factor Id2 and interferon-regulatory factor Irf8, have also been implicated in CD8$^+$ cDC lineage specification, but also have an indirect or dual role in the pDC lineage. Id2 is expressed on all cDCs, more so in CD8$^+$ than CD11b$^+$ subsets, but is not expressed on precursor cells[133,144]. Accordingly, mice that lack Id2 show a significant reduction in CD8$^+$ cDCs but not CD11b$^+$, whereas pDCs show an increase in numbers, in agreement with the fact that forced expression of Id2 leads to a decrease in pDCs in human cells[145]. Irf8 is expressed highly in CD8$^+$ cDCs and pDCs but not in CD11b$^+$ cDCs[146]. Unlike in Id2 knockout models, depletion of Irf8 leads to significant reductions in both CD8$^+$ cDCs and pDCs, while leaving CD8$^-$ cDCs relatively intact[147].

pDCs. Our lab has identified E-protein E2-2 as a specific and crucial regulator of pDC fate. The long isoform of E2-2 is specifically expressed in pDCs, but not cDCs (L. Grajkowska, unpublished). Complete deletion of E2-2 in adult mice leads to a complete loss of pDCs in bone marrow and spleen, and haploinsufficiency of E2-2 in mice is enough to impair pDC development[27]. E2-2 seems to regulate a cohort of transcription factors that have been shown to govern pDC fate decisions, such as Irf8 (as described above), Bcl11a, and Spi-B[27,148]. Adult mice deficient in Bcl11a within the hematopoietic system show decreases in pDCs but normal levels of cDCs and CDPs, while Spi-B has been shown to be an important factor in generating human pDCs and plays a role in murine pDC development and function[149-151]. Interestingly, E2-2 also works to repress cDC fate by suppressing *Id2* expression in complex with Eto family protein Mtg16[133].

While the last decade and a half has unveiled a number of transcriptional regulators involved in various aspects of DC development, no transcription factors have been identified that specifically promote cDC fate over pDC fate. Recently, Zbtb46 was found to be specifically expressed in the cDC lineage[152,153]. While it may become a useful tool for cDC identification *in vivo*, it is clear the transcription factor itself is largely dispensable for DC development[154]. Therefore, our complete knowledge of how exactly the bifurcation from the CDP level occurs still remains unclear.

Mycl1/L-myc

Mycl1 was originally discovered as an amplified gene in human small cell lung carcinoma[155]. Mycl1 is a member of the Myc oncogene family, which includes other more recognized members c-Myc and N-Myc. Similarly to its other family members, Mycl1 encodes three exons and contains a conserved carboxyl-terminal basic-helix-loops-helix (bHLH) zipper domain that interacts with other small bHLH proteins, thus allowing the heterodimer to bind to DNA E-box sequences[156,157]. While structurally similar, Mycl1 expression during development and its activity differ significantly from the other members in a context-dependent manner. For example, the *in vitro* transforming abilities of Mycl1 are weaker than that of c-Myc in rat fibroblasts[157]. *In vivo,* Mycl1 overexpression under the control of an immunoglobulin enhancer leads to T cell lymphoma, as opposed to B cell malignancies seen with c-Myc or N-Myc[158].

Furthermore, in stark contrast to mice deficient in c-Myc, mice that lack Mycl1 show no apparent phenotype and are viable and fertile[159].

Most studies on Mycl1 have focused on its role in cancer, while its role in the steady state still remains to be determined. Mycl1 is highly expressed in the developing murine brain, and to a lesser extent the developing kidney, lung, intestine, and adult intestine and lung[160]. While Mycl1 was initially not detected in the spleen, a closer look at the various cell types within the hematopoietic system shows that Mycl1 is highly and specifically expressed in DCs in both mice and human[132,161,162]. Given the unique expression pattern of Mycl1 and its relation to a family that has significant roles in proliferation, growth, and differentiation, we sought to explore the role of Mycl1 in DC development and function.

RESULTS

Mycl1$^{-/-}$ mice show normal DC numbers

In order to investigate the potential role of Mycl1 *in vivo*, we analyzed mice in which all three exons of the *Mycl1* gene was removed. As reported before using a different mouse model[159], no gross abnormalities were observed and mice were viable and fertile. Given the specific expression pattern of Mycl1 in DCs, we analyzed DC populations in the spleen, a lymphoid organ that has an abundant representation of DCs. Analysis of DC populations in the spleen showed normal cell numbers and frequencies for both types of cDCs as well as pDCs (Figure 2.2A-D). The only notable characteristic was a very slight downregulation of CD8α expression in CD11b^{-} cDCs, however this change was not significant (2.2A,E). Analysis of other lymphoid organs like the bone marrow and skin-draining lymph nodes also showed normal frequencies of both cDCs (Figure 2.3A) and pDCs (Figure 2.3C). Overall, there were no overt differences in DC populations in the steady state. This was true also for mice in which Mycl1 was specifically deleted in the DC compartment using the *CD11c-Cre* mouse strain (Figure 2.2F-G; Figure 2.3B,D).

While there did not seem to be drastic differences in the spleen, we investigated analogous DC populations in nonlymphoid tissues. Tissues like the intestine, lung, and skin constantly encounter foreign material, and therefore may highlight any development or functional phenotype not seen in steady-state lymphoid tissues. Analysis of the lamina propria of small intestine showed a slight overall decrease in cDC populations mainly in the small intestine (Figure 2.4A), but not in the large intestine (Figure 2.4B) or mesenteric lymph nodes (Figure 2.4C). Closer analysis of the subpopulations of cDCs showed a slight reduction in the proportion of CD103^{+} cDCs in the small intestine and large intestine, but not in CD11b^{+} CD103^{+} cDCs. In contrast, analysis of epidermal Langerhan cells (Figure 2.5A), dermal cDCs (Figure 2.5B), migratory cDCs in skin-draining lymph nodes (Figure 2.5C), and lung cDCs (Figure 2.6A-B) showed normal DC numbers and cDC subset proportions. Overall, we conclude that mice deficient in Mycl1 quantitatively display a normal DC phenotype in both lymphoid and nonlymphoid tissues.

Mycl1$^{-/-}$ mice show normal DC development and proliferation

Because mature DC numbers looked normal in the steady state, we decided to test the function of early DC progenitors by inducing DC development *in vitro* and *in vivo.* Flt3L is a key cytokine required for the development of DCs and administration *in vitro* and *in vivo* is sufficient to drive early progenitors to produce DCs[69]. To this end, we tested DC development *in vitro* by first culturing whole bone marrow suspensions from WT or *Mycl1*$^{-/-}$ mice in Flt3L-rich supernatant obtained from a Flt3L-secreting B16 melanoma cell line. As seen in Figure 2.7, *Mycl1*$^{-/-}$ bone marrow was able to produce a comparable proportion and number of cDCs and pDCs. Moreover, these DCs looked phenotypically similar by cell surface markers. We also administered Flt3L *in vivo* to test whether presence of other extracellular cues may affect *Mycl1*$^{-/-}$ DC development. Similar to what we see *in vitro, Mycl1*$^{-/-}$ mice were completely capable of driving DC development *in vivo* and generated the same frequencies of cDCs and pDCs compared to WT in the spleen (Figure 2.8A-B) and small intestine lamina propria (Figure 2.8C-D). This was also true for the bone marrow, skin-draining lymph nodes, and mesenteric lymph nodes (data not shown). Thus, Mycl1 does not affect Flt3L-induced DC development *in vitro* or *in vivo*.

In vivo, IL-12 administration increases the number of CD8$^+$ cDCs in WT mice and is sufficient to drive regeneration of CD8$^+$ cDCs in *Batf3*$^{-/-}$ mice that normally lack these cells in the steady state[163]. Thus, as another means to drive DC development *in vivo*, we also administered murine IL-12 to WT or *Mycl1*$^{-/-}$ mice and analyzed DC subsets in the spleen. As expected, we saw an increase in CD8$^+$ cDCs in the spleens of IL-12-treated WT mice versus PBS-treated (Figure 2.9B). We also saw an increase CD11b$^+$ cDCs (Figure 2.9B) along with an overall increase in cDC numbers (Figure 2.9A). However, *Mycl1*$^{-/-}$ mice responded similarly to WT mice, indicating that there was no defect in IL-12-induced DC development. The same was true for the bone marrow (data not shown).

While overall DC numbers did not change, it may be possible that Mycl1 affects mature DC turnover and that earlier progenitors are compensating for this change. Therefore, we tested the proliferation of mature DCs by measuring BrDU incorporation shortly after the initial pulse. As described before, splenic CD8$^+$ cDCs showed the highest proliferation rate compared to other DCs, while pDCs show the lowest (Figure 2.10). Comparison of WT and *Mycl1*$^{-/-}$ DC populations showed no difference in BrDU uptake. Thus, Mycl1 does not control the proliferation of DCs.

Mycl1$^{-/-}$ DCs show normal T cell responses

While Mycl1-deficient DCs do not seem to be phenotypically different from their WT counterparts, these observations do not preclude the possibility that Mycl1 may govern the function of these DCs. Because most of the subtle changes that we saw were restricted to the CD8^{+} and CD8^{+}-like cDCs, we sought to test their cross-presentation ability *in vivo*. Using OVA protein as an antigen source, we injected apoptotic, antigen-pulsed BALB/c splenocytes into WT or *CD11c-Cre Mycl1$^{fl/fl}$* 129 recipients and quantified the frequency of OVA-specific CD8^{+} T cells one week later. Because BALB/c and 129 express different MHC I haplotypes, only CD8^{+} cDCs from the recipient and not the donor are able to present to 129 T cells. Flow cytometric analysis of recipient spleens showed a trend of fewer antigen-specific CD8^{+} T cells generated, however this slight reduction was not significant (Figure 2.11).

In addition to using OVA, we also measured cross-presentation under more physiological conditions of a viral and bacterial infection. WT or *CD11c-Cre Mycl1$^{fl/fl}$* mice were infected with influenza virus and tetramer-specific CD8^{+} T cells in the lung, mediastinal lymph node, and spleen were measured 1 week later. As shown in Figure 2.12A, recipients show no change in virus-specific T cell numbers, nor did they show a significant change succumbing to the disease, as measured by weight loss (2.12B). WT or *Mycl1$^{-/-}$* mice were also infected with OVA-expressing *Listeria monocytogenes* and measured for OVA-specific T cell responses 1 week later. *Mycl1$^{-/-}$* mice exhibited no difference in proportion or number of tetramer-positive CD8^{+} T cells (Figure 2.12C). Overall, we conclude that mice deficient in Mycl1 still retain a normal ability to cross-present to CD8^{+} T cells.

Mycl1$^{-/-}$ CD8^{+} cDC gene expression is similar to Mycl1$^{+/+}$

Because we did not see any significant differences in DC development or DC function, we investigated whether there were changes in the genetic program of *Mycl1$^{-/-}$* DCs, again focusing on CD8^{+} cDCs. Hence, we performed microarray analysis on sorted WT and *Mycl1$^{-/-}$* splenic CD8^{+} cDCs. As shown in Figure 2.13, surprisingly little difference in expression pattern was seen between WT and *Mycl1$^{-/-}$* splenic CD8^{+} cDCs. Among the genes that were downregulated, Mycl1 came up as the top hit, validating the gene targeting. Genes that were upregulated upon Mycl1 encoded mainly immunoglobulin proteins. Of note, Mfsd2, which is a neighboring gene of Mycl1, was also upregulated, suggesting that the

deletion of the Mycl1 locus may have disrupted negative regulatory elements of *Mfsd2* transcription. Nevertheless, aside from Mycl1 itself, the overall genetic landscape of Mycl1-deficient splenic $CD8^+$ cDCs showed very little difference compared to that of WT splenic $CD8^+$ cDCs.

Overall, these results support the conclusion that Mycl1 does not impair the development, homeostasis, function, or genetic landscape of DCs.

DISCUSSION

Mycl1 is dispensable for DC development and function

Our current knowledge on how an early hematopoietic progenitor commits to the DC fate is still under active investigation. While several transcription factors have been identified to be crucial for DC development, we have yet to identify a single molecule that specifically regulates the cDC fate. Zbtb46 was indeed a prime candidate given its specific expression in pre-DCs and mature cDCs. Unfortunately Zbtb46-deficient cDCs seem to develop normally, indicating that it mostly does not play a role in cDC development[152,153]. Similar to Zbtb46, Mycl1 becomes increasingly expressed in the cDC lineage, instead starting from the CDP, and thus, was a potential candidate to regulate cDC fate decisions. However, our work has shown that Mycl1 is entirely dispensable for DC development and function. Analysis of DC proportions in spleen, skin-draining lymph nodes, epidermis, dermis, lung, small intestine LPL, large intestine LPL, and mesenteric lymph nodes show normal phenotypes as in WT mice. The only potential difference was in $CD8^+$ and $CD8^+$-like cDCs, and still the phenotype was quite subtle. Functionally, *Mycl1*$^{-/-}$ $CD8^+$ cDCs are capable of cross-presenting antigen from apoptotic cells, viral antigen, and bacterial antigen to $CD8^+$ T cells, with some variation between assays. Finally, the genomic expression pattern of *Mycl1*$^{-/-}$ $CD8^+$ cDCs only narrowly differs, with the biggest change in expression being in *Mycl1* transcripts.

Discrepancies on the functional role of Mycl1 in DCs

Another group has published work on the role of Mycl1 in dendritic cell development using a GFP knockin/knockout model of Mycl1[164]. While our conclusion that Mycl1 does not play a role in DC development corroborates with their results, our studies in the functional role of Mycl1 in DCs do not agree. Their microarray analysis performed on steady-state $CD8^+$ cDCs revealed a select number of Mycl1 targets involved in cell proliferation and apoptosis, and accordingly Mycl1-deficient cDCs showed a reduction in BrdU uptake. This is in contrast to our results, in which very few genes were downregulated and no difference was seen in proliferation. Additionally, KC et al show a deficiency in T cell priming during *L. monocytogenes* infection, along with protection against a lethal infection. This contradicts our

results, in which we do not see a difference in T cell priming under various conditions, including *L. monocytogenes* infection.

Several considerations can be taken into account in order to reconcile this clear discrepancy. The foremost difference between our studies and the studies of KC et al is the mouse model and gene targeting. Our mouse model deletes the entirety of the Mycl1 gene: exon 1, an untranslated region that may have regulatory elements in it; exon 2, which encodes the transactivation domain; and exon 3, which encodes the DNA/protein-binding bHLH and leucine zipper domain[165]. The mouse model of KC et al targets only the first coding exon (exon 2). Although unlikely, it is possible that a protein containing only exon 3 may have been transcribed and generated either dominant negative isoform or protein that aberrantly blocks DNA binding. Depending on the epitope of the antibody and the target sequence of the hybridized probe, this aberrant protein may have remained undetected and therefore interpreted as deficient in Mycl1 protein. Another main difference between our mouse models is the strain background. While our model remained on a 129 background, several experiments done by KC et al were done on C57BL/6, including the proliferation experiments. Indeed, mouse strain backgrounds do make a difference in phenotype in certain cases. For example, C57BL/6 are known to be more resistant to *L. monocytogenes* infection than other strains[166]. Furthermore, steady-state distributions of splenic WT 129 and C57BL/6 are slightly different, with the former often containing fewer $CD8^+$ cDCs than the latter (data not shown). Therefore, it may be possible that compensatory mechanisms in the 129 background not present in the C57BL/6 strain may have masked the phenotype that KC et al see. Technical differences may also account for the disparity in results specifically in the role of Mycl1 in T cell priming. In particular, we measured the priming of endogenous T cells, rather than transgenic OT I cells, which are particularly sensitive to OVA stimulation. Therefore, subtle differences that may not have reached significance in our hands may have been amplified using OT I cells. However, the most likely explanation for the lack of phenotype observed in our model is the genetic redundancy of Myc transcription factors. KC et al, while describing a reduced expression of c-Myc expression in mature DCs, still demonstrate some basal expression in mature DCs, especially in cDCs. It is likely that this basal expression of c-Myc is sufficient to compensate for lack of Mycl1 expression, and that abrogation of both Myc transcription factors would reveal the function of Mycl1 in cDCs.

Other potential roles of Mycl1 in DC biology

KC et al provide additional evidence for other roles that Mycl1 may play in DC function that we did not address. For example, they show that Mycl1 protein is maintained during inflammatory conditions and generally downregulates a genetic program induced by GM-CSF signaling. Additionally, they provide evidence for a potential connection with Irf8 regulation. The most striking phenotype of their Mycl1-deficient model is the resistance to a lethal infection by *L. monocytogenes,* which was due to the reduction of intracellular cell growth, and not due to reduced bacterial capture or DC viability, despite their claim that Mycl1 controls proliferation and survival of DCs. These observations collectively paint a very broad but disjointed role for Mycl1, which may mirror the broad regulatory role that other Myc family members encompass[167]. Nevertheless, it is clear from our studies and the studies of KC et al that Mycl1 alone, like Zbtb46, is dispensable for DC development in the steady state, and that the search for the cDC-specific transcription factor continues on.

MATERIALS AND METHODS

Animals

Mycl1$^{fl/fl}$ mice were made by Robert Eisenman and acquired from Jackson. To generate germ-line deletions, *Mycl1*$^{fl/fl}$ mice were bred to a *Prm-Cre* strain[168] that deletes in the male germline. To generate DC-specific deletion, *Mycl1*$^{fl/fl}$ mice were bred to *Itgax-Cre (CD11c-Cre)* developed in our lab[143]. All mice were on 129 backgrounds. BALB/c mice were acquired from Taconic. All animal studies were performed according to the investigator's protocol approved by the Institutional Animal Care and Use Committee of Columbia University.

Cell preparations

Spleen, thymus, and lymph nodes were minced and pressed through a nylon cell strainer to yield single cell suspensions and then subjected to red blood cell (RBC) lysis before being filtered. Bone marrow was prepared by flushing femurs and tibias with phosphate buffer saline (PBS) using a 27-gauge needle before RBC lysis. For lymphoid organ DC analysis, organs were digested with collagenase D (1 mg/mL) and DNAseI (20μg/mL) in for 30-60 min at 37°C prior to generating cell suspensions. Small intestine lamina propria lymphocytes were prepared as described before[131]. For epidermis/dermis DC analysis, dorsal and ventral earflaps were "floated" on HBSS and 4 u/mL Dispase for 90 min at 37°C to separate dermis and epidermis. Epidermis and dermis were minced and digested with collagenase D (400 u/mL) and DNaseI (100 μg/mL) for 45 min at 37°C with an additional 4 u/mL Dispase for the dermis. EDTA was added, and tissues were pressed into a cell strainer to yield single cell suspensions. For DC lung analysis, lungs were perfused with PBS and digested with collagenase D (400 u/mL). DC preparations were performed by Aleksey Chudnovskiy and Brandon Hogstad from the lab of Miriam Merad at Mount Sinai School of Medicine (NY, New York).

Flow cytometry

Cells were stained with the following fluorochrome- or biotin-conjugated antibodies from eBioscience or as indicated: anti-CD11c (N418), MHC II (M5/114.15.2), CD11b (M1/70), CD8α (53-6.7), CD103 (2E7),

B220 (RA3-6B2), mPDCA-1/Bst2 (Miltenyi Biotec), CD317/PDCA/Bst2 (Biolegend clone 927), CD24 (M1/69), TCRβ (H57-597), CD3 (17A2), CD4 (RM4-5 and GK1.5), CD44 (IM7), F4/80 (BM8), and CD45 (30-F11). Cell acquisition was done on LSR II (BD Biosciences) using FACSDiva (BD Biosciences) and analysis was done on FlowJo (Tree Star). DC analyses were performed by Aleksey Chudnovskiy and Brandon Hogstad from the lab of Miriam Merad at Mount Sinai School of Medicine (NY, New York).

***In vitro* BM-derived DC cultures**

Bone marrow cells were harvested as described above. RBC-lysed cells were plated in triplicates in a 24-well plate at 2 x 10^6 per well in DMEM/10% FCS and 20% supernatant from cultured Flt3L-secreting B16 melanoma cell lines. Suspension and adherent cells were harvested after 8 days and triplicates were pooled for counting and flow cytometric analysis.

Flt3L administration

Mice were injected intraperitoneally (i.p.) with 10 µg recombinant Flt3L-Fc (LakePharma) every 3 days (d0, d3) and analyzed on day 6 after initial treatment. Spleens, bone marrow, skin-draining lymph nodes, mesenteric lymph nodes, and small intestine were harvested for flow cytometry and prepared as described above for DC analysis.

IL-12 administration

Mice were injected i.p. with PBS or 0.5 µg murine IL-12 (PeproTech) for four consecutive days and analyzed 6 days after initial treatment. Spleens and bone marrow were harvested for flow cytometry and prepared as described above for DC analysis.

BrDU incorporation

For BrDU labeling, mice were injected i.p. with 2 mg of BrDU (Sigma) or PBS and analyzed 4 hours later for flow cytometry. Spleens were prepared, as described above, and single cell suspensions were stained for cell surface markers, fixed, permeabilized, and stained for BrDU using the APC BrDU Flow Kit from BD Biosciences as per manufacturer's instructions.

***In vivo* cross presentation assay**

Chicken ovalbumin protein (Sigma) was hypertonically pulsed into BALB/c (H-2^d) splenocytes and lymph node cells. Briefly, cells were incubated with a hypertonic solution of 10% polyethylene glycol, 0.5 M sucrose, 10 mM HEPES, and 10 mg/mL ovalbumin in RPMI buffer for 10 minutes at 37°C and then immediately flushed with a hypotonic solution of 40% water in RPMI. Cells were incubated for 2 min at 37°C and washed with cold PBS. Cells were irradiated with 2000cGy and injected into *Mycl1*$^{fl/fl}$ or *CD11c-Cre Mycl1*$^{fl/fl}$ (H-2^b) at a dose of ~40 x 10^6 cells per recipient.

Influenza infection

Mice were infected with a sublethal dose (500 $TCID_{50}$) of PR8 H1N1 virus. Spleens, lungs, and mediastinal lymph nodes were analyzed 7 days later for T cell analysis. Antigen-specific $CD8^+$ T cells were identified using a mix of PE-conjugated hemagluttinin (HA) or polymerase (PA) peptide-loaded MHC I tetramer complexes (MBL International). Infection, cell preparations, and flow cytometry were performed in collaboration with Damian Turner from the lab of Donna Farber at Columbia University Medical Center.

***Listeria monocytogenes* infection**

Mice were infected with 5 x 10^4 CFU of *Listeria monocytogenes* expressing OVA in PBS and injected intravenously. Spleens were analyzed 8 days later for T cell analysis. Antigen-specific $CD8^+$ T cells were identified using a PE-conjugated SIINFEKL peptide-loaded MHC I tetramer complexes (Beckman Coulter). Infection was performed in collaboration with Simone Nish from the lab of Steven Reiner at Columbia University Medical center.

Gene expression analysis

Splenocytes from *Mycl1*$^{+/+}$ or *Mycl1*$^{-/-}$ were depleted of lymphoid and erythroid cells by negative selection using MACS columns and the following biotinylated antibodies: anti-CD19 (eBio1D3), Gr-1 (RB6-8C5), CD3 (17A2), Ter119 (TER-119), CD49b (DX5). $CD8^+$ cDCs were sorted as $CD11c^{hi}$ $MHCII^+$ $CD11b^-$ $CD8\alpha^+$ $Bst2^-$ $B220^-$ on BD Influx (BD Biosciences) and RNA was isolated by Trizol (Life Technologies)

extraction per manufacturer's instructions. Samples were reverse-transcribed, labeled, and hybridized onto GeneChip Mouse Gene 1.0 ST array (Affymetrix) according to manufacturer's instructions. RMA-normalized gene expression values were analyzed using NIA Array software[169].

Statistical analysis

Statistical significance was estimated with unpaired, two-tailed Student's T test, unless otherwise indicated.

CHAPTER II FIGURES

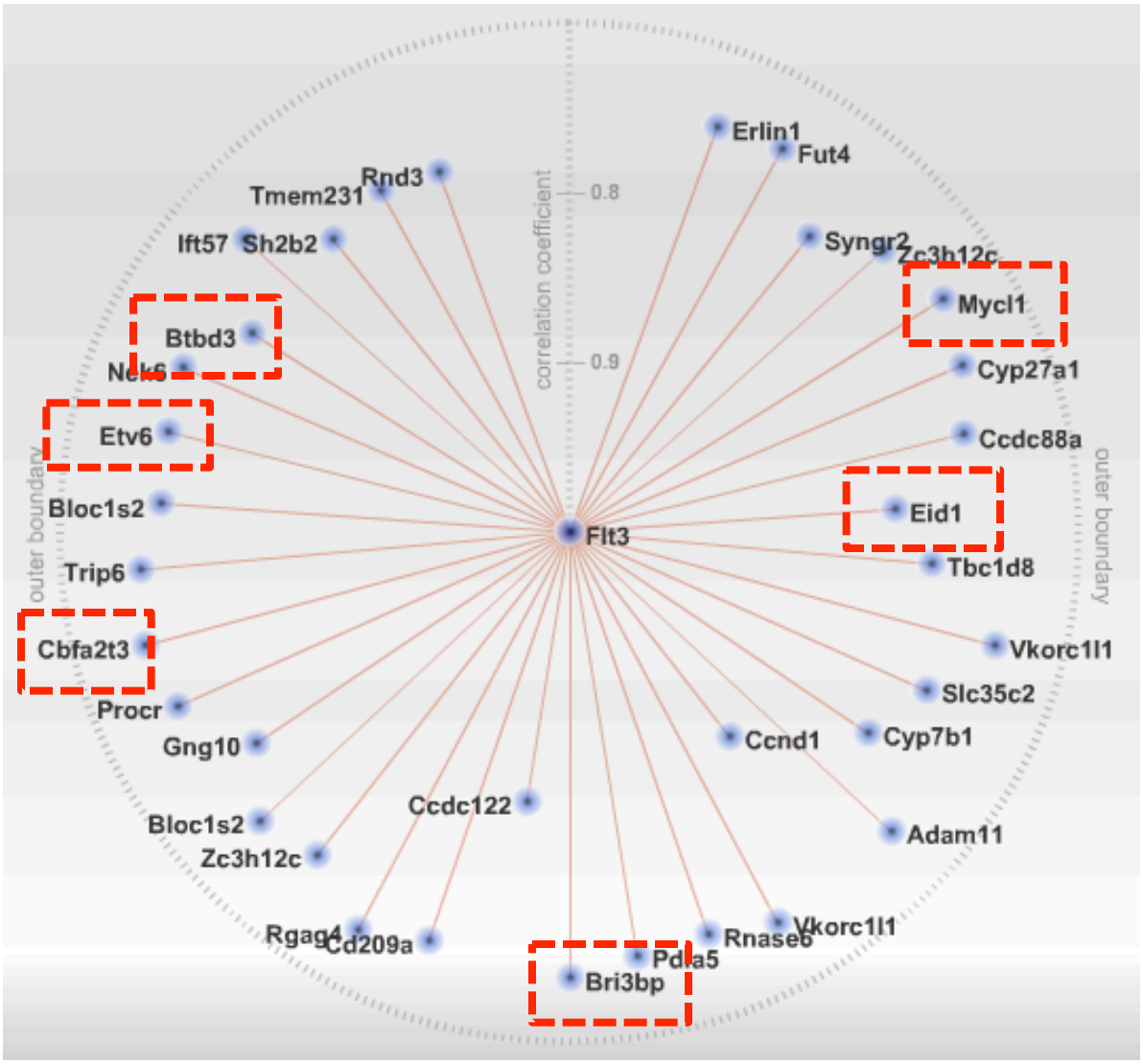

Figure 2.1. Genes correlated with Flt3 expression.

Shown are murine genes found to be correlated with the expression pattern of Flt3 within the hematopoietic system using the Immgen database (ref. 132). Genes outlined in red indicate described or putative transcription factors. Distance of gene from center indicates tightness of correlation, with the closest genes being more tightly correlated. Correlation was calculated using Pearson correlation.

Figure 2.2. Mycl1-deficient mice show normal DC numbers in the spleen.

(A) Representative staining profiles of splenic cDC populations in naïve *Mycl1*$^{+/+}$ (WT) and *Mycl1*$^{-/-}$ (KO) . CD11b^{+} and CD8^{+} cDC populations are labeled. Numbers in FACS plots indicate percent of gated population. Mean fluorescent intensity (MFI) numbers above histogram indicates CD8α MFI among CD11b^{-} population. Percentages in histogram indicate proportion of CD8^{+} cDCs.

(B) Representative staining profiles of splenic pDC populations in naïve *Mycl1*$^{+/+}$ (WT) and *Mycl1*$^{-/-}$ (KO) mice.

(C) Absolute numbers (top row) and frequencies (bottom row) of total cDCs and cDC subsets as identified in (A) (mean ± SD, n = 4).

(D) Absolute number (top row) and frequency (bottom row) of pDCs identified in (B) (mean ± SD, n = 4).

(E) Pair-wise comparison of CD8α MFI among CD11b^{-} population, as described in (A). Statistics were analyzed using paired two-tailed Student's t-test.

(F) Representative staining profiles of splenic cDC populations in naïve *Mycl1*$^{fl/fl}$ (WT) and *CD11c-Cre*$^{+/-}$ *Mycl1*$^{fl/fl}$ (CKO) mice. Numbers in FACS plots indicate percent of gated population. Mean fluorescent intensity (MFI) numbers above histogram indicates CD8α MFI among CD11b^{-} population. Percentages in histogram indicate proportion of CD8^{+} cDCs. Data is representative of 3 experiments.

(G) Representative staining profiles of splenic pDC populations in naïve *Mycl1*$^{fl/fl}$ (WT) and *CD11c-Cre*$^{+/-}$ *Mycl1*$^{fl/fl}$ (CKO) . Data is representative of 3 experiments.

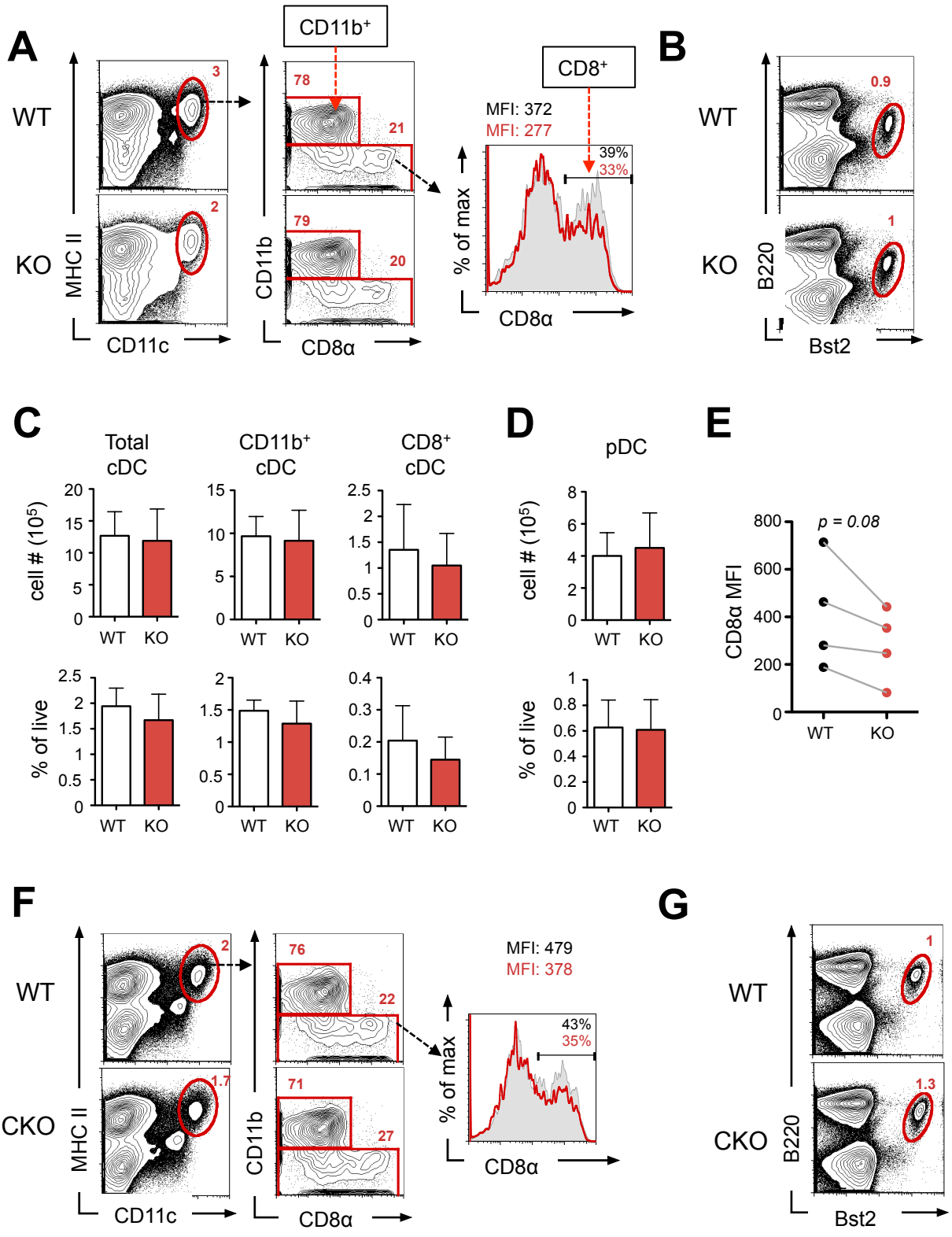
A
WT
KO
MHC II
CD11c
3
2
CD11b⁺
78
21
79
20
CD11b
CD8α
CD8⁺
MFI: 372
MFI: 277
39%
33%
% of max
CD8α
B
WT
KO
B220
Bst2
0.9
1
C
Total cDC
CD11b⁺ cDC
CD8⁺ cDC
cell # (10⁵)
% of live
WT
KO
D
pDC
cell # (10⁵)
% of live
E
CD8α MFI
p = 0.08
F
WT
CKO
MHC II
CD11c
2
1.7
76
22
71
27
CD11b
CD8α
MFI: 479
MFI: 378
43%
35%
% of max
CD8α
G
WT
CKO
B220
Bst2
1
1.3

Figure 2.3. Mycl1-deficient mice show normal DC numbers in other lymphoid tissues.

(A) Representative staining profiles of cDC populations in *Mycl1*$^{+/+}$ (WT) and *Mycl1*$^{-/-}$ (KO) bone marrow and skin-draining lymph nodes (inguinal, brachial, axillary, cervical). Numbers indicate percent of gated population. Resident cDCs are identified as CD11c^{hi} MHCII^{+} and migratory cDCs as CD11c^{+} MHCII^{hi}. CD11b^{+} and CD11b^{-} cDCs are shown. Data is representative of 2-3 experiments.

(B) Representative staining profiles of cDC populations in *Mycl1*$^{fl/fl}$ (WT) and *CD11c-Cre*$^{+/-}$ *Mycl1*$^{fl/fl}$ (CKO), as in (A). Bone marrow data is representative of one experiment, while lymph node data is representative of 3 independent experiments.

(C) Representative staining profiles of pDC populations in *Mycl1*$^{+/+}$ (WT) and *Mycl1*$^{-/-}$ (KO) bone marrow and skin-draining lymph nodes. Data is representative of 2-3 independent experiments.

(D) Representative staining profiles of pDC populations in *Mycl1*$^{fl/fl}$ (WT) and *CD11c-Cre*$^{+/-}$ *Mycl1*$^{fl/fl}$ (CKO). Bone marrow data is representative of one experiment, while lymph node data is representative of 3 independent experiments.

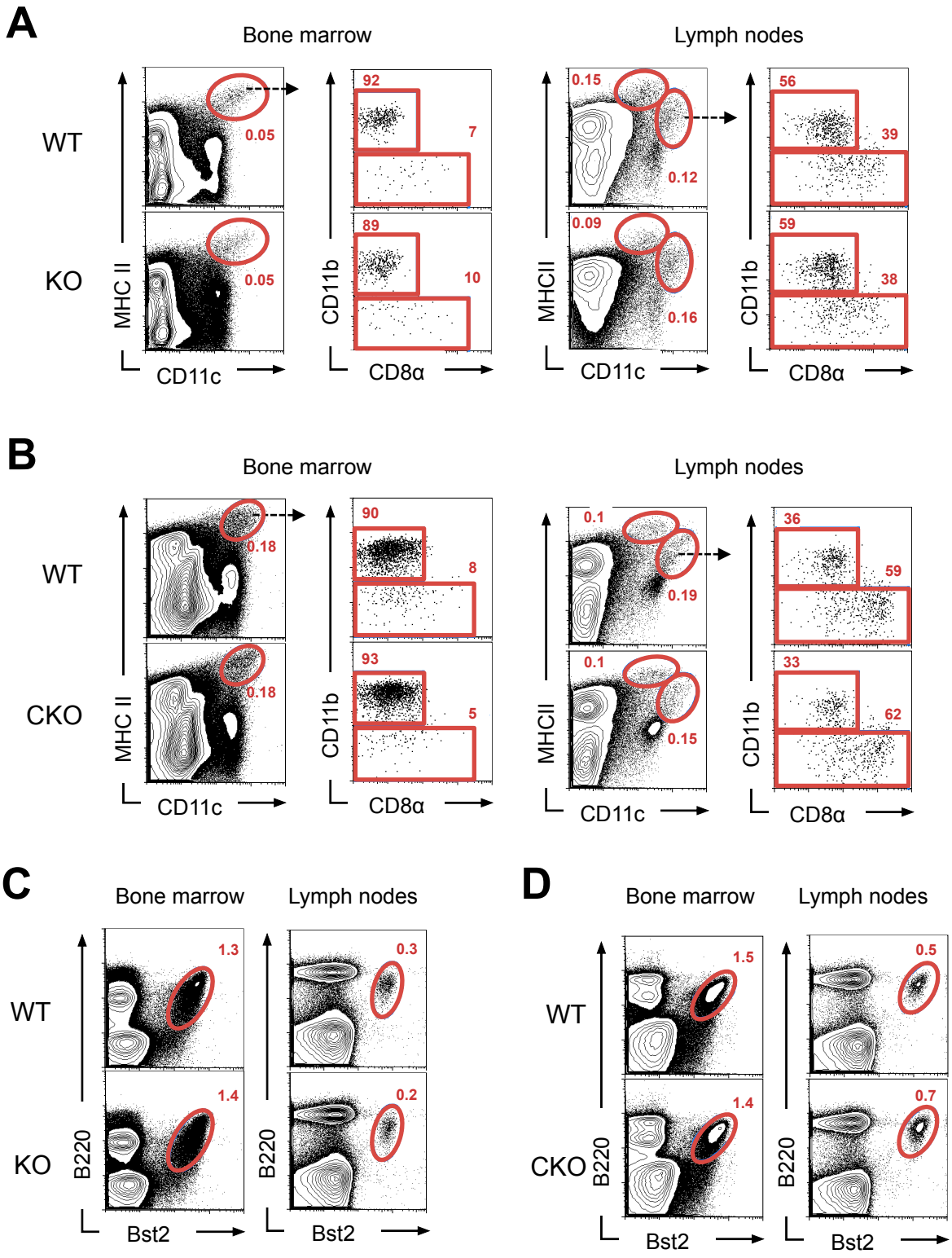
A
Bone marrow
Lymph nodes
WT
KO
MHC II
CD11c
CD11b
CD8α
MHCII
0.05
0.05
92
7
89
10
0.15
0.12
0.09
0.16
56
39
59
38
B
Bone marrow
Lymph nodes
WT
CKO
0.18
0.18
90
8
93
5
0.1
0.19
0.1
0.15
36
59
33
62
C
Bone marrow
Lymph nodes
WT
KO
B220
Bst2
1.3
1.4
0.3
0.2
D
Bone marrow
Lymph nodes
WT
CKO
1.5
1.4
0.5
0.7

Figure 2.4. Mycl1-deficient mice show slight reduction of DC numbers in the small intestine.

(A) Representative staining profile of cDCs isolated from small intestine lamina propria lymphocytes (LPL) of *Mycl1*$^{+/+}$ (WT) and *Mycl1*$^{-/-}$ (KO) mice. Plots are pre-gated on CD45^{+} cells. Numbers show percent of gated population. Data is representative of 2 independent experiments.

(B) Representative staining profiles of cDCs isolated from large intestine LPL as in (A).

(C) Representative staining profiles of cDCs isolated from mesenteric lymph nodes (LN) as in (A)

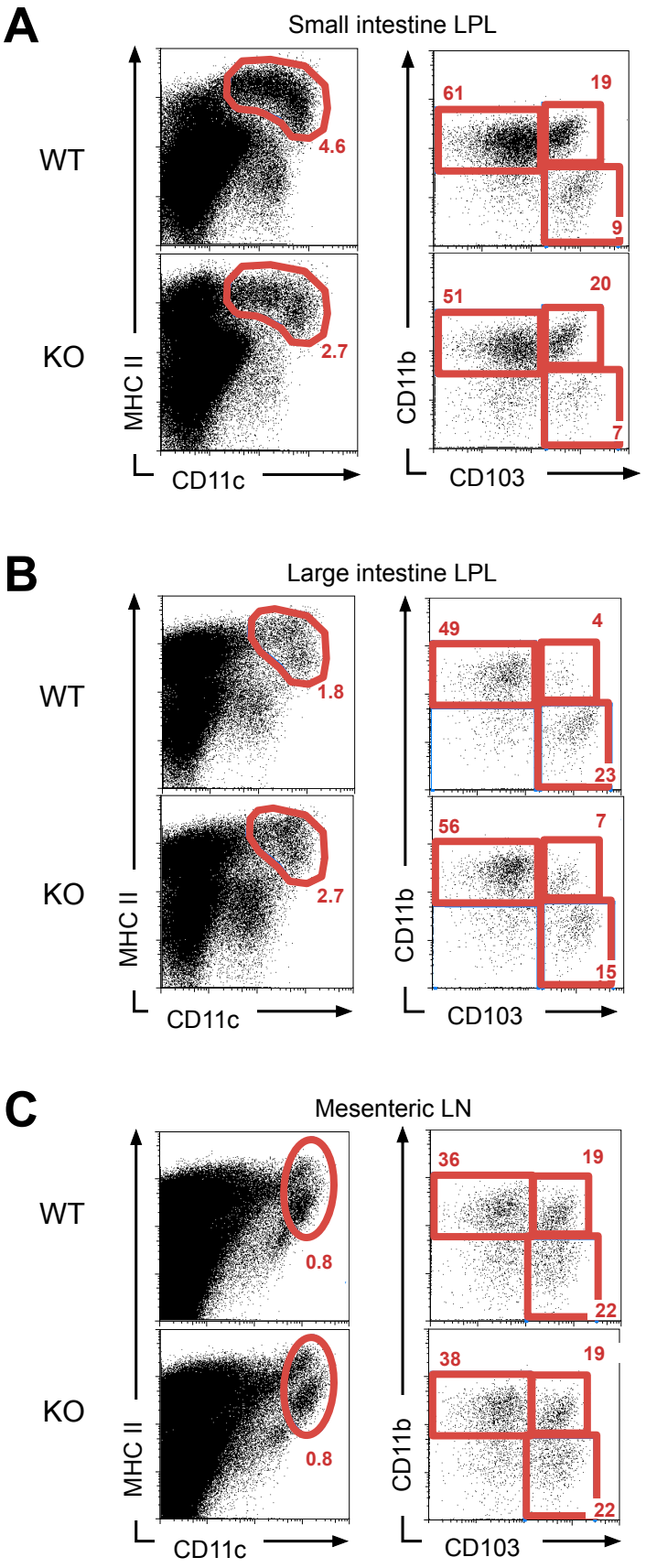
A
Small intestine LPL
WT
KO
MHC II
CD11c
4.6
2.7
CD11b
CD103
61
19
9
51
20
7
B
Large intestine LPL
WT
KO
MHC II
CD11c
1.8
2.7
CD11b
CD103
49
4
23
56
7
15
C
Mesenteric LN
WT
KO
MHC II
CD11c
0.8
0.8
CD11b
CD103
36
19
22
38
19
22

Figure 2.5. Mycl1-deficient mice show normal DC numbers in the dermis and epidermis.

(A) Representative staining profiles of epidermal Langerhan cells (LC) in *Mycl1*$^{+/+}$ (WT) and *Mycl1*$^{-/-}$ (KO) mice. Plots are pre-gated on CD45^{+} cells. Numbers show percent of gated population as mean ± SD, n = 2-3.

(B) Representative staining profiles of dermal DCs in WT and KO mice. Plots are pre-gated on CD45^{+} MHCII^{+} F4/80^{-} SSC^{lo} cells. Numbers show percent of gated population as mean ± SD, n = 2-3.

(C) Representative staining profiles of migratory DCs in WT and KO skin-draining lymph nodes (brachial, inguinal, and popliteal). Plots are pre-gated on CD11c^{+} MHCII^{hi} cells. Three populations of DCs are shown and are marked in WT graphs: migratory CD103^{+} cDCs (i), migratory LCs (ii), and migratory CD11b^{+} cDCs (iii). Numbers show percent of gated population as mean ± SD, n = 2-3.

Analyses were performed by A. Chudnovskiy and B. Hogstad.

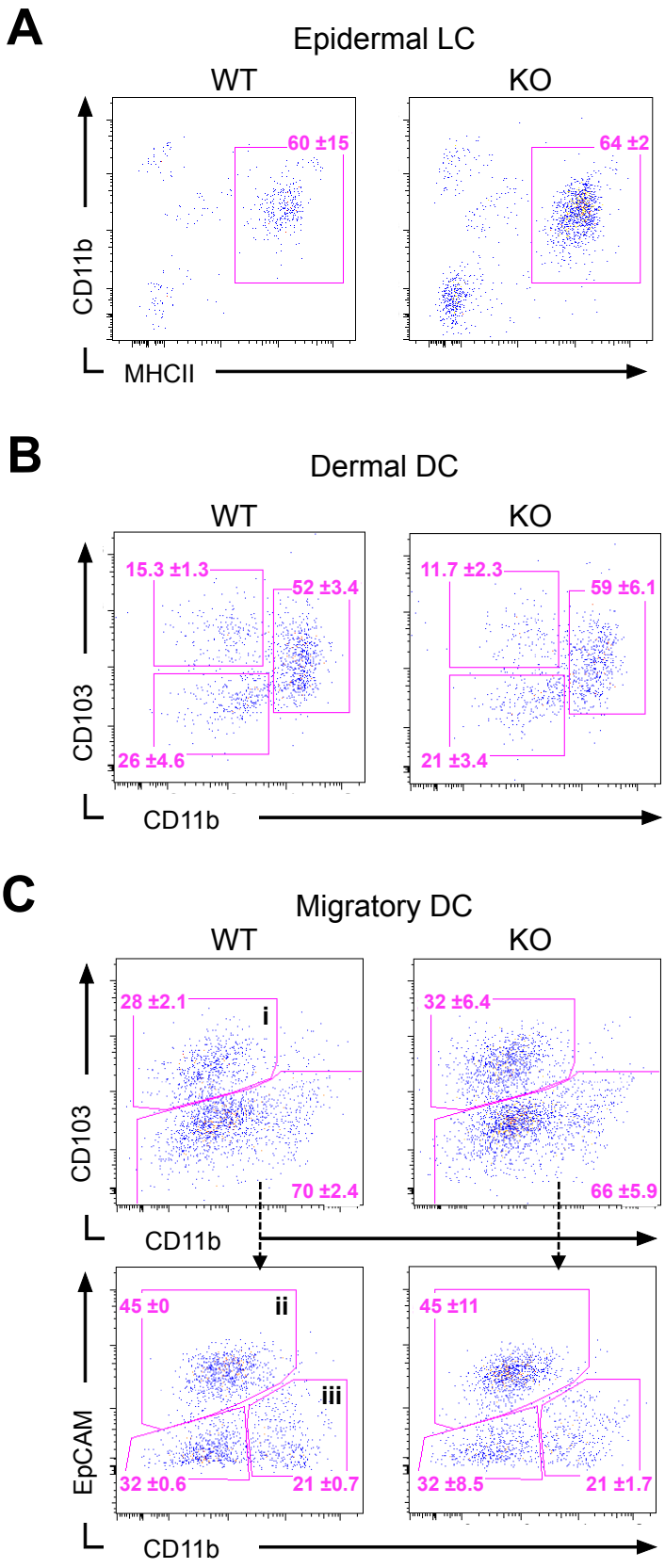
A
Epidermal LC
WT
KO
60 ±15
64 ±2
CD11b
MHCII
B
Dermal DC
WT
KO
15.3 ±1.3
52 ±3.4
26 ±4.6
11.7 ±2.3
59 ±6.1
21 ±3.4
CD103
CD11b
C
Migratory DC
WT
KO
28 ±2.1
i
70 ±2.4
32 ±6.4
66 ±5.9
CD103
CD11b
45 ±0
ii
iii
32 ±0.6
21 ±0.7
45 ±11
32 ±8.5
21 ±1.7
EpCAM
CD11b

Figure 2.6. Mycl1-deficient mice show normal DC numbers in the lung.

(A) Representative gating strategy for identifying $CD103^+$ and $CD11b^+$ cDC populations in the lung.

(B) Representative staining profiles of lung cDCs in *Mycl1*$^{+/+}$ (WT) and *Mycl1*$^{-/-}$ (KO) mice. Plots are pre-gated as shown in (A). Numbers show percent of gated population as mean ± SD, n = 2-3.

Analyses were performed by A. Chudnovskiy and B. Hogstad.

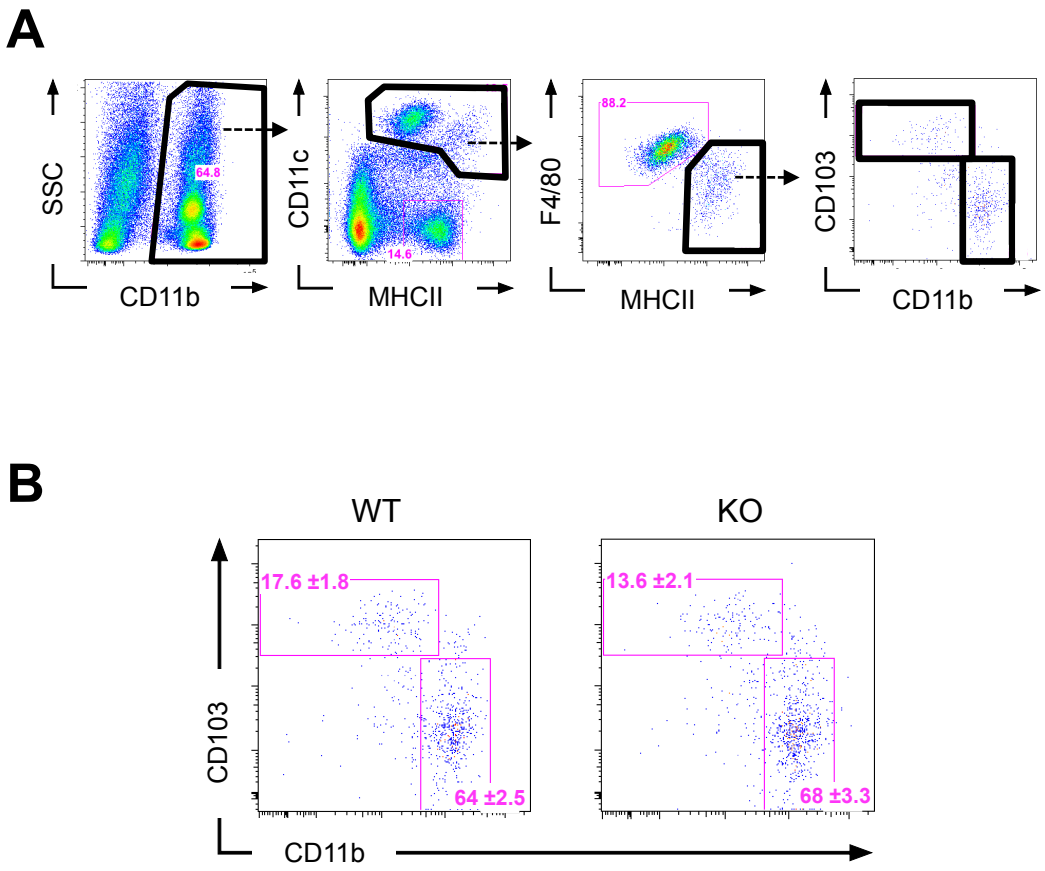
A
SSC
CD11b
64.8
CD11c
MHCII
14.6
F4/80
MHCII
88.2
CD103
CD11b
B
WT
KO
CD103
CD11b
17.6 ±1.8
64 ±2.5
13.6 ±2.1
68 ±3.3

Figure 2.7. Mycl1-deficient mice show normal DC numbers in Flt3L-driven development *in vitro*.

Whole bone marrow from naïve *Mycl1*$^{+/+}$ (WT) and *Mycl1*$^{-/-}$ (KO) mice was cultured 20% Flt3L-rich supernatant for 8 days. Shown are representative staining profiles of cDC subsets pre-gated on CD11c^{+} MHCII^{+} (left) and pDC subsets pre-gated on B220^{+} cells. Numbers on plot indicate fraction of cells within gated population. Numbers below are absolute total live cell numbers from each condition.

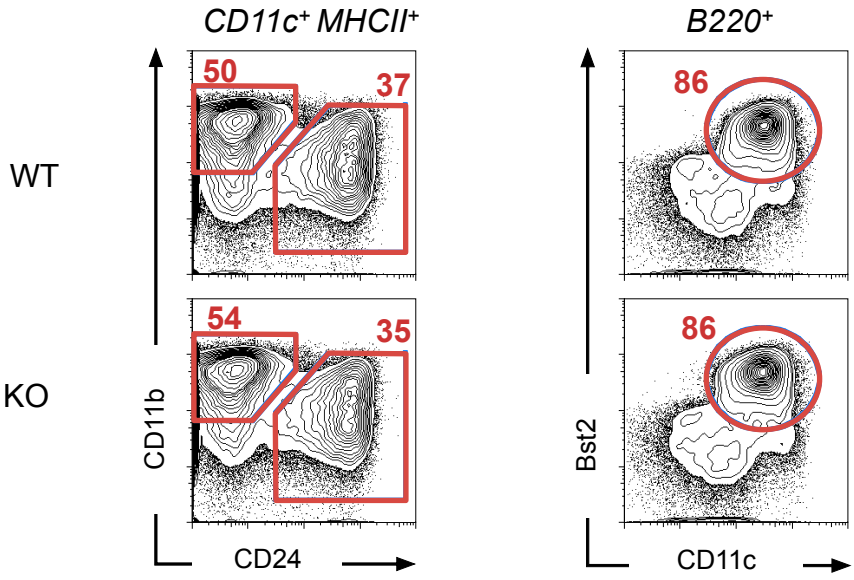

WT: 1.6 x 10^6 cells
KO: 1.3 x 10^6 cells

Figure 2.8. Mycl1-deficient mice show normal DC numbers in Flt3L-driven development *in vivo*.

Mycl1$^{+/+}$ (WT) and *Mycl1*$^{-/-}$ (KO) mice were injected intraperitoneally with 2 doses of 10 μg of Flt3L every three days and analyzed 6 days after initial treatment.

(A) Representative staining profiles of cDCs isolated from spleens of WT and KO mice. Numbers show percent of gated population.

(B) Frequencies of total cDC (top) and cDC subset (bottom) expansion, as gated in (A). CD11b^{-} CD8^{-} population was not included in analysis. Graphs are shown as mean of 3 animals per condition.

(C) Representative FACS plots of cDCs isolated from small intestine lamina propria lymphocytes (LPL) of WT and KO mice. Numbers show percent of gated population.

(D) Frequencies of total cDC (top left) and cDC subset (top right, bottom) expansion, as gated in (C). CD11b^{-} CD103^{-} population was not included in analysis. Graphs are shown as mean of 3 animals per condition.

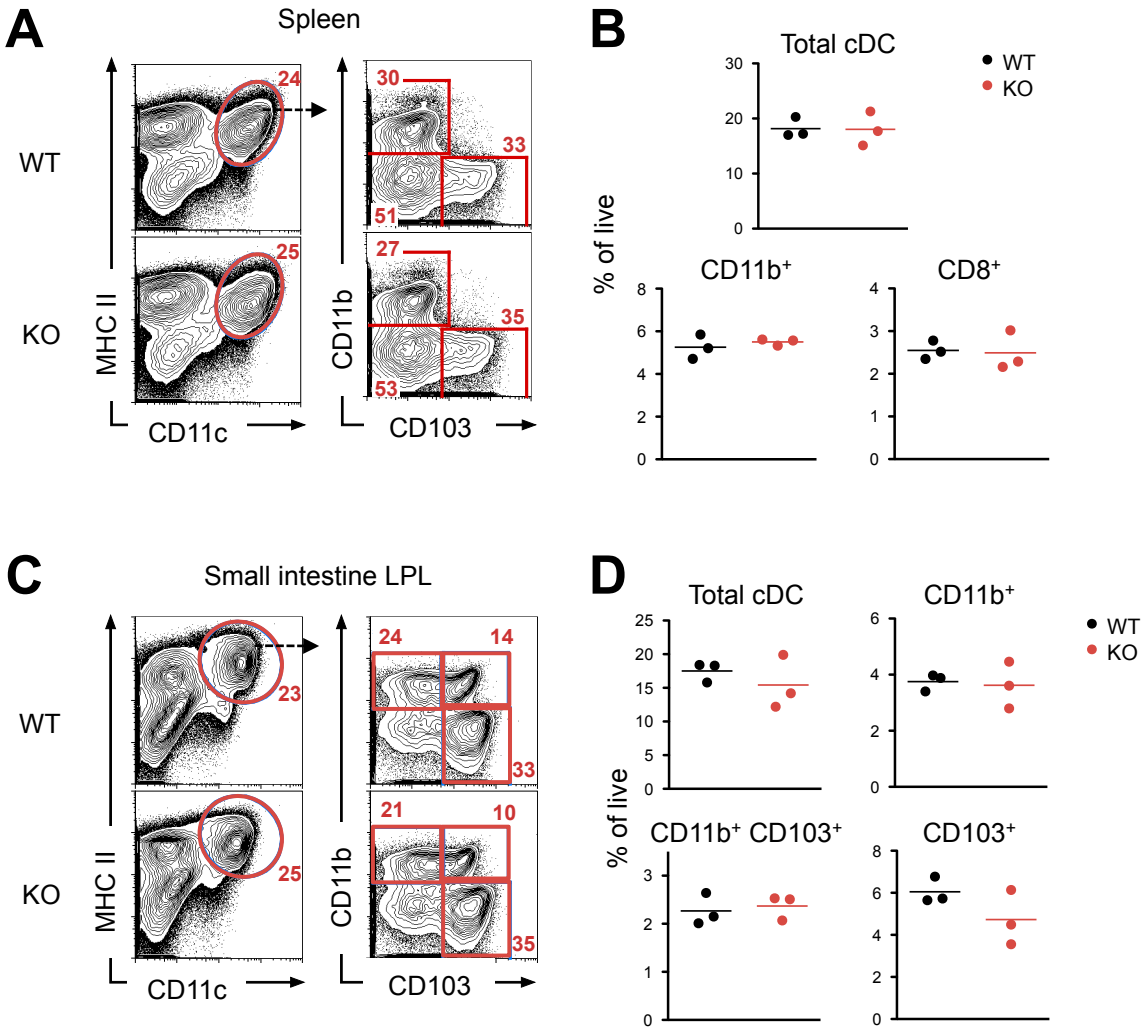
A
Spleen
WT
KO
MHC II
CD11c
CD11b
CD103
24
25
30
33
51
27
35
53
B
Total cDC
WT
KO
% of live
CD11b+
CD8+
C
Small intestine LPL
23
25
24
14
33
21
10
35
D
Total cDC
CD11b+
CD11b+ CD103+
CD103+

Figure 2.9. Mycl1-deficient mice show normal DC numbers in IL-12-driven development *in vivo*.

Mycl1$^{+/+}$ (WT) and *Mycl1*$^{-/-}$ (KO) mice were injected intraperitoneally with PBS or 0.5 µg of murine IL-12 once a day for 4 days and analyzed 6 days after initial treatment.

(A) Frequencies of total cDC from WT and KO spleen, gated as CD11c^{hi} MHCII^{+}. Graphs are shown as mean of 2-3 animals per condition.

(B) Frequencies of cDC subsets from WT and KO spleen, pre-gated as CD11c^{hi} MHCII^{+}. Graphs are shown as mean of 2-3 animals per condition.

A

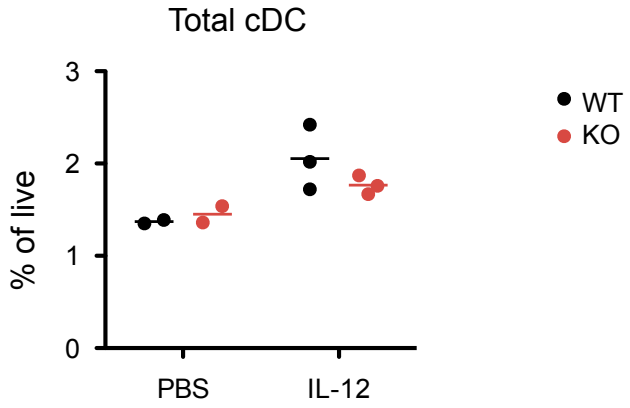
Total cDC
% of live
3
2
1
0
PBS
IL-12
WT
KO

B

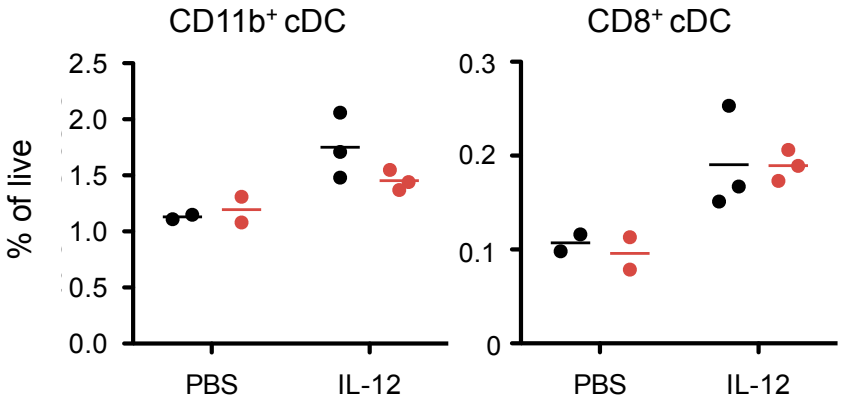
CD11b+ cDC
CD8+ cDC
% of live
2.5
2.0
1.5
1.0
0.5
0.0
0.3
0.2
0.1
0
PBS
IL-12
PBS
IL-12

Figure 2.10. Mycl1-deficient mice show normal proliferation rates.

Mycl1$^{+/+}$ (WT) and *Mycl1*$^{-/-}$ (KO) cells were labeled *in* vivo by injecting mice intraperitoneally with 2 mg of BrDU. Mice were sacrificed 4 hours later and spleens were analyzed for BrDU incorporation. Shown are graphs depicting the percentage of cells that have incorporated BrDU within each indicated cell population. Graphs are shown as mean of 5 animals per condition.

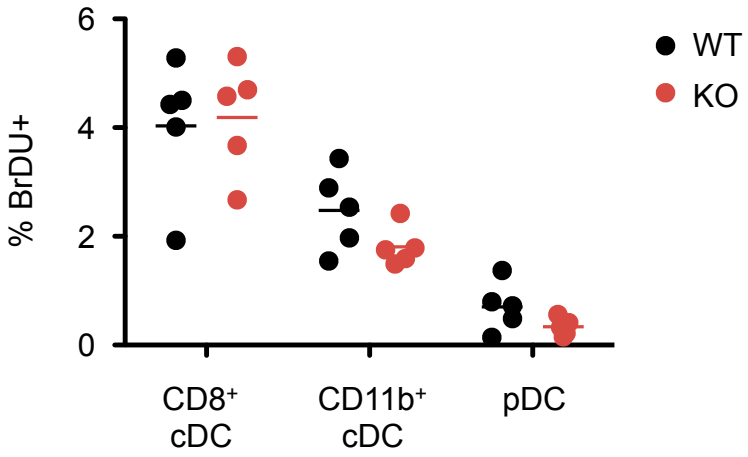
6
4
2
0
% BrDU+
WT
KO
CD8+
cDC
CD11b+
cDC
pDC

Figure 2.11. Mycl1-deficient mice show normal cross-presentation of antigen from apoptotic cells.

Apoptotic ovalbumin (OVA)-pulsed BALB/c cells were injected into *Mycl1*$^{fl/fl}$ (WT) and *Mycl1*$^{fl/fl}$ (CKO) and analyzed 7 days after transfer for OVA-specific CD8$^+$ T cells.

(A) Representative staining profiles of CD8$^+$ T cells from immunized mice. Number in FACS plot indicates percent of tetramer-positive (and thus OVA-specific) cells out of total CD8$^+$ T cells in spleen.

(B) Percent of tetramer-positive cells out of total CD8$^+$ T cell population (left) and absolute numbers (right) of tetramer-positive cells in splenic leukocytes. Graphs are shown as mean of 4 animals per condition.

A

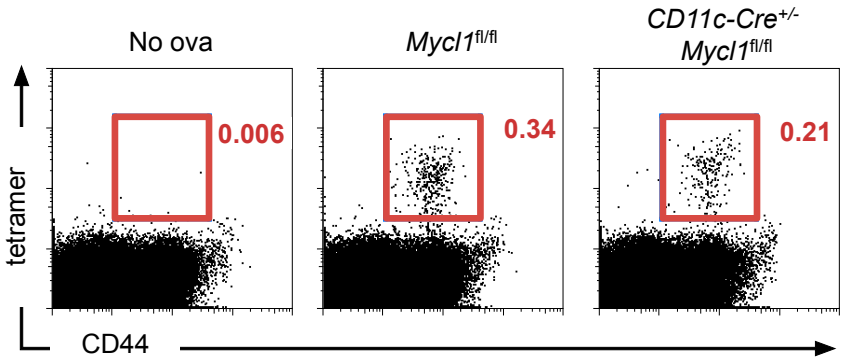
No ova
Mycl1fl/fl
CD11c-Cre+/-
Mycl1fl/fl
0.006
0.34
0.21
tetramer
CD44

B

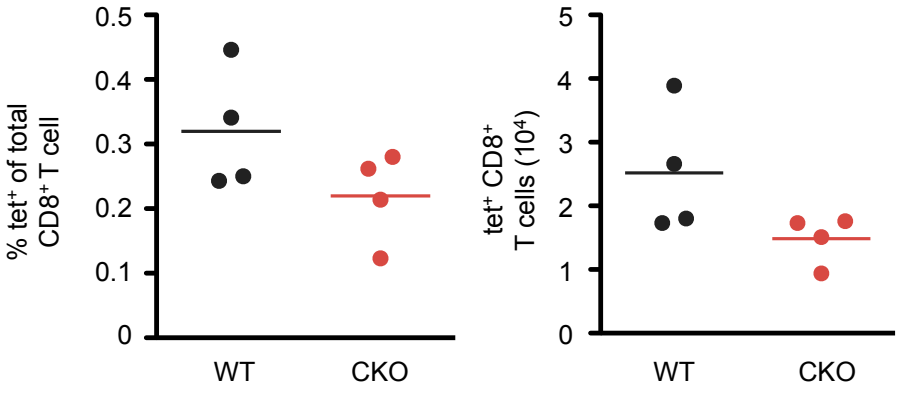
% tet+ of total CD8+ T cell
0.5
0.4
0.3
0.2
0.1
0
WT
CKO
tet+ CD8+ T cells (10^4)
5
4
3
2
1
0
WT
CKO

Figure 2.12. Mycl1-deficient mice show normal cross-presentation during viral and bacterial infections.

(A) *Mycl1*$^{fl/fl}$ (WT) and *Mycl1*$^{fl/fl}$ (CKO) mice were infected with a sublethal dose of influenza virus and analyzed after 7 days for viral antigen-specific CD8$^+$ T cells. Shown are percentages of tetramer-positive (viral antigen-specific) cells out of total CD8$^+$ T cells within lungs, spleens, and mediastinal lymph nodes. Cells were gated on CD8$^+$ CD11a$^+$ tet$^+$. Graphs show data as mean from 3 animals per condition.

(B) Time course of weight loss of mice in (A) after infection.

(C) *Mycl1*$^{+/+}$ (WT) and *Mycl1*$^{-/-}$ (KO) mice were infected with *Listeria monocytogenes* expressing OVA at a sublethal dose of 5 x 10^4 CFU and analyzed after 8 days for SIINFEKL tetramer-positive CD8$^+$ T cells. Shown are percentages of tetramer-positive cells out of total CD8$^+$ T cells (left) and absolute numbers of tetramer-positive CD8$^+$ T cells (right). Cells were gated on B220$^-$ TCRb$^+$ CD8$^+$ CD44$^+$ tet$^+$. Graphs show data as mean from 4-5 animals per condition.

Influenza infection and cell analysis were performed by D. Turner. Listeria infection was performed by S. Nish.

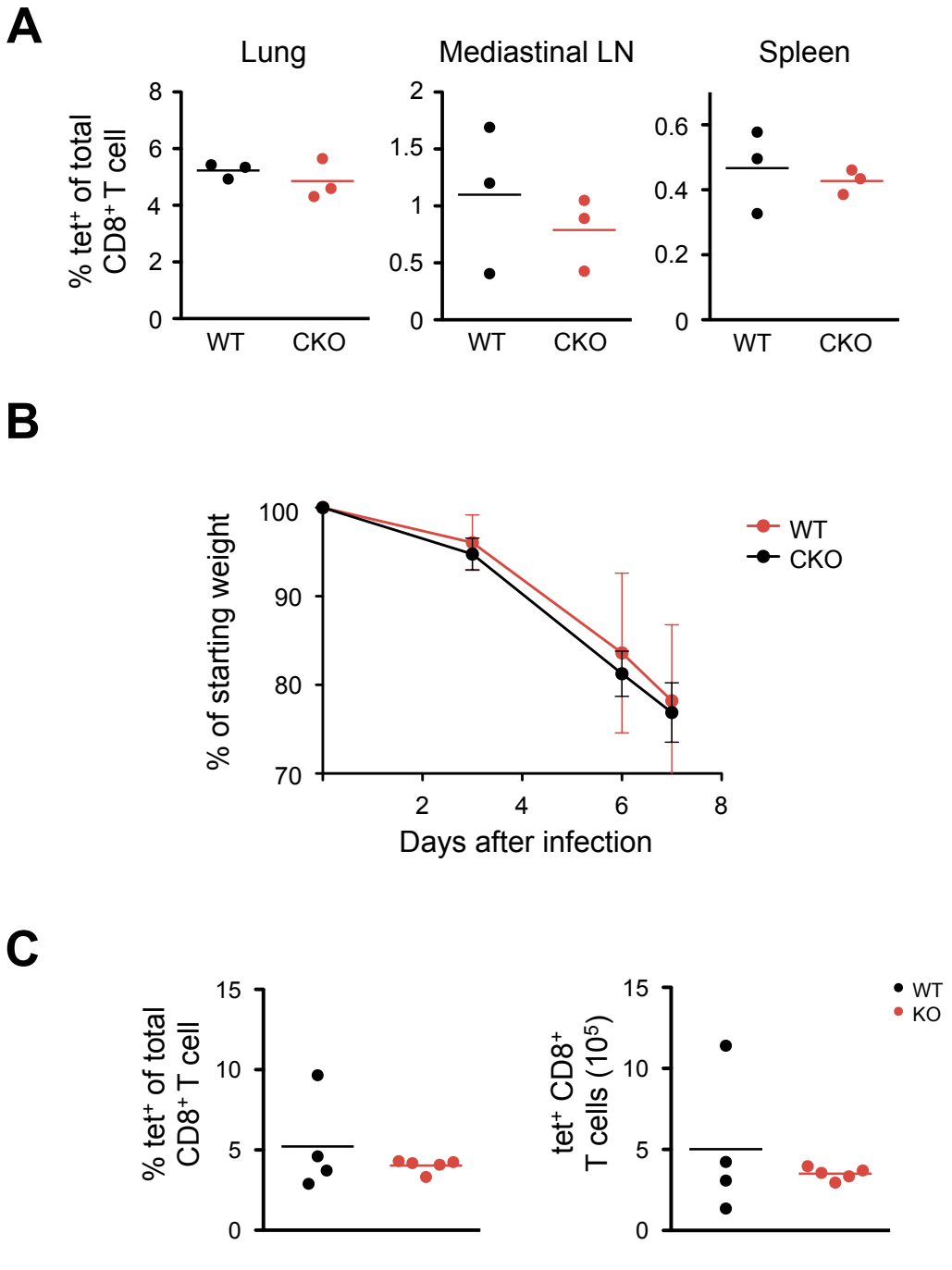
A
Lung
Mediastinal LN
Spleen
% tet+ of total CD8+ T cell
8
6
4
2
0
2
1.5
1
0.5
0
0.6
0.4
0.2
0
WT
CKO
WT
CKO
WT
CKO
B
% of starting weight
100
90
80
70
2
4
6
8
Days after infection
WT
CKO
C
% tet+ of total CD8+ T cell
15
10
5
0
tet+ CD8+ T cells (10^5)
15
10
5
0
WT
KO

Figure 2.13. Mycl1-deficient CD8$^+$ cDCs show minimal change in gene expression.

Mycl1$^{+/+}$ and *Mycl1*$^{-/-}$ splenic DCs were enriched from total splenocytes by MACS depletion and CD8$^+$ cDC populations were sorted for RNA extraction. RNA was prepared for hybridization onto Affymetrix GenChip Mouse Gene 1.0 ST Array and analyzed for differential gene expression using the NIA Array online software tool (ref. 169). Shown is a scatter plot of log intensity comparing gene expression between Mycl1-deficient and wild-type mice. Red dots signify overexpressed genes and green dots signify underexpressed genes upon Mycl1 depletion that have more than a two-fold change in expression. Highlighted genes are indicated. False discovery rate was set at <0.05.

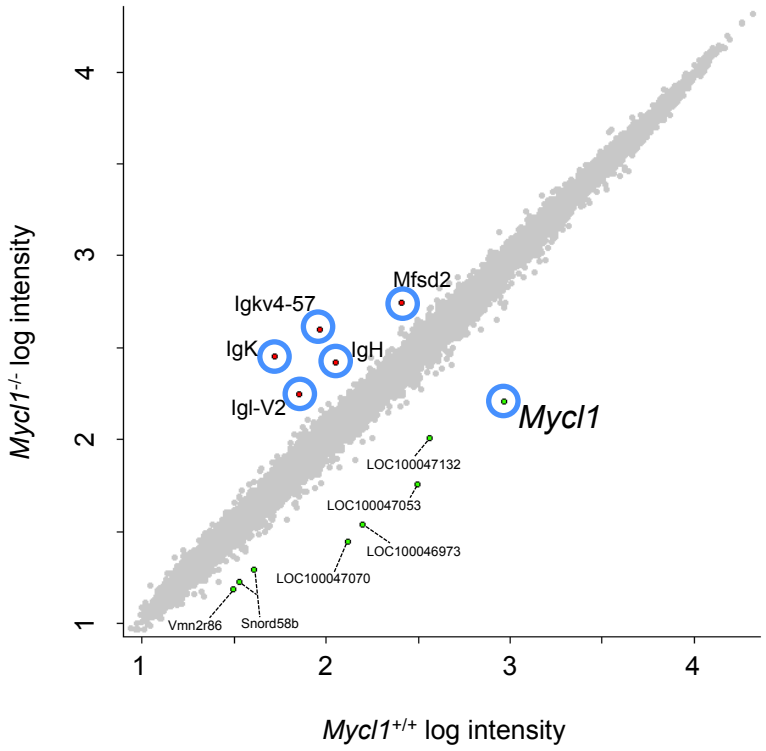
Mycl1-/- log intensity
Mycl1+/+ log intensity
1
2
3
4
Mfsd2
Igkv4-57
IgK
IgH
Igl-V2
Mycl1
LOC100047132
LOC100047053
LOC100046973
LOC100047070
Vmn2r86
Snord58b

CHAPTER III

THE ROLE OF EVT6 IN DENDRITIC CELL AND MONOCYTE DEVELOPMENT, HOMEOSTASIS, AND FUNCTION

INTRODUCTION

In this last chapter, we focus on our second candidate transcription factor whose expression pattern correlated with that of Flt3, the Ets-family protein Etv6. Its closest ortholog in *Drosophila* is an important regulator of cell differentiation during development, and recently Etv6 has been shown to have a role in hematopoietic cell differentiation. In addition to its well-documented expression in hematopoietic stem cells (HSC) and progenitors, we observed that Etv6 is prominently expressed in DCs and monocytes[136]. In accordance to its role in HSC biology, Etv6 is well known in the hematopoietic cancer field, as multiple genes are translocated onto its locus, forming fusion oncoproteins that deregulate signaling or transcription. However, a role for Etv6 in DCs and monocytes has yet to be determined. This section focuses on the effect of Etv6 deletion in the DC and monocyte compartment, and describes several alterations in their development, homeostasis, and differentiation. In addition, we provide evidence that implicates Etv6 in the suppression of interferon signaling. Overall, our studies reveal a novel and complex role for Etv6 in the hematopoietic system that goes beyond the cell-intrinsic role in the HSC compartment.

BACKGROUND

The Monocyte Compartment

Monocytes are highly plastic mononuclear phagocytes that originate from the bone marrow and are found mainly in the blood and spleen. Historically, circulating monocytes have been considered precursor cells that differentiate into tissue-resident macrophages and DCs. But several studies over the years have challenged this generalization; adult tissue macrophages develop before definitive hematopoeisis during embryogenesis and can self renew *in situ*[170], while steady-state DCs are not of monocyte-origin[171]. On the other hand, it is clear that monocytes can and do differentiate into macrophages and DCs under inflammatory and pathogenic conditions. Nevertheless, increasing evidence has revealed a new perspective on the role of monocytes, not just as precursor cells, rather as effector cells.

Monocyte development

During adult hematopoiesis, monocytes originate and develop in the bone marrow. Seminal studies that took place more than 30 years ago laid the foundation for the classical model of monocyte development: the first committed progenitor is the monoblast, which gives rise to the pro-monocyte, which finally gives rise to the monocyte[172-174]. Since then, studies within the last decade have updated this model with the characterization of a macrophage/dendritic cell progenitor (MDP), the dedicated progenitor to the monocytic lineage and (debatably) the DC lineage[14,175]. This MDP has been shown to give rise to the more restricted monocyte progenitor, the common monocyte progenitor (cMoP)[176]. Using adoptive transfer studies, the cMoP has been shown to give rise to both "classical" Ly6C^{hi} and "nonclassical" Ly6C^{lo} monocytes, which are released into circulation from the bone marrow and cease to proliferate. It has been proposed that the MDP and cMoP together make up subpopulations of the classical monoblasts[176]. Accumulating evidence suggests that Ly6C^{hi} monocytes can differentiate into Ly6C^{lo} monocytes in circulation, portraying a more linear stage of development rather than parallel[170,177].

Monocyte subsets and function

Development and survival of monocytes require signaling through colony-stimulating factor 1 (CSF1 or M-CSF) and its receptor M-CSFR (CD115)[178-180]. Accordingly, all monocytes can be readily identified by expression of the receptor for M-CSF, M-CSFR (CD115), in addition to CD11b. As mentioned above, blood monocytes can be categorized into two groups: the "classical" inflammatory Ly6C^{hi} monocytes, and "nonclassical" macrophage-like Ly6C^{lo} monocytes. In addition to Ly6C, classical monocytes express CCR2 which is required for their release into the periphery, and express intermediate levels of CX_3CR1[181,182]. On the other hand, nonclassical Ly6C^{lo} monocytes do not express CCR2 and express high levels of CX_3CR1[181]. In addition, nonclassical monocytes can be distinguished from their Ly6C^{hi} counterparts by the expression of CD43[183]. Importantly, defined monocyte subsets within the murine model have characteristically analogous counterparts in humans. Ly6C^{hi} monocytes most resemble human CD14^{+} monocytes, which also express CCR2 and low levels of CX_3CR1[181,184,185]. Meanwhile, Ly6C^{lo} monocytes most resemble human CD16^{+} CD14^{lo} monocytes, which show low levels of CCR2 and high levels of CX_3CR1[181,184,185].

Classical Ly6C^{hi} monocytes circulate in the blood and are readily recruited to sites of inflammation or infection. They have very short half-lives of only about 20 hours[170]. Once extravasated, they differentiate into macrophages and DCs, depending on the non-steady state context. For example, infection with *Listeria monocytogenes* induces monocytes to differentiate into inflammatory DCs, also known as Tip-DCs, that secrete TNFα and iNOS[186]. On the other hand, infection with *Toxoplasma gondii* drives monocytes to differentiate into macrophages[187].

Nonclassical Ly6C^{lo} monocytes are a distinct subset of monocytes that seem to have divergent roles from its Ly6C^{hi} counterparts. Using intravital microscopy, researchers have been able to show that Ly6C^{lo} monocytes crawl along the luminal side of blood vessels, and are hypothesized to patrol the vascular endothelium microenvironment for any signs of injury or infection in the steady state[188]. Moreover, in cases like *Listeria* infection and muscle necrosis, Ly6C^{lo} monocytes acquired late in the infection or injury seem to exhibit properties that most resemble M2-macrophages, which promote resolution of the inflammation, rather than its initiation[188-190]. These Ly6C^{lo} monocytes were originally termed "resident" monocytes because of their persistence in uninflamed and inflamed tissues after

adoptive transfer[181]. Indeed, compared to Ly6C^{hi} monocytes, nonclassical monocytes have an estimated half-life of about 2.2 days, which interestingly can be extended upon depletion of Ly6C^{hi} monocytes[170].

Etv6/Tel

Structure

Etv6/Tel belongs to the Ets family of transcription factors, one of the largest families of transcriptional regulators found within metazoans[191]. As the family name suggests, all members contain the highly conserved Ets domain, which confers its DNA binding activity. In addition to the Ets domain, Etv6 also contains the well-conserved HLH or pointed domain, which provides its protein binding activity for homodimeric or heterodimeric interactions[191], as well as an autoinhibitory region downstream of the Ets domain that blocks its DNA binding surface[192]. Etv6 is a transcriptional repressor, making it the only Ets family repressor found in human malignancies[193].

Etv6 in cancer

ETV6 was originally discovered as part of a chromosomal aberration associated with human chronic myelomonocytic leukemia[194]. Since then, *ETV6* has been discovered to be a frequently rearranged gene in several hematopoietic malignancies with over 40 associated translocations reported[195]. These commonly include the formation of a chimeric protein containing the pointed domain of Etv6 fused to protein tyrosine kinases (e.g. *ETV6-ABL1*), or DNA binding domains of other transcription factors like *ETV6-RUNX1,* which is the most common fusion gene found in pediatric B cell lymphoblastic leukemia[195]. Furthermore, mutations have also been reported in the rare blastic plasmacytoid neoplasm and more recently in familial cases of thrombocytopenia[196,197].

Expression and function within the hematopoietic system

While Etv6 is broadly expressed in many tissues, it is more selectively expressed among cell types within the hematopoietic compartment, with the most prominent expression in the HSC compartment[132,198]. Germline deletion of Etv6 in murine models show impaired angiogenesis in the yolk sac as well as impairment in bone marrow hematopoiesis[199]. Accordingly, deletion in adult HSCs show

impairments in HSC survival and repopulating activity, whereas in downstream lineages like B cells, T cells, and erythroid cells, Etv6 is dispensable. The role and expression of Etv6 in HSCs therefore may partially explain its prominence in leukemia.

Ets factors play important roles in cell fate decisions across species and tissues. In *Drosophila*, for example, Ets transcriptional repressor Yan, the closest ortholog to Etv6, was initially shown to regulate the differentiation of neurons in the developing eye, and later found to regulate differentiation in a number of additional processes[200,201]. Within the murine hematopoietic compartment, PU.1 is a major regulator of the lymphoid and myeloid lineage, SpiB has been implicated to play a role in pDC development, and Ets1 has important contributions for plasma cell differentiation and T cell development[151,202]. The role of Etv6 in cell fate decisions has also been demonstrated within the hematopoietic system, as overexpression of Etv6 seems to promote T_H17 differentiation[203].

Interestingly, Etv6 is also highly expressed in all splenic DC populations as well murine blood monocytes[132] and human DCs[161,162], however its role in these populations still remains to be elucidated. Given the precedent role of Ets factors in cell fate decisions, and the correlated expression pattern of Etv6 with Flt3 (Figure 2.1), we hypothesized that Etv6 may regulate a developmental transcription program within the DC compartment, and possibly the monocyte compartment. Here, we present data of ongoing research on the role of Etv6 in DC and monocyte development and function.

RESULTS

Mice deficient for Etv6 show impaired development of bone marrow pDCs and splenic $CD8^+$ cDCs

Mice that harbor germline deletions of *Etv6* show severe impairment in yolk sac angiogenesis and therefore the deletion is embryonic lethal[198]. To study Etv6 in the adult mouse, we bred mice that harbored a lox-P-flanked (floxed) allele of Etv6 to a mouse strain that expressed a tamoxifen-inducible Cre-ERT2 recombinase protein under the control of the ubiquitous, endogenous *Rosa26* promoter. Administration of tamoxifen allows temporal deletion of exon 7 of *Etv6*, which encodes a crucial component of the DNA binding domain. Analysis of splenic DC populations after deletion in these mice (*R26-Etv6*$^{\Delta}$) showed a minor decrease in frequency in cDCs but not splenic pDCs (Figure 3.1A-D). In contrast, pDC populations in the bone marrow were reduced by about half in absolute numbers (Figure 3.1C-D).

A closer look at cDC subsets showed that the overall decrease in cDC frequency was due to the specific decrease in the $CD8^+$ cDC populations, which comprise canonical $DEC205^+$ cDCs and non-canonical $DEC205^-$ cDCs (Figure 3.2A-B). In *R26-Etv6*$^{\Delta}$ mice, both $CD8^+$ populations showed a decrease in both frequency and absolute numbers (Figure 3.2B). Meanwhile, neither the Notch2-dependent $Esam^{hi}$ nor Notch2-independent $Esam^{lo}$ $CD11b^+$ cDC subsets showed any difference in numbers within the spleen (Figure 3.2B).

We also investigated whether this developmental phenotype could be recapitulated *in vitro*. To this end, we cultured whole bone marrow from *R26-Etv6*$^{\Delta}$ mice in Flt3L-containing supernatant to drive DC development. Consistent with what we see *in vivo*, Etv6-deficient bone marrow yielded significantly less $CD24^+$ ($CD8^+$-like) cDCs and pDCs, whereas $CD11b^+$ cDC numbers were not significantly altered (Figure 3.3). Overall, these data suggest that ubiquitous deletion of Etv6 during adult hematopoiesis leads to an impairment of DC development, particularly in the development of $CD8^+$ cDCs and pDCs.

To analyze whether this developmental phenotype occurs early or late in DC development, we crossed our Etv6 floxed mice to a mouse strain carrying a transgene of Cre recombinase expressed under the control of the *CD11c* promoter. This deleter strain, termed *CD11c-Cre*, deletes late in DC development after the common DC progenitor (CDP) stage, and in mature DCs. To improve deletion

efficiency, we crossed the *CD11c-Cre* strain to floxed mice that were heterozygous for the excised (null) *Etv6* allele, identified as *CD11c-Etv6*$^{\Delta/-}$. Similar to what was seen in the *R26-Etv6*$^{\Delta}$, *CD11c-Etv6*$^{\Delta/-}$ mice showed reduced pDC numbers in the bone marrow, and no change in CD11b^{+} cDC subset numbers were observed (Figure 3.4A-B). In contrast to what was seen in *R26-Etv6*$^{\Delta}$ DCs, CD8^{+} cDC subsets showed a specific reduction in DEC205^{-} cDCs and not DEC205^{+} cDCs. *In vitro* bone cultures showed a similar reduction in cell numbers of CD24^{+} cDCs and pDCs, but to a much lesser extent than seen in ubiquitous deletion of Etv6 (Figure 3.5A-C). Based on this data, it appears that Etv6 acts late in DC development to support the generation of DEC205^{-} cDCs and pDCs, while it acts earlier to support the generation of DEC205^{+} cDCs.

Given the consistent decrease of DEC205^{-} cDCs, we further asked whether or not Etv6 played a role in the survival and maintenance of these cells, rather than the development. To test this, we crossed our Etv6 floxed mice to a mouse strain expressing a tamoxifen-inducible CreER and YFP cassette, both under the control of the endogenous CX_3CR1 promoter. Since DEC205^{-} cDCs as well as Esam^{lo} cDCs express high levels of CX_3CR1 (Figure 3.10A), we could induce deletion of Etv6 in these cells and analyze the effect shortly after deletion, before any DC precursors (like the CX_3CR1 expressing CDP or pre-DC) could completely replenish the pool. We found that treated *Cx3cr1-CreER*$^{+/-}$ *Etv6*$^{fl/fl}$ mice (*Cx3cr1-Etv6*$^{\Delta}$) resulted in a slight decrease in overall cDCs (Figure 3.6A), which was mainly caused by the decrease in cDCs that only expressed CX_3CR1, namely DEC205^{-} and Esam^{lo} cDCs (Figure 3.6B). In contrast, pDCs and DEC205^{+} cDCs, which express low amounts of CX_3CR1, were not affected as they were with *CD11c-Etv6*$^{\Delta/-}$ and *R26-Etv6*$^{\Delta}$ deletion, confirming that potential Etv6-deficient precursors did not fully give rise to these cells. These results suggest that Etv6 may play a role in the maintenance and survival of DEC205^{-} and Esam^{lo} cDCs.

<u>cDCs deficient for Etv6 show an altered cell surface phenotype</u>

While ubiquitous deletion of Etv6 did not result in a significant decrease in all DC numbers, closer analysis of the DC subtypes showed an altered cell surface phenotype. In particular, both CD8^{+} cDC subsets showed a reduction in cell surface expression of CD8α (Figure 3.2C-D), most notably in DEC205^{+} cDCs, which normally express very high levels compared to DEC205^{-} cDCs. In addition, Esam^{hi}

CD11b^{+} cDCs showed a slight reduction in proportion as well as an increase in cell surface expression of CD11b (Figure 3.2E-F). Esam^{lo} cDCs also showed an increase in CD11b expression to a similar extent (Figure 3.2E-F). These results suggest that Etv6 may not only play a role in DC development, but it may also affect the differentiation of these DCs. To test this notion, we more closely analyzed the cell surface markers of mature DC populations in *CD11c-Etv6*$^{\Delta/-}$ mice. Analysis of splenic cDC populations showed similar phenotypes in CD8^{+} cDC subsets and CD11b^{+} cDC subsets, namely the decrease in CD8α expression in the former (Figure 3.4C), and the decreased proportion and increased CD11b expression in the latter (Figure 3.4D). In addition, *in vitro* cultures of *CD11c-Etv6*$^{\Delta/-}$ showed an abnormal increase in CD11b expression in CD24^{+} cDCs (Figure 3.5D). Overall, the alteration in cell surface phenotype in both early deletion and late deletion of Etv6 suggest that Etv6 may also play a role in cDC differentiation in addition to DC development. Interestingly, the deletion of Etv6 in CX_3CR1-expressing DCs did not show any change in cell surface expression (Figure 3.6C-D), suggesting that Etv6 may play a role specifically regulating the quality of DEC205^{+} and Esam^{hi} cDCs, and not their CX_3CR1 counterparts.

Monocytes deficient for Etv6 show a subtle impairment in homeostasis

Because Etv6 is also highly expressed within the monocyte compartment, we investigated how deletion of Etv6 affected monocyte development. CD115^{+} monocytes can be categorized into two groups: classical inflammatory Ly6C^{hi} and the nonclassical patrolling Ly6C^{lo} monocytes. Both subsets express CX_3CR1, with nonclassical Ly6C^{lo} monocytes expressing the highest levels (Figure 3.10). Thus, we analyzed monocyte subsets in our *Cx3cr1-Etv6*$^{\Delta}$ mice. The flow cytometric staining profile of monocyte subsets are shown in Figure 3.7A. We found that deletion of Etv6 in the monocyte compartment led to a decrease in both subsets in absolute numbers but not significantly in frequencies in bone marrow (Figure 3.7B; data not shown). In the periphery, *Cx3cr1-Etv6*$^{\Delta}$ deletion mostly affected the Ly6C^{lo} population (Figure 3.7B-C). To see if Etv6 deletion affected early progenitors, we analyzed the recently described cMoP populations in the bone marrow, which also express CX_3CR1[176]. A representative gating strategy is shown in Figure 3.8A. Deletion of Etv6 in the cMoP showed no difference in numbers (Figure 3.8B), suggesting that Etv6 does not affect monocytes at the early monocyte progenitor stage, and therefore may affect maintenance and homeostasis.

Mice deficient for Etv6 show increased Sca1 expression on multiple immune cells

Analysis of the most primitive hematopoietic progenitors like HSCs in *R26-Etv6*$^{\Delta}$ mice was confounded by the occasional observation that c-Kit^{hi} Sca1^{-} erythromyeloid progenitors showed increased expression of Sca1 (data not shown). Sca1 induction in myeloid progenitors was inconsistent likely due to the inefficient deletion of the Etv6 allele and/or the rapid selection for non-deleters in this proliferative population, as prominence of the floxed allele assessed by PCR was correlated with lack of Sca1 induction (data not shown). Nevertheless, analysis of downstream mature B cells both in the bone marrow and spleen showed slight and consistent increases in Sca1 expression (Figure 3.9). Since Sca1 is an interferon-responsive gene[204], we speculated that these mice may be exhibiting signs of interferon signaling. While many cells produce interferon, pDCs are especially adept at producing massive amounts of type I interferon. To this end, we analyzed B cells of *CD11c-Etv6*$^{\Delta/-}$ mice to see if this same Sca1 induction occurred when Etv6 was deleted in DCs, particularly pDCs. As seen in Figure 3.9B, no Sca1 induction was observed in B cells, suggesting that DCs are not the source of the interferon production. Since Etv6 is also highly expressed in monocytes, and deletion of Etv6 in the monocyte compartment does have an effect on the compartment, we also investigated whether monocytes were involved in the Sca1 induction. Surprisingly, deletion of Etv6 in CX_3CR1-expressing cells led to a robust induction of Sca1 induction in early myeloid progenitors (Figure 3.8C) and B cells (Figure 3.9C) as seen with ubiquitous deletion of Etv6, in addition to other hematopoietic populations known not to express CX_3CR1, like granulocytes (Figure 3.9D-G). Interestingly, monocytes consistently showed one of the highest changes in Sca1 expression in the bone marrow, spleen and blood compared to other cell types (Figure 3.9E-G). Overall, these experiments suggest that Etv6 may be controlling the secretion of interferon in a CX_3CR1-expressing cell.

DISCUSSION

The role of Etv6 in early and late DC development

Ubiquitous deletion and *CD11c-Cre* deletion both led to the reduction of pDCs and $CD8^+$ cDCs *in vivo* and *in vitro*, though the *CD11c-Cre* deletion only affected the $DEC205^-$ cDC population *in vivo* and the *in vitro* phenotype was significantly more mild. The difference in the reduction of $CD8^+$ cDCs between ubiquitous deletion and *CD11c-Cre* deletion may reflect the dual effect of Etv6 on both early and late DC development. *R26-Etv6*$^{\Delta}$ mice delete in both DC progenitors and mature DCs, and the effect on the progenitor pool would explain the almost complete depletion of pDCs and $CD8^+$ cDCs *in vitro*, and the broad reduction in pDCs, $DEC205^-$, and $DEC205^+$ cDC *in vivo.* On the other hand, continued expression of Etv6 late in development may also affect the maintenance of pDCs and $DEC205^-$ cDCs specifically, and thus explain the persistence of $DEC205^+$ cDCs in late deletion. Consistent with this, CX_3CR1-expressing DCs, like $DEC205^-$ cDCs, also showed slight reduction in numbers very soon after deletion. Evidence *in vivo* would suggest that the slight reduction of $CD24^+$ cDCs is reflective of the specific depletion of *in vitro* $DEC205^-$ counterparts. In support of this, bone marrow cultures derived from *Batf3*$^{-/-}$ mice, which are devoid of $DEC205^+$ cDCs, do still develop variable amounts of residual $CD24^+$ cDCs (unpublished data), suggesting that these non-canonical $DEC205^-$ cDCs can develop *in vitro.* Interestingly, the dual effect on $CD8^+$ cDCs and pDCs is reminiscent of Irf8 deletion, in which both cell types are completely depleted from several lymphoid tissues[147]. However, the phenotype that we see is much less severe, and only seems to effect pDCs in the bone marrow.

Even though *CD11c-Etv6*$^{\Delta/-}$ mice did not show quantitative differences in $DEC205^+$ cDC or $CD11b^+$ cDC populations, the significant difference in cell surface phenotype in these cells suggest that they are still altered qualitatively by the lack of Etv6. Both subsets of $CD8^+$ cDCs showed a reduction in CD8α expression, which was much more severe in $DEC205^+$ cDCs. At the same time, $Esam^{hi}$ and $Esam^{lo}$ cDCs showed an increase in CD11b expression, with a very subtle reduction in the proportion of $Esam^{hi}$ cDCs. On the surface, it appears that $DEC205^+$ and $Esam^{hi}$ populations are converting to their CX_3CR1-expressing counterparts, as $DEC205^-$ cDCs already show low levels of CD8α expression and similarly $Esam^{lo}$ populations show high levels of CD11b expression. Further studies are clearly required to confirm

this notion, specifically with functional studies of T cell priming as well as genome-wide expression analysis. Overall, it seems that Etv6 has multiple roles in development, homeostasis, and differentiation across the different DC subtypes.

The role of Etv6 in monocyte homeostasis

Among hematopoietic cells, CX_3CR1 can be detected on subsets of DC populations, a very small proportion of NK cells, and most prominently in the monocyte compartment[117]. To this end, we used *Cx3cr1-CreER* to delete Etv6 more specifically in the monocyte compartment and evaluate the effect on their development. Deletion of Etv6 showed a subtle reduction in the absolute cell numbers in both types of monocytes in the bone marrow, whereas deletion in the periphery mostly affected $Ly6C^{lo}$ monocytes. Early progenitors of monocytes include the MDP and the cMoP, both of which express moderate levels of CX_3CR1, and therefore should have also deleted Etv6. Even though analysis was done soon after the deletion of Etv6 (5 days), monocytes are a very-short lived cell type and we would expect that any developmental defect originating from progenitors would present itself in the mature compartment within this time period. Analysis of the precursor cMoP population showed no difference in absolute numbers, suggesting that Etv6 functions on the mature monocyte level and that the reduction in numbers is due to a defect in homeostasis. However, this does not preclude the possibility that Etv6 may effect monocyte development at a more primitive level than the MDP or cMoP. Furthermore, $Ly6C^{hi}$ monocytes have been proposed to be precursors to $Ly6C^{lo}$ monocytes in the blood, so further experiments are necessary to dissect the differentiation potential of Etv6-deficient $Ly6C^{hi}$ monocytes into $Ly6C^{lo}$. Nevertheless, the results from *Cx_3cr1-Etv6$^{\Delta}$* analyses suggest that Etv6 functions in the monocyte compartment as well.

The role of Etv6 in regulating interferon signaling

The most striking phenotype of the deletion of Etv6 was the induction of Sca1 expression in multiple hematopoietic cell types. Interestingly, Sca1 induction was consistently seen in *Cx_3cr1-Etv6$^{\Delta}$* mice. More importantly, non-CX_3CR1 expressing cells like B cells showed a significant induction of Sca1 expression, suggesting a cell-extrinsic effect from a CX_3CR1-expressing cell. Mature cell types that prominently express CX_3CR1 include monocytes, DCs and a small subset of NK cells. Given that Sca1

induction was not observed in *CD11c-Etv6*$^{\Delta/-}$ mice, the most likely candidate for the cytokine source is monocytes. In support of this, monocytes consistently showed one of the highest levels of Sca1 induction in all tissues analyzed. We cannot rule out the possibility that NK cells may be a source of interferon induction as well, however their minimal presence compared to monocytes argues otherwise. Sca1 induction was only occasionally seen in *R26-Etv6*$^{\Delta}$ mice, likely due to the inefficiency of allele deletion (data not shown) and the selective pressure coming from the HSC compartment to maintain Etv6 expression, which has been described before[199]. Given the timing of analysis, it may be possible that non-deleters may have infiltrated more downstream compartments, especially those that have high turnover like monocytes, and attenuated the transient interferon response. Quantitative analysis of Etv6 expression within individual cell populations would confirm this notion. Nevertheless, these results suggest that Etv6 may be a negative regulator of interferon production. In line with this, the interaction of Ets factors and interferon regulating factors has precedence. For example, Spi1/PU.1 has been shown to interact with Irf4 and Irf8 and induce transcription of interferon genes[205]. Interestingly, Etv6 has also been proposed to interact with Irf8 and repress transcription at interferon response elements through the recruitment of a histone deacetylase[206]. Confirmation of the interferon signature and pinpointing the exact cell source of interferon secretion is currently under active investigation. Future studies establishing the functional implications of this signaling are warranted.

Overall, the studies presented in this chapter identify Etv6 as a potential multi-faceted regulator in DC and monocyte development, homeostasis and/or function. Using several models of conditional deletion, we have shown that Etv6 developmentally affects pDCs and CD8^{+} cDCs, and potentially affects the homeostasis and differentiation of several cDC subsets. We have also provided evidence for a role of Etv6 in monocyte homeostasis, selectively in Ly6C^{lo} monocytes, as well as uncovered a potential role for Etv6 in the repression of interferon signaling. Elucidation of these features will provide key insight on potentially new mechanisms regulating DC and monocyte homeostasis and function.

MATERIALS AND METHODS

Animals

Etv6$^{fl/fl}$ were a kind gift from H. Hock[199]. *R26-CreER* mice were a kind gift from T. Ludwig[207]. *Itgax-Cre (CD11c-Cre)* was developed in our lab[143]. *Cx3cr1-CreER*[208] mice were acquired from Jackson. All mice were on C57BL/6 background. All animal studies were performed according to the investigator's protocol approved by the Institutional Animal Care and Use Committee of Columbia University.

Cell preparations

Spleens were minced and digested with collagenase D (1 mg/mL) and DNaseI (20μg/mL) in for 30-60 min at 37°C. Tissues were pressed through a nylon cell strainer to yield single cell suspensions and then subjected to red blood cell (RBC) lysis before being filtered. Bone marrow was prepared by flushing femurs and tibias with phosphate buffer saline (PBS) using a 27-gauge needle before RBC lysis. Blood was acquired by cardiac puncture and subject to RBC lysis.

Flow cytometry

Cells were stained with the following fluorochrome- or biotin-conjugated antibodies from eBioscience or as indicated: anti-CD11c (N418), MHC II (M5/114.15.2), CD11b (M1/70), CD8α (53-6.7), DEC205 (NLDC-145; BioLegend), Esam (IG8), B220 (RA3-6B2), mPDCA-1/Bst2 (Miltenyi Biotec), CD317/PDCA/Bst2 (Biolegend clone 927), CD24 (M1/69), Ly6C (HK1.4), Ly6G (IA8), F4/80 (BM8), NK1.1 (PK136), Ter119 (TER-119), CD49b (DX5), TCRβ (H57-597), CD3 (17A2), Flt3 (A2F10), c-Kit (2B8), Sca-1 (D7), and CD115 (AFS98). Cell acquisition was done on LSR II (BD Biosciences) using FACSDiva (BD Biosciences) and analysis was done on FlowJo (Tree Star).

In vitro BM-derived DC cultures

Bone marrow cells were harvested as described above. RBC-lysed cells were plated in triplicates in a 24-well plate at 2 x 10^6 per well in DMEM/10% FCS and 20% supernatant from cultured Flt3L-secreting B16

melanoma cell lines. Suspension and adherent cells were harvested after 8 days and triplicates were pooled for counting and flow cytometric analysis.

Tamoxifen treatment

Mice were treated by oral gavage for three consecutive days with 5 mg of tamoxifen suspended in sunflower seed oil. *R26-CreER* mice and *Cx3cr1-CreER* were analyzed 9 and 5 days after the last treatment, respectively.

CHAPTER III FIGURES

Figure 3.1. Ubiquitous deletion of Etv6 shows a decrease in bone marrow pDCs.

R26-CreER$^{+/-}$ *Etv6*$^{+/+}$ or *Etv6*$^{fl/fl}$ (Ctrl) and *R26CreER*$^{+/-}$ *Etv6*$^{fl/fl}$ (R26-Etv6$^{\Delta}$) were treated with 5 mg of tamoxifen by oral gavage for 3 consecutive days. Mice were sacrificed 9 days after the last treatment.

(A) Representative staining profiles of splenic cDC populations. Numbers in plots indicate percent of gated population.

(B) Absolute numbers (top) and frequencies (bottom) of total cDCs as identified in (A) (mean ± SD, n = 4-5).

(C) Representative staining profiles of pDC populations in spleen (SPL) and bone marrow (BM).

(D) Absolute numbers (top) and frequencies (bottom) of pDCs as identified in (C) (mean ± SD, n = 4-5).

Statistically significant differences are indicated as: * $p < 0.05$; ** $p < 0.01$; *** $p < 0.001$

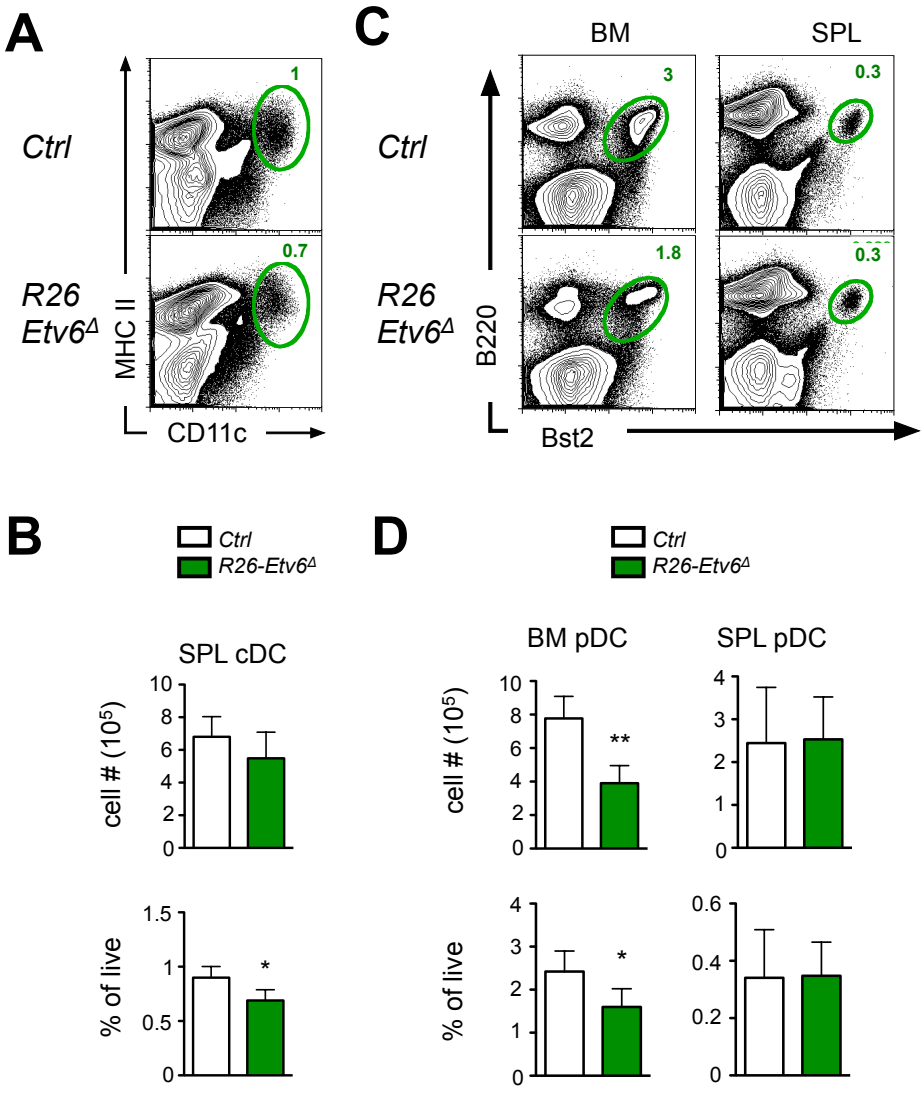
A
Ctrl
R26
Etv6Δ
MHC II
CD11c
1
0.7
C
BM
SPL
Ctrl
R26
Etv6Δ
B220
Bst2
3
0.3
1.8
0.3
B
Ctrl
R26-Etv6Δ
SPL cDC
cell # (10⁵)
% of live
*
D
Ctrl
R26-Etv6Δ
BM pDC
SPL pDC
cell # (10⁵)
% of live
**
*

Figure 3.2. Ubiquitous deletion of Etv6 shows a decrease in CD8$^+$ cDCs and alterations in cDC cell surface phenotype.

R26-CreER$^{+/-}$ *Etv6*$^{+/+}$ or *Etv6*$^{fl/fl}$ (Ctrl) and *R26CreER*$^{+/-}$ *Etv6*$^{fl/fl}$ (R26-Etv6$^{\Delta}$) were treated with 5 mg of tamoxifen by oral gavage for 3 consecutive days. Mice were sacrificed 9 days after the last treatment.

(A) Representative staining profile cDC subsets pre-gated on CD11c^{hi} MHCII$^+$. Numbers in plots indicate percent of gated population.

(B) Absolute numbers (top row) and frequencies (bottom row) of cDC subsets as identified in (A) (mean ± SD, n = 4-5).

(C) Representative histograms of CD8α expression in CD8$^+$ cDC subsets. Dotted line shows means fluorescent intensity (MFI) of CD8α expression in Ctrl DEC205$^+$ cDCs.

(D) MFI of CD8α expression as depicted in (C) (mean ± SD, n = 4-5).

(E) Representative histograms of CD11b expression in CD11b$^+$ cDC subsets. Dotted line shows MFI of CD11b expression in Ctrl Esam^{hi} cDCs.

(F) MFI of CD11b expression (left) as depicted in (E) and percent of Esam^{hi} cDCs out of total CD11b$^+$ cDCs (right) as depicted in (A) (mean ± SD, n = 4-5).

Statistically significant differences are indicated as: * $p < 0.05$; ** $p < 0.01$; *** $p < 0.001$

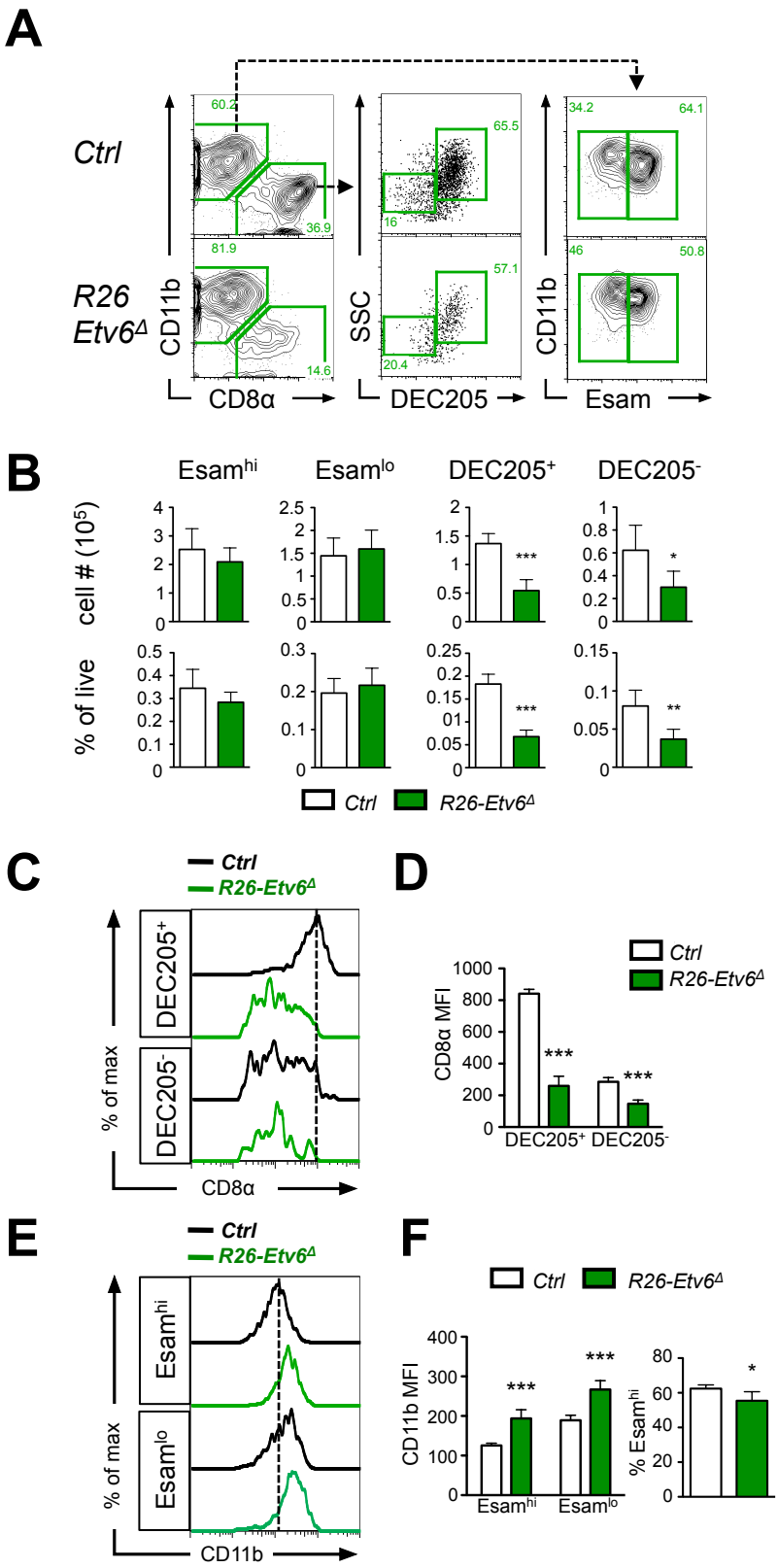
A
Ctrl
R26 Etv6Δ
CD11b
CD8α
SSC
DEC205
CD11b
Esam
60.4
36.9
81.9
14.6
65.5
16
57.1
20.4
34.2
64.1
46
50.8
B
Esamhi
Esamlo
DEC205+
DEC205-
cell # (10^5)
% of live
Ctrl
R26-Etv6Δ
C
Ctrl
R26-Etv6Δ
DEC205+
DEC205-
% of max
CD8α
D
Ctrl
R26-Etv6Δ
CD8α MFI
DEC205+ DEC205-
E
Ctrl
R26-Etv6Δ
Esamhi
Esamlo
% of max
CD11b
F
Ctrl
R26-Etv6Δ
CD11b MFI
% Esamhi
Esamhi
Esamlo

Figure 3.3. Etv6-deficient mice show impairment in Flt3L-driven DC development *in vitro*.

R26-CreER$^{+/-}$ *Etv6*$^{+/+}$ or *Etv6*$^{fl/fl}$ (Ctrl) and *R26CreER*$^{+/-}$ *Etv6*$^{fl/fl}$ (R26-Etv6$^{\Delta}$) were treated with 5 mg of tamoxifen by oral gavage for 3 consecutive days. Mice were sacrificed 9 days after the last treatment. Whole bone marrow from treated mice was cultured in 20% Flt3L-rich supernatant for 7 days.

(A) Representative staining profiles of cDC subsets pre-gated on CD11c^{+} MHCII^{+}. Numbers on plot indicate fraction of cells within gated population.

(B) Representative staining profiles of pDC subsets pre-gated on B220^{+} cells. Numbers on plot indicate fraction of cells within gated population.

(C) Absolute numbers of DC populations identified as in (A-B)(mean ± SD, n = 4-5).

Statistically significant differences are indicated as: * $p < 0.05$; ** $p < 0.01$; *** $p < 0.001$

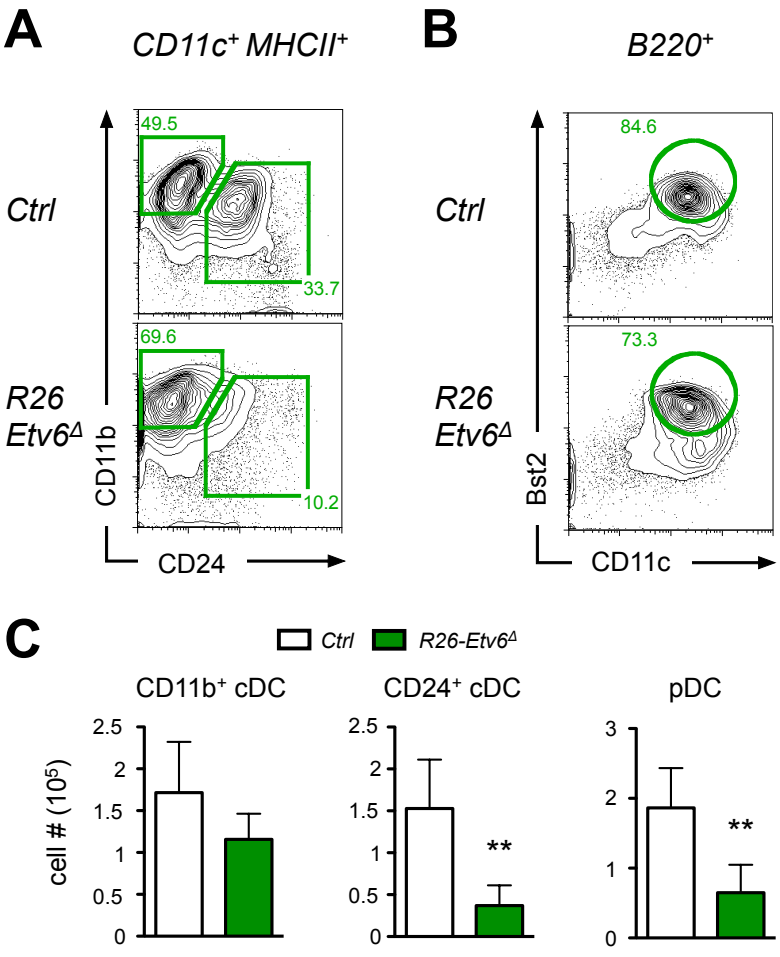
A
CD11c+ MHCII+
B
B220+
Ctrl
R26 Etv6Δ
49.5
33.7
69.6
10.2
84.6
73.3
CD11b
CD24
Bst2
CD11c
C
Ctrl
R26-Etv6Δ
CD11b+ cDC
CD24+ cDC
pDC
cell # (10^5)
2.5
2
1.5
1
0.5
0
3
**

Figure 3.4. DC-specific deletion of Etv6 results in a mild decrease in DEC205^{-} CD8^{+} cDCs and pDCs, and alters cDC phenotypes.

(A) Absolute numbers (top row) and frequencies (bottom row) of DCs as identified in (Fig. 3.1A,C) in *Etv6*$^{fl/fl}$ (Ctrl) and *CD11c-Cre*$^{+/-}$ *Etv6*$^{fl/-}$ (CD11c-Etv6$^{\Delta/-}$) mice (mean ± SD, n = 4).

(B) Absolute numbers (top row) and frequencies (bottom row) of cDC subsets as identified in (Fig. 3.2A) in Ctrl and CD11c-Etv6$^{\Delta/-}$ mice (mean ± SD, n = 4).

(C) Mean fluorescent intensity (MFI) of CD8α expression as depicted in (Fig. 3.2C) in Ctrl and CD11c-Etv6$^{\Delta/-}$ mice (mean ± SD, n = 4).

(D) MFI of CD11b expression (left) as depicted in (Fig. 3.2E) and percent of Esam^{hi} cDCs out of total CD11b^{+} cDCs (right) as depicted in (Fig. 3.2A) (mean ± SD, n = 4).

Statistically significant differences are indicated as: * $p < 0.05$; ** $p < 0.01$; *** $p < 0.001$

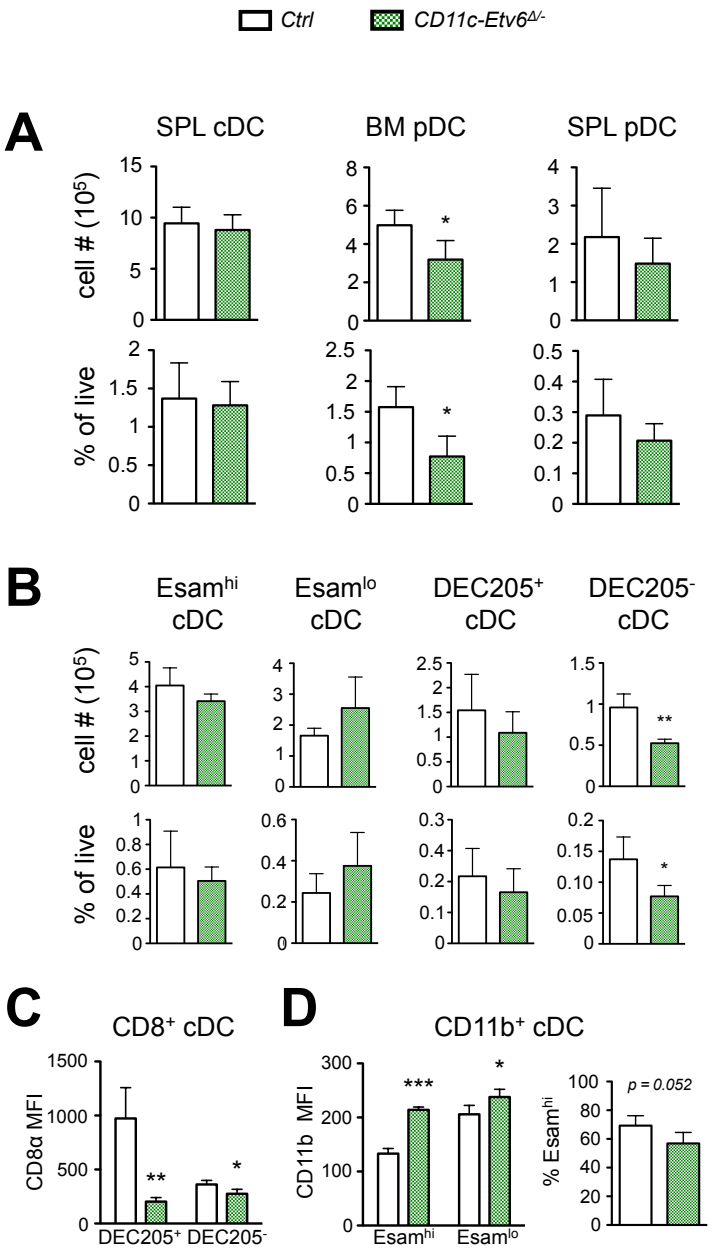
Ctrl
CD11c-Etv6Δ/-
A
SPL cDC
BM pDC
SPL pDC
cell # (10^5)
% of live
B
Esamhi cDC
Esamlo cDC
DEC205+ cDC
DEC205- cDC
cell # (10^5)
% of live
C
CD8+ cDC
CD8α MFI
DEC205+ DEC205-
D
CD11b+ cDC
CD11b MFI
Esamhi Esamlo
% Esamhi
p = 0.052

Figure 3.5. Deletion of Etv6 late in DC development shows a subtle impairment of Flt3L-driven DC development and alters CD24$^+$ cDCs *in vitro*.

Whole bone marrow from *Etv6*$^{fl/fl}$ (Ctrl) and *CD11c-Cre*$^{+/-}$ *Etv6*$^{fl/-}$ (CD11c-Etv6$^{\Delta/-}$) mice was cultured in 20% Flt3L-rich supernatant for 7 days.

(A) Representative staining profiles of cDC subsets pre-gated on CD11c$^+$ MHCII$^+$. Numbers on plot indicate fraction of cells within gated population.

(B) Representative staining profiles of pDC subsets pre-gated on B220$^+$ cells. Numbers on plot indicate fraction of cells within gated population.

(C) Absolute numbers of DC populations identified as in (A-B) (mean ± SD, n = 3).

(D) Representative histograms of CD11b expression on CD24$^+$ cDCs. Bar graph shows mean fluorescent intensity (MFI) of CD11b expression (mean ± SD, n = 3).

Statistically significant differences are indicated as: * $p < 0.05$; ** $p < 0.01$; *** $p < 0.001$

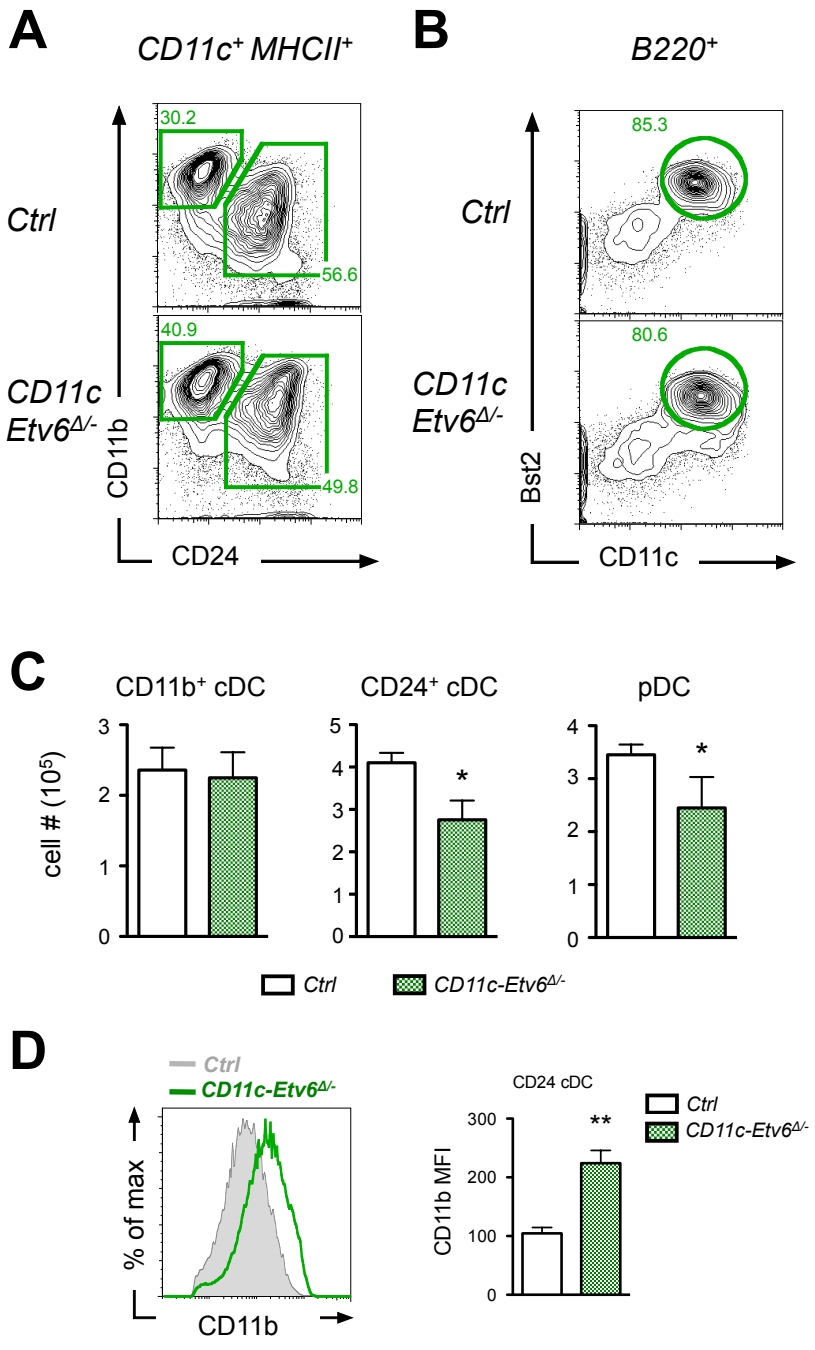
A
CD11c+ MHCII+
Ctrl
CD11c Etv6Δ/-
30.2
56.6
40.9
49.8
CD11b
CD24
B
B220+
85.3
80.6
Bst2
CD11c
C
CD11b+ cDC
CD24+ cDC
pDC
cell # (10^5)
Ctrl
CD11c-Etv6Δ/-
D
Ctrl
CD11c-Etv6Δ/-
% of max
CD11b
CD24 cDC
CD11b MFI

Figure 3.6. Deletion of Etv6 in CX_3CR1-expressing cells results in a mild decrease in DEC205$^-$ CD8$^+$ and Esam^{lo} CD11b$^+$ cDCs.

Etv6$^{fl/fl}$ (Ctrl) *Cx3cr1-CreER*$^{+/-}$ *Etv6*$^{fl/fl}$ (Cx3cr1-Etv6$^{\Delta}$) were treated with 5 mg of tamoxifen by oral gavage for 3 consecutive days. Mice were sacrificed 5 days after the last treatment.

(A) Absolute numbers (top row) and frequencies (bottom row) of DCs as identified in (Fig. 3.1A-B) (mean ± SD, n = 6).

(B) Absolute numbers (top row) and frequencies (bottom row) of cDC subsets as identified in (Fig. 3.2A) (mean ± SD, n = 6).

(C) Mean fluorescent intensity (MFI) of CD8α expression as depicted in (Fig. 3.2C) (mean ± SD, n = 6).

(D) MFI of CD11b expression (left) as depicted in (Fig. 3.2E) and percent of Esam^{hi} cDCs out of total CD11b$^+$ cDCs (right) as depicted in (Fig. 3.2A) (mean ± SD, n = 6).

Statistically significant differences are indicated as: * $p < 0.05$; ** $p < 0.01$; *** $p < 0.001$

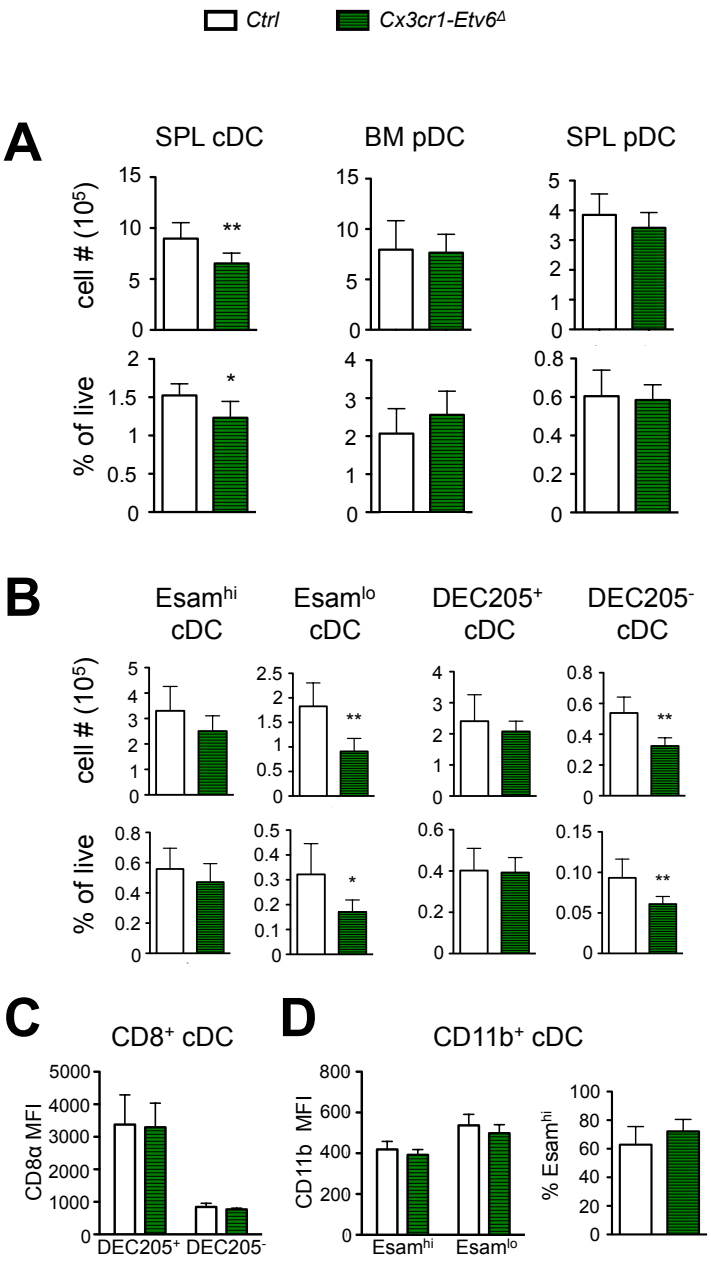
Ctrl
Cx3cr1-Etv6Δ
A
SPL cDC
BM pDC
SPL pDC
cell # (10^5)
% of live
B
Esam^hi cDC
Esam^lo cDC
DEC205^+ cDC
DEC205^- cDC
C
CD8^+ cDC
CD8α MFI
DEC205^+ DEC205^-
D
CD11b^+ cDC
CD11b MFI
% Esam^hi
Esam^hi Esam^lo

Figure 3.7. Deletion of Etv6 in CX_3CR1-expressing cells results in slight reduction in bone marrow and peripheral monocytes.

Etv6$^{fl/fl}$ (Ctrl) *Cx3cr1-CreER*$^{+/-}$ *Etv6*$^{fl/fl}$ (Cx3cr1-Etv6$^{\Delta}$) were treated with 5 mg of tamoxifen by oral gavage for 3 consecutive days. Mice were sacrificed 5 days after the last treatment.

(A) Representative staining profile Ly6C^{hi} and Ly6C^{lo} monocytes in the bone marrow. Similar gating strategies were used to quantify monocytes in the spleen and blood. Lineage markers include Ly6G, CD49b, B220, and CD3.

(B) Absolute numbers of Ly6C^{hi}, Ly6C^{lo}, and granulocytes in bone marrow (BM) and spleen (SPL). Granulocytes were identified as Lineage(Ly6G)$^{+}$ CD11b^{+} FSC^{hi} SSC^{hi} (mean ± SD, n = 6).

(C) Frequency of Ly6C^{lo} monocytes in blood (mean ± SD, n = 6)

Statistically significant differences are indicated as: * $p < 0.05$; ** $p < 0.01$; *** $p < 0.001$

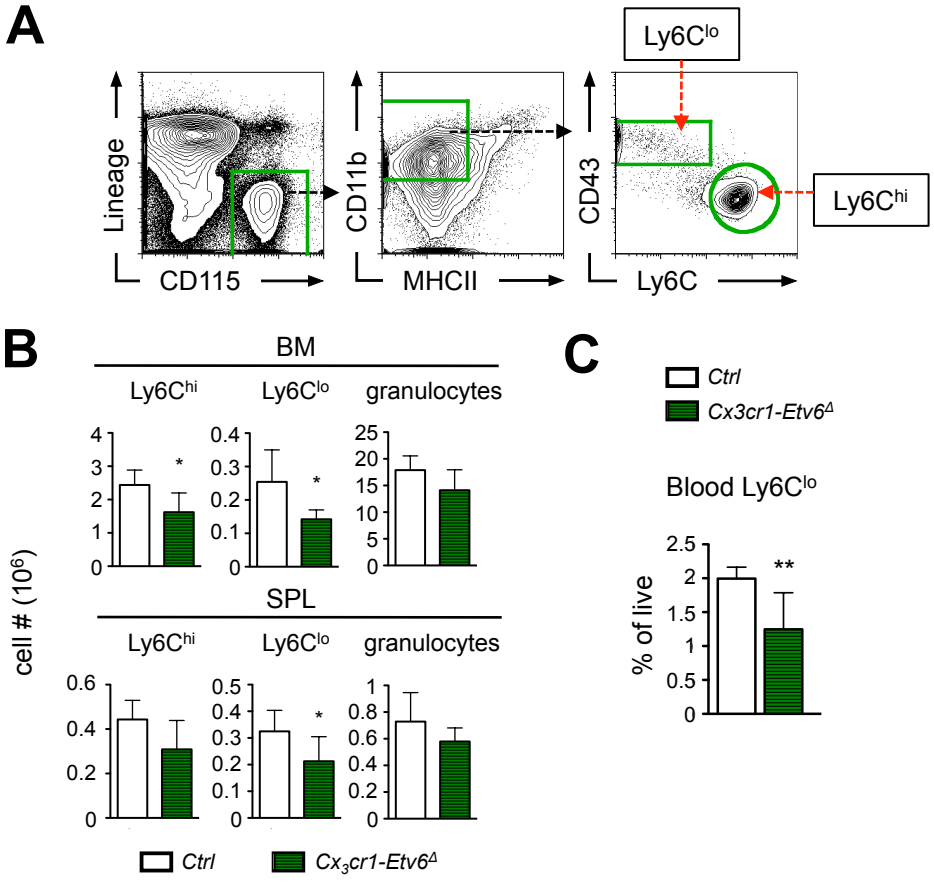
A
Ly6C^lo
Lineage
CD115
CD11b
MHCII
CD43
Ly6C
Ly6C^hi
B
BM
Ly6C^hi
Ly6C^lo
granulocytes
SPL
cell # (10^6)
Ctrl
Cx3cr1-Etv6^Δ
C
Ctrl
Cx3cr1-Etv6^Δ
Blood Ly6C^lo
% of live

Figure 3.8. Deletion of Etv6 in CX_3CR1-expressing does not change cMoP numbers but induces Sca1 expression on stem/progenitor populations.

Etv6$^{fl/fl}$ (Ctrl) and *Cx$_3$cr1-CreER*$^{+/-}$ *Etv6*$^{fl/fl}$ (Cx$_3$cr1-Etv6$^{\Delta}$) were treated with 5 mg of tamoxifen by oral gavage for 3 consecutive days. Mice were sacrificed 5 days after the last treatment.

(A) Representative gating strategy for common monocyte progenitors (cMoPs) in bone marrow. Lineage markers include Ly6G, CD11c, CD49b, B220, TCRb, and Ter119.

(B) Absolute numbers of cMoPs in the bone marrow (mean ± SD, n = 6).

(C) Representative staining profiles of Lin$^-$ Ly6C$^-$ CD11b$^-$ cells in bone marrow and histograms of gated populations showing Sca1 expression.

Statistically significant differences are indicated as: * $p < 0.05$; ** $p < 0.01$; *** $p < 0.001$

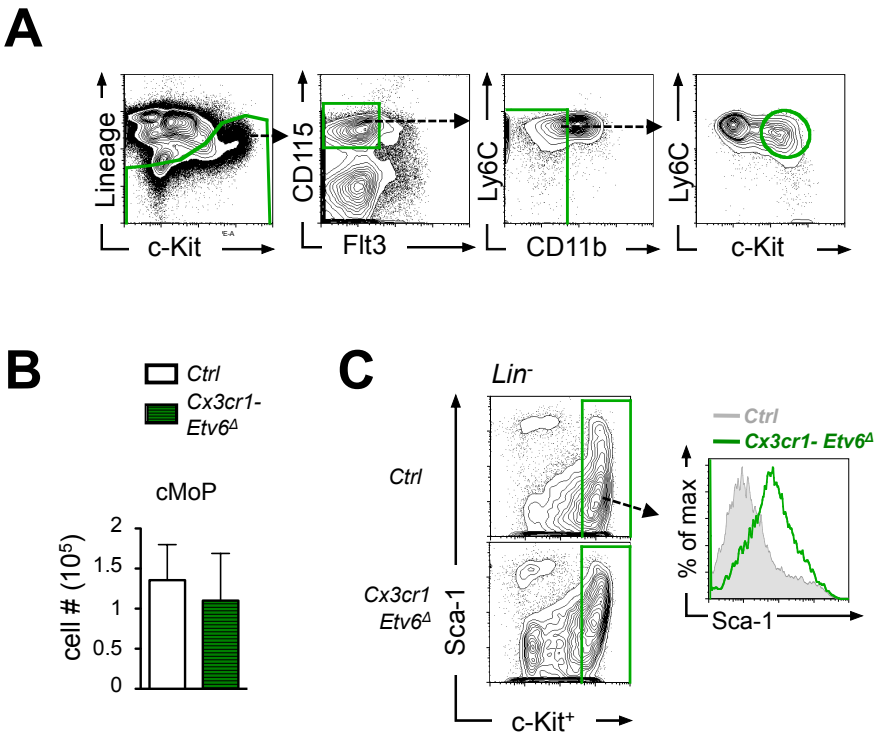
A
Lineage
c-Kit
CD115
Flt3
Ly6C
CD11b
Ly6C
c-Kit
B
Ctrl
Cx3cr1-
Etv6Δ
cMoP
cell # (10^5)
2
1.5
1
0.5
0
C
Lin-
Ctrl
Cx3cr1
Etv6Δ
Sca-1
c-Kit+
Ctrl
Cx3cr1- Etv6Δ
% of max
Sca-1

Figure 3.9. Deletion of Etv6 in CX_3CR1-expressing cells results in global Sca1 induction.

(A) Mean fluorescent intensity (MFI) of Sca1 expression in mature B cells in *R26-CreER*$^{+/-}$ *Etv6*$^{+/+}$ or *Etv6*$^{fl/fl}$ (Ctrl) and *R26CreER*$^{+/-}$ *Etv6*$^{fl/fl}$ (R26-Etv6$^{\Delta}$) spleen (SPL) and bone marrow (BM) (mean ± SD, n = 4-5). Mice were treated with 5 mg of tamoxifen by oral gavage for 3 consecutive days and analyzed 9 days after last treatment. B cells were identified as B220^{+} MHCII^{hi}.

(B) MFI of Sca1 expression in mature B cells in *Etv6*$^{fl/fl}$ (Ctrl) and *CD11c-Cre*$^{+/-}$ *Etv6*$^{fl/-}$ (CD11c-Etv6$^{\Delta/-}$) SPL and BM (mean ± SD, n = 4). B cells were identified as B220^{+} MHCII^{hi}.

For C-G, *Etv6*$^{fl/fl}$ (Ctrl) and *Cx3cr1-CreER*$^{+/-}$ *Etv6*$^{fl/fl}$ (Cx3cr1-Etv6$^{\Delta}$) mice were treated with 5 mg of tamoxifen by oral gavage for 3 consecutive days and analyzed 5 days after last treatment. B cells were identified as B220^{+} MHCII^{hi} IgD^{+}.

(C) MFI of Sca1 expression in mature B cells in SPL and BM (mean ± SD, n = 6).

(D) Representative histograms of Sca1 expression in various immune cells in SPL and BM. Cell types were identified as follows: granulocytes - Lineage(Ly6G)$^{+}$ CD11b^{+} FSC^{hi} SSC^{hi}; monocytes (as in Fig. 3.7A); pDCs (as in Fig. 3.1C); B cells - B220^{+} MHCII^{hi} IgD^{+}; cDC subsets (as in Fig. 3.2A).

(E) Fold change of Sca1 MFI in various immune cells as defined in (D) in SPL. To calculate fold change, individual Cx3cr1-Etv6$^{\Delta}$ Sca1 MFIs were normalized to the Ctrl mean MFI for each tissue cell type. Dotted line delineates fold change of 1 (mean ± SD, n = 6).

(F) Fold change of Sca1 MFI in various immune cells as defined in (D) in BM (mean ± SD, n = 6). Fold change was calculated as in (E). c-Kit hi progentiors were defined as in (Fig. 3.8C).

(G) Fold change of Sca1 MFI in various immune cells as defined in (D) in blood (mean ± SD, n = 6). Fold change was calculated as in (E). B cells were defined as Lineage(B220)$^{+}$ MHCII^{+} SSC^{lo} FSC^{lo}.

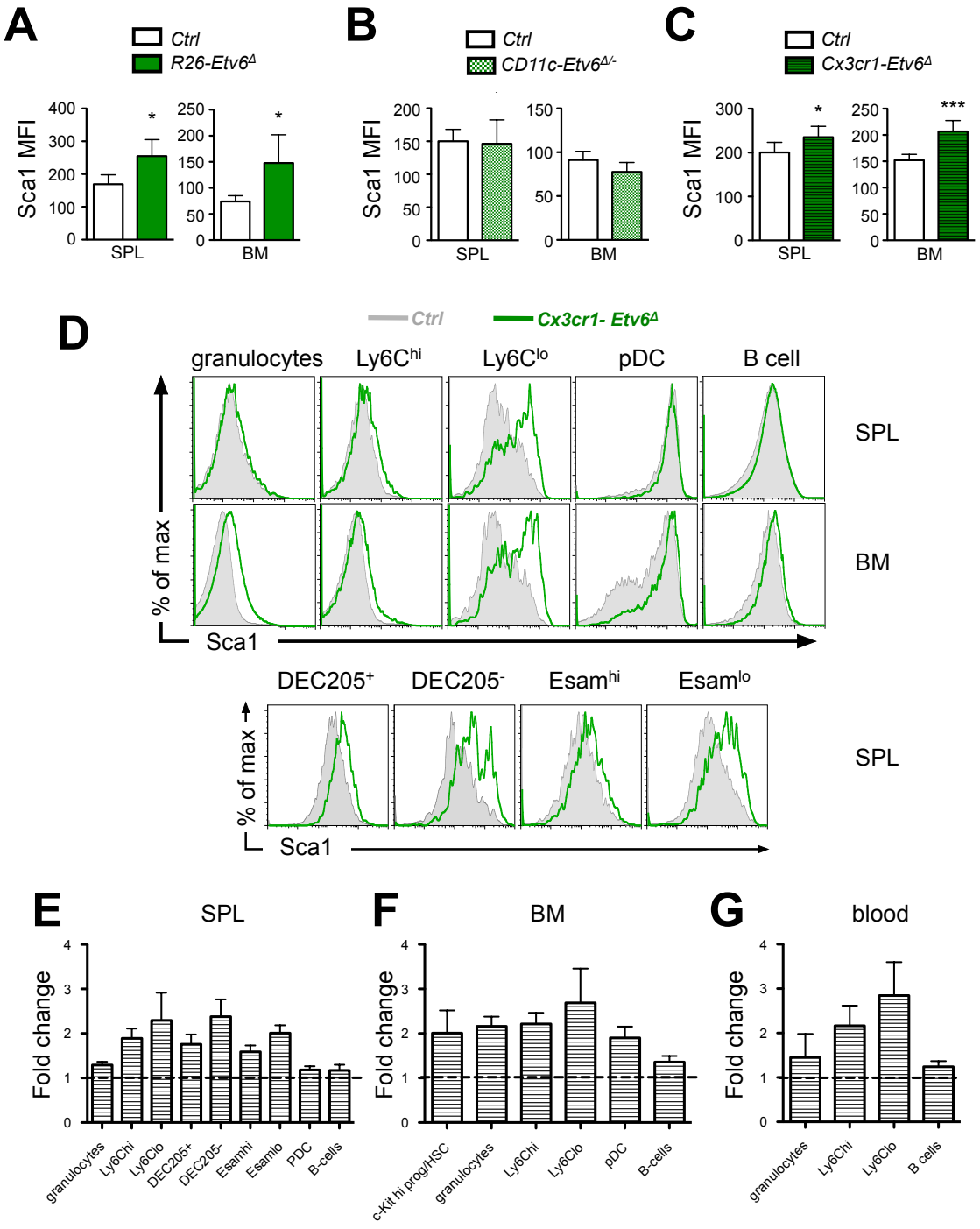
A
Ctrl
R26-Etv6Δ
Sca1 MFI
SPL
BM
B
Ctrl
CD11c-Etv6Δ/-
C
Ctrl
Cx3cr1-Etv6Δ
D
Ctrl
Cx3cr1- Etv6Δ
granulocytes
Ly6Chi
Ly6Clo
pDC
B cell
% of max
Sca1
DEC205+
DEC205-
Esamhi
Esamlo
E
SPL
F
BM
G
blood
Fold change
granulocytes
Ly6Chi
Ly6Clo
DEC205+
DEC205-
Esamhi
Esamlo
PDC
B-cells
c-Kit hi prog/HSC
pDC

Figure 3.10. YFP expression in untreated *Cx3cr1-CreER* mice.

(A) Representative staining profiles of YFP expression in spleen. Cell types were identified as follows: granulocytes - Lineage(Ly6G)$^{+}$ CD11b^{+} FSC^{hi} SSC^{hi}; monocytes (as in Fig. 3.7A); pDCs (as in Fig. 3.1C); B-cells - B220^{+} MHCII^{hi} IgD^{+}; cDC subsets (as in Fig. 3.2A).

(B) Representative staining profiles of YFP expression in bone marrow. Cell types were defined as in (A).

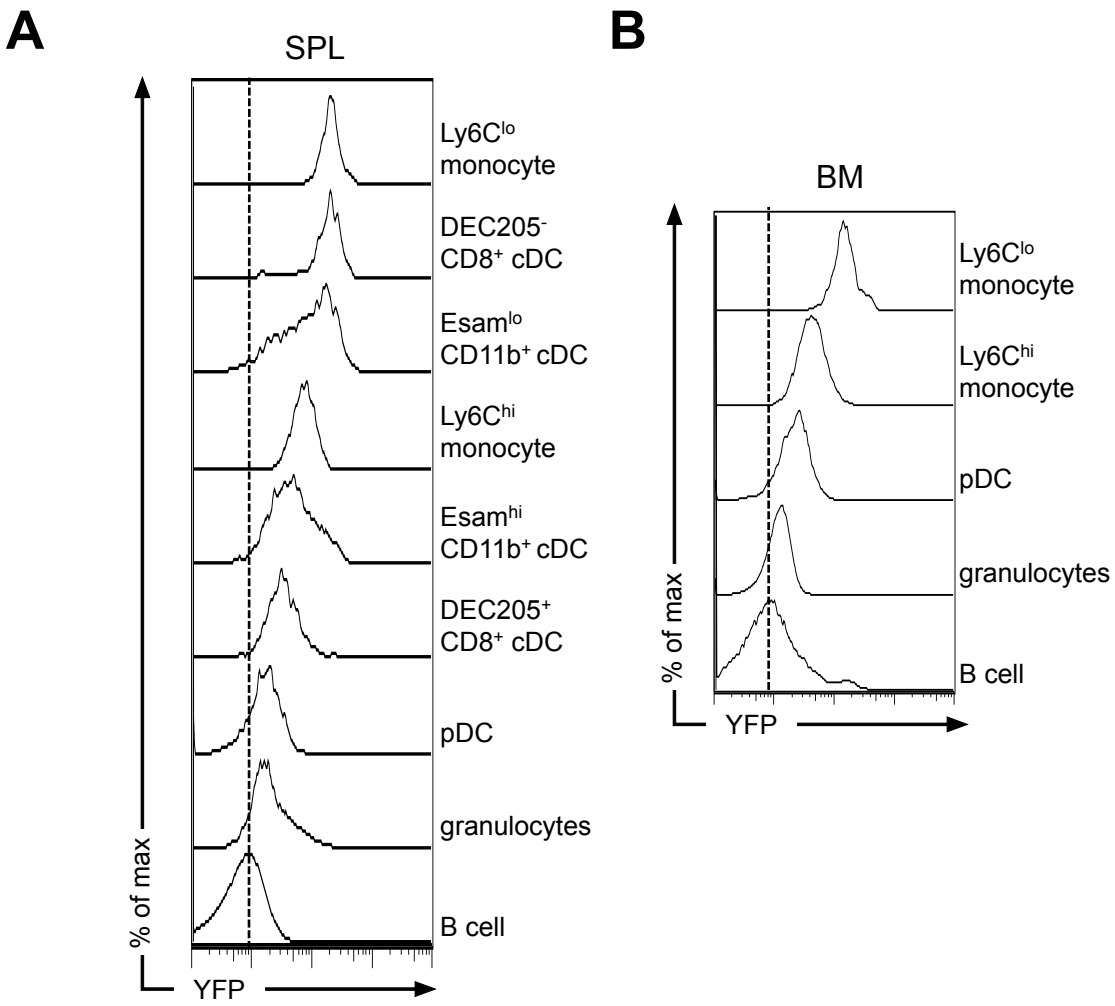
A
SPL
Ly6C^lo monocyte
DEC205^- CD8^+ cDC
Esam^lo CD11b^+ cDC
Ly6C^hi monocyte
Esam^hi CD11b^+ cDC
DEC205^+ CD8^+ cDC
pDC
granulocytes
B cell
% of max
YFP
B
BM
Ly6C^lo monocyte
Ly6C^hi monocyte
pDC
granulocytes
B cell
% of max
YFP

CONCLUSIONS AND FUTURE DIRECTIONS

The role of immunosurveillance in acute myeloid leukemia: a new perspective

Acute myeloid leukemia (AML), like other tumors, is not simply a disease of uncontrolled, cell-intrinsic cell expansion – it is also a disease of immunodeficiency specific to tumor immunosurveillance. The role of the immune system during cancer development has only recently been appreciated as one of the hallmarks of cancer[101]. Pioneering studies using carcinogen-induced tumors established a clear role for the immune system in eliminating and shaping cancer development, and since then several studies have validated the concept of cancer immunosurveillance[100,105,209,210]. But while immunosurveillance in solid tumors has been well studied, immunosurveillance in hematological tumors has been relatively under-explored, especially in leukemia. Moreover, even fewer studies exist that explore the role of DCs in the immunosurveillance of leukemia.

In this study, we focus on Flt3, an established developmental regulator of the DC lineage. Our knowledge of this fundamental pathway paved the way to investigate the effect of its dysregulated activation in DC homeostasis and explore the potential consequences on the immune system. We found that a prominent form of the mutated receptor, Flt3-ITD, found in AML, causes the expansion of DC subsets and supports the modulation of T cell responses, including the increased presence of regulatory T cells. Collectively, we offer a new mechanism in which DCs can promote leukemogenesis before the clinical manifestations of the disease. Because of their important role in facilitating immune tolerance, the DC lineage would be an attractive target for tumor exploitation. Indeed, AML DCs have been described to be abnormal and/or dysfunctional, and have also been proposed to affect T cell activity and promote T_{reg} induction[113-115]. But these mechanisms have been restricted to mainly *in vitro* systems, and to our knowledge, no specific mechanisms have been tied to these phenomena *in vivo* until now.

Beyond implicating an active role for DCs in leukemogenesis, this work also underlines the unique ability of AML mutations in infiltrating the immune system, which prompts a new perspective on leukemogenesis. More often than not, mutations involved in immune evasion in AML have been described in a similar fashion as in solid tumors, that is, as a separate entity from the immune system (Figure 4.1A). For example, relapsed leukemia has been described to downregulate mismatched HLA

molecules to avoid cytotoxicity from graft-versus-leukemia effects, and there is an increased frequency of AMLs that express inhibitory molecules that promote escape from NK-cell mediated cytotoxicity[211,212]. However, the genetic landscape of AML is quite different from solid tumors, in that relatively few genetic mutations are present[213]. This phenomenon would suggest that prominent AML mutations serve additional purposes beyond cell-intrinsic transformation. Because both the leukemia and immune cells arise from the same source, AML out of all tumors would have the unique ability to co-opt the immune system, requiring the least amount of genetic manipulation if it can target an opportune gene. Specific stem/progenitor mutations like the Flt3-ITD mutation, which like many other genetic lesions intrinsically promotes the proliferation and survival of the tumor itself, may carry down the mutation to downstream immune cells and thereby have a dual role in modulating immunosurveillance (Figure 4.1B). We propose that other single mutations found in leukemia likely exist that harbor the same kind of multi-tasking ability of intrinsically transforming a cell and disabling immunosurveillance. While our observations on the DC lineage and regulatory T cells are specific to the Flt3-ITD mutation, certainly mutations that affect other immune cells may support their own strategies of immune evasion. Therefore, future directions require the re-evaluation of prominently occurring AML mutations, not just as factors that promote cell-intrinsic survival, growth, or proliferation, but also as factors that promote immune modulation. This altered perspective may unveil potentially new features of tumor promotion and provide more nuanced mechanistic explanations as to why particular mutations are associated with more aggressive disease. It is clear that the current standard of broad-spectrum chemotherapy that targets proliferating cells is insufficient and obsolete, thus this new perspective will be imperative for developing new therapeutic strategies for AML that are tailored for specific subgroups, and thus will highlight the most important signaling pathways to target.

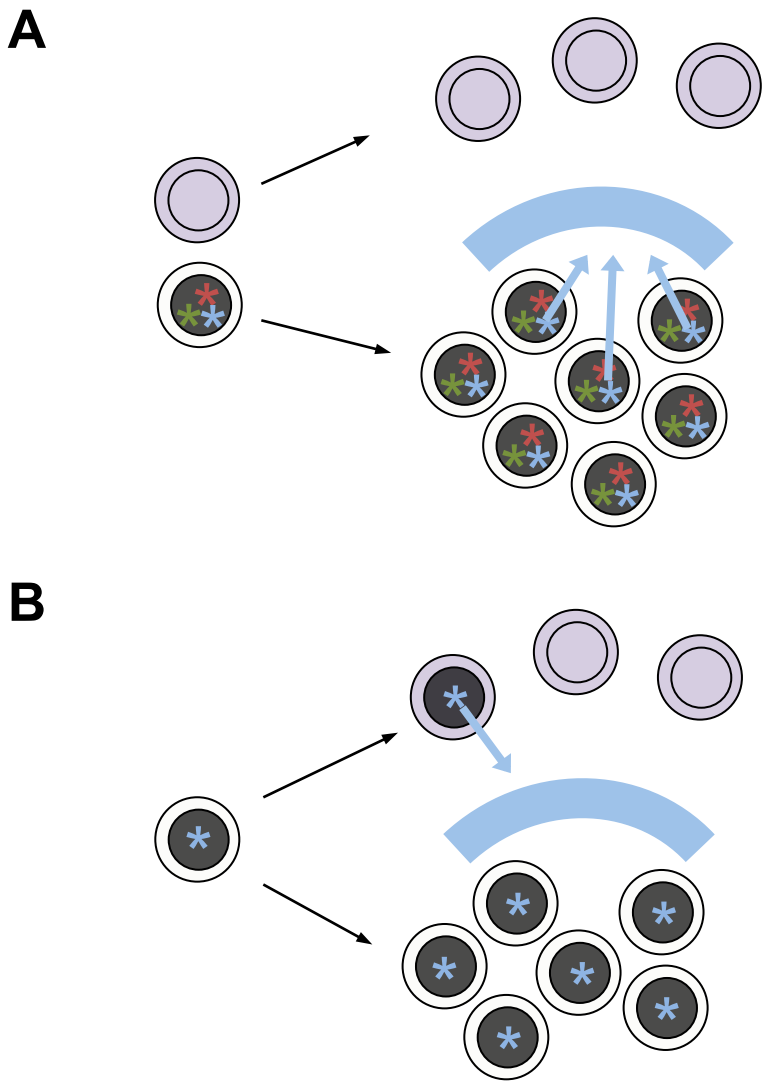

Figure 4.1. Immune evasion in solid tumors versus leukemias.

(A) Tumor cells from solid tumors acquire several mutations that separately promote cell-intrinsic transformation and protection from the immune system. Purple cells represent immune cells, and black cells with white borders represent tumor cells. Blue bar signifies protection from immune elimination. Asterisks signify different mutations.

(B) Leukemic cells acquire few mutations that dually promote transformation and protection from the immune system at the same time. Purple cells represent immune cells, black cells with white border represent leukemic cells, and black cell with purple border represents leukemia-derived immune cell. Blue bar signifies protection from immune elimination. Asterisk signifies one mutation.

Uncovering new mechanisms of DC fate decisions

The central role of DCs in facilitating the adaptive immune response prompts a comprehensive examination of the basic mechanisms that control their development and function. Their clear functional heterogeneity highlights the need to better understand how these subsets develop in order to take advantage of this division of labor for therapeutic use. Several questions still remain on the basic development of DCs in the steady state, such as which factors specifically control the lineage specification of cDCs over pDCs, and the precise mechanism of cDC differentiation. By studying the roles of two candidate genes, this thesis work enhances our understanding of cDC development.

We explored the implication of two transcription factors, Mycl1 and Etv6, in regulating genetic programs that would affect DCs in the steady state. Despite its expression specificity in DCs, several lines of phenotypic and functional analyses provide support for a negligible role of Mycl1 in the general development and function of DCs (Figure 4.2), and raises debate on its recently described role in DC function and proliferation. While technical considerations and genetic redundancy may account for the disparity, we conclude that cDCs are relatively functional in the absence of Mycl1, and that Mycl1 does not influence the development of the cDC lineage. Etv6, on the other hand, shows a more apparent influence in DC homeostasis and development. Early on in DC development, it seems to affect the development of $CD8^+$ cDCs, and late in DC development, it may continue to play a role in mature pDC and cDC commitment, quite possibly function (Figure 4.2). In addition, it may also play a potential role in monocyte homeostasis and a functional role as a suppressor of unwarranted cytokine secretion. All of these observations are still in their nascent state, so clearly future actions are required to corroborate these claims. Functional studies in T cell priming will be required to assess whether the effect of Etv6 on mature DCs compromises their identity, while infection models that induce inflammation like *Listeria monocytogenes* will be useful in examining the effector functions of Etv6 monocytes. Furthermore, a more comprehensive analysis of the interferon signature will be required, using genome-wide analysis and genetic models to elucidate a mechanism.

Nevertheless, while it is clear that Etv6 may have multiple roles during DC development, this promising role of Etv6 in cDC differentiation will provide significant insight on a portion of DC development that is not well described. Few transcription factors have been identified as regulators of the late terminal

commitment of cDC subsets. These include Batf3, Id2, and Irf8 for $CD8^+$ cDCs, and RelB and Irf4 for $CD11b^+$ cDCs. However, these transcription factors selectively affect one cDC subset over the other, and currently there is yet to be a common transcription factor that has been described to be important for the commitment of both. Bcl6-deficiency has been shown lead to the depletion of both cDC subtypes, however it seems to promote the survival of these cells, rather than their commitment[214]. In contrast, deletion of Etv6 late in DC development does not seem to grossly alter the quantity of these cDCs, but instead grossly alters the quality of the cDCs as observed by cell surface phenotype, which is a feature that already distinguishes it from other transcription factors. The effect on differentiation may ultimately have a significant impact on cDC function and identity. Furthermore, as a member of one of the biggest families of transcription factors among metazoans, the study of Etv6 and the nature of other Ets-family binding partners throughout DC development may provide a versatile mechanism for which the DC lineage could resolve DC fate commitment. Overall, Etv6 remains as a prospective, novel regulator of cDC differentiation and function, and the dissection of its regulation will provide key insight on the mechanisms of cDC development.

Collectively, the work presented here dissects the normal regulatory mechanisms that govern the development of mononuclear phagocytes, with emphasis on DC development. We provide new insight on how normal regulatory mechanisms in DC development can be misappropriated for pathological conditions such as leukemia. Furthermore, we provide support for a dispensable role of Mycl1 in DC development and function, which conflicts with previous findings. Finally, we lay a foundation for an uncharacterized role of Etv6 in DC and monocyte homeostasis and the regulation of cytokine signaling. Overall, the examination of these basic regulatory mechanisms will advance our understanding of DC biology, and ultimately provide further support for therapeutic application.

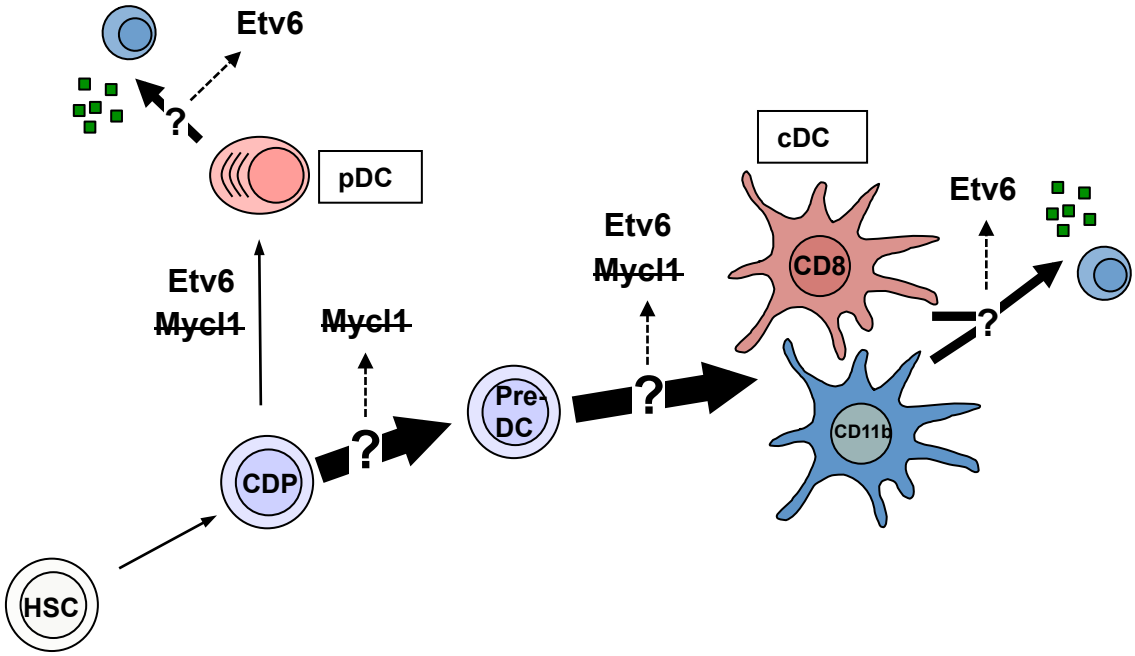

Figure 4.2. Summary of the roles of Mycl1 and Etv6 during DC development.

Questions still remain on what transcriptional factors control the cDC lineage commitment, differentiation, and function. This thesis work rules out Mycl1 as an important regulator of overall DC development, while implicates Etv6 as a promising candidate that regulates DC differentiation and potentially function.

REFERENCES

1. Akira S, Uematsu S, Takeuchi O. Pathogen recognition and innate immunity. *Cell*. 2006;124(4):783-801.

2. Long EO, Kim HS, Liu D, Peterson ME, Rajagopalan S. Controlling natural killer cell responses: integration of signals for activation and inhibition. *Annu Rev Immunol*. 2013;31:227-258.

3. Litman GW, Rast JP, Fugmann SD. The origins of vertebrate adaptive immunity. *Nat Rev Immunol*. 2010;10(8):543-553.

4. Bonilla FA, Oettgen HC. Adaptive immunity. *J Allergy Clin Immunol*. 2010;125(2 Suppl 2):S33-40.

5. Janeway CA, Jr. How the immune system protects the host from infection. *Microbes Infect*. 2001;3(13):1167-1171.

6. Langerhans P. Über die Nerven der menschlichen Haut. *Virchows Archiv*. 1868;44(2-3):325-337.

7. Steinman RM, Cohn ZA. Identification of a novel cell type in peripheral lymphoid organs of mice. I. Morphology, quantitation, tissue distribution. *J Exp Med*. 1973;137(5):1142-1162.

8. Steinman RM, Witmer MD. Lymphoid dendritic cells are potent stimulators of the primary mixed leukocyte reaction in mice. *Proc Natl Acad Sci U S A*. 1978;75(10):5132-5136.

9. Merad M, Sathe P, Helft J, Miller J, Mortha A. The dendritic cell lineage: ontogeny and function of dendritic cells and their subsets in the steady state and the inflamed setting. *Annu Rev Immunol*. 2013;31:563-604.

10. Liu K, Waskow C, Liu XT, Yao KH, Hoh J, Nussenzweig M. Origin of dendritic cells in peripheral lymphoid organs of mice. *Nature Immunology*. 2007;8(6):578-583.

11. Traver D, Akashi K, Manz M, et al. Development of CD8alpha-positive dendritic cells from a common myeloid progenitor. *Science*. 2000;290(5499):2152-2154.

12. Schlenner SM, Madan V, Busch K, et al. Fate mapping reveals separate origins of T cells and myeloid lineages in the thymus. *Immunity*. 2010;32(3):426-436.

13. Liu K, Victora GD, Schwickert TA, et al. In vivo analysis of dendritic cell development and homeostasis. *Science*. 2009;324(5925):392-397.

14. Sathe P, Metcalf D, Vremec D, et al. Lymphoid tissue and plasmacytoid dendritic cells and macrophages do not share a common macrophage-dendritic cell-restricted progenitor. *Immunity*. 2014;41(1):104-115.

15. Dudziak D, Kamphorst AO, Heidkamp GF, et al. Differential antigen processing by dendritic cell subsets in vivo. *Science*. 2007;315(5808):107-111.

16. Mebius RE, Kraal G. Structure and function of the spleen. *Nat Rev Immunol*. 2005;5(8):606-616.

17. Hildner K, Edelson BT, Purtha WE, et al. Batf3 deficiency reveals a critical role for CD8alpha+ dendritic cells in cytotoxic T cell immunity. *Science*. 2008;322(5904):1097-1100.

18. Lewis KL, Caton ML, Bogunovic M, et al. Notch2 receptor signaling controls functional differentiation of dendritic cells in the spleen and intestine. *Immunity*. 2011;35(5):780-791.

19. Mashayekhi M, Sandau MM, Dunay IR, et al. CD8alpha(+) dendritic cells are the critical source of interleukin-12 that controls acute infection by Toxoplasma gondii tachyzoites. *Immunity*. 2011;35(2):249-259.

20. Bar-On L, Birnberg T, Lewis KL, et al. CX3CR1+ CD8alpha+ dendritic cells are a steady-state population related to plasmacytoid dendritic cells. *Proc Natl Acad Sci U S A*. 2010;107(33):14745-14750.

21. Edelson BT, Kc W, Juang R, et al. Peripheral CD103+ dendritic cells form a unified subset developmentally related to CD8alpha+ conventional dendritic cells. *J Exp Med*. 2010;207(4):823-836.

22. Jaensson E, Uronen-Hansson H, Pabst O, et al. Small intestinal CD103+ dendritic cells display unique functional properties that are conserved between mice and humans. *J Exp Med*. 2008;205(9):2139-2149.

23. Bedoui S, Whitney PG, Waithman J, et al. Cross-presentation of viral and self antigens by skin-derived CD103+ dendritic cells. *Nat Immunol*. 2009;10(5):488-495.

24. del Rio ML, Rodriguez-Barbosa JI, Kremmer E, Forster R. CD103- and CD103+ bronchial lymph node dendritic cells are specialized in presenting and cross-presenting innocuous antigen to CD4+ and CD8+ T cells. *J Immunol*. 2007;178(11):6861-6866.

25. Mildner A, Jung S. Development and function of dendritic cell subsets. *Immunity*. 2014;40(5):642-656.

26. Bogunovic M, Ginhoux F, Helft J, et al. Origin of the lamina propria dendritic cell network. *Immunity*. 2009;31(3):513-525.

27. Cisse B, Caton ML, Lehner M, et al. Transcription factor E2-2 is an essential and specific regulator of plasmacytoid dendritic cell development. *Cell*. 2008;135(1):37-48.

28. Reizis B, Bunin A, Ghosh HS, Lewis KL, Sisirak V. Plasmacytoid dendritic cells: recent progress and open questions. *Annu Rev Immunol*. 2011;29:163-183.

29. Stirewalt DL, Radich JP. The role of FLT3 in haematopoietic malignancies. *Nat Rev Cancer*. 2003;3(9):650-665.

30. Agnes F, Shamoon B, Dina C, Rosnet O, Birnbaum D, Galibert F. Genomic structure of the downstream part of the human FLT3 gene: exon/intron structure conservation among genes encoding receptor tyrosine kinases (RTK) of subclass III. *Gene*. 1994;145(2):283-288.

31. Griffith J, Black J, Faerman C, et al. The structural basis for autoinhibition of FLT3 by the juxtamembrane domain. *Mol Cell*. 2004;13(2):169-178.

32. Turner AM, Lin NL, Issarachai S, Lyman SD, Broudy VC. FLT3 receptor expression on the surface of normal and malignant human hematopoietic cells. *Blood*. 1996;88(9):3383-3390.

33. Heiss E, Masson K, Sundberg C, et al. Identification of Y589 and Y599 in the juxtamembrane domain of Flt3 as ligand-induced autophosphorylation sites involved in binding of Src family kinases and the protein tyrosine phosphatase SHP2. *Blood*. 2006;108(5):1542-1550.

34. Lyman SD, James L, Vanden Bos T, et al. Molecular cloning of a ligand for the flt3/flk-2 tyrosine kinase receptor: a proliferative factor for primitive hematopoietic cells. *Cell*. 1993;75(6):1157-1167.

35. Hannum C, Culpepper J, Campbell D, et al. Ligand for FLT3/FLK2 receptor tyrosine kinase regulates growth of haematopoietic stem cells and is encoded by variant RNAs. *Nature*. 1994;368(6472):643-648.

36. Lyman SD, James L, Johnson L, et al. Cloning of the human homologue of the murine flt3 ligand: a growth factor for early hematopoietic progenitor cells. *Blood*. 1994;83(10):2795-2801.

37. Lyman SD, Jacobsen SE. c-kit ligand and Flt3 ligand: stem/progenitor cell factors with overlapping yet distinct activities. *Blood*. 1998;91(4):1101-1134.

38. McKenna HJ, Stocking KL, Miller RE, et al. Mice lacking flt3 ligand have deficient hematopoiesis affecting hematopoietic progenitor cells, dendritic cells, and natural killer cells. *Blood*. 2000;95(11):3489-3497.

39. Mendoza MC, Er EE, Blenis J. The Ras-ERK and PI3K-mTOR pathways: cross-talk and compensation. *Trends Biochem Sci*. 2011;36(6):320-328.

40. Dosil M, Wang S, Lemischka IR. Mitogenic signalling and substrate specificity of the Flk2/Flt3 receptor tyrosine kinase in fibroblasts and interleukin 3-dependent hematopoietic cells. *Mol Cell Biol*. 1993;13(10):6572-6585.

41. Rottapel R, Turck CW, Casteran N, et al. Substrate specificities and identification of a putative binding site for PI3K in the carboxy tail of the murine Flt3 receptor tyrosine kinase. *Oncogene*. 1994;9(6):1755-1765.

42. Zhang S, Mantel C, Broxmeyer HE. Flt3 signaling involves tyrosyl-phosphorylation of SHP-2 and SHIP and their association with Grb2 and Shc in Baf3/Flt3 cells. *J Leukoc Biol*. 1999;65(3):372-380.

43. Zhang S, Broxmeyer HE. Flt3 ligand induces tyrosine phosphorylation of gab1 and gab2 and their association with shp-2, grb2, and PI3 kinase. *Biochem Biophys Res Commun*. 2000;277(1):195-199.

44. Zhang S, Broxmeyer HE. p85 subunit of PI3 kinase does not bind to human Flt3 receptor, but associates with SHP2, SHIP, and a tyrosine-phosphorylated 100-kDa protein in Flt3 ligand-stimulated hematopoietic cells. *Biochem Biophys Res Commun*. 1999;254(2):440-445.

45. Sathaliyawala T, O'Gorman WE, Greter M, et al. Mammalian target of rapamycin controls dendritic cell development downstream of Flt3 ligand signaling. *Immunity*. 2010;33(4):597-606.

46. Choudhary C, Brandts C, Schwable J, et al. Activation mechanisms of STAT5 by oncogenic Flt3-ITD. *Blood*. 2007;110(1):370-374.

47. Zhang S, Fukuda S, Lee Y, et al. Essential role of signal transducer and activator of transcription (Stat)5a but not Stat5b for Flt3-dependent signaling. *J Exp Med*. 2000;192(5):719-728.

48. Birkenkamp KU, Geugien M, Lemmink HH, Kruijer W, Vellenga E. Regulation of constitutive STAT5 phosphorylation in acute myeloid leukemia blasts. *Leukemia*. 2001;15(12):1923-1931.

49. Hayakawa F, Towatari M, Kiyoi H, et al. Tandem-duplicated Flt3 constitutively activates STAT5 and MAP kinase and introduces autonomous cell growth in IL-3-dependent cell lines. *Oncogene*. 2000;19(5):624-631.

50. Mizuki M, Fenski R, Halfter H, et al. Flt3 mutations from patients with acute myeloid leukemia induce transformation of 32D cells mediated by the Ras and STAT5 pathways. *Blood*. 2000;96(12):3907-3914.

51. Kiyoi H, Ohno R, Ueda R, Saito H, Naoe T. Mechanism of constitutive activation of FLT3 with internal tandem duplication in the juxtamembrane domain. *Oncogene*. 2002;21(16):2555-2563.

52. Spiekermann K, Bagrintseva K, Schwab R, Schmieja K, Hiddemann W. Overexpression and constitutive activation of FLT3 induces STAT5 activation in primary acute myeloid leukemia blast cells. *Clin Cancer Res*. 2003;9(6):2140-2150.

53. Rocnik JL, Okabe R, Yu JC, et al. Roles of tyrosine 589 and 591 in STAT5 activation and transformation mediated by FLT3-ITD. *Blood*. 2006;108(4):1339-1345.

54. Masson K, Liu T, Khan R, Sun J, Ronnstrand L. A role of Gab2 association in Flt3 ITD mediated Stat5 phosphorylation and cell survival. *Br J Haematol*. 2009;146(2):193-202.

55. Rosnet O, Marchetto S, deLapeyriere O, Birnbaum D. Murine Flt3, a gene encoding a novel tyrosine kinase receptor of the PDGFR/CSF1R family. *Oncogene*. 1991;6(9):1641-1650.

56. deLapeyriere O, Naquet P, Planche J, et al. Expression of Flt3 tyrosine kinase receptor gene in mouse hematopoietic and nervous tissues. *Differentiation*. 1995;58(5):351-359.

57. Rosnet O, Schiff C, Pebusque MJ, et al. Human FLT3/FLK2 gene: cDNA cloning and expression in hematopoietic cells. *Blood*. 1993;82(4):1110-1119.

58. Adolfsson J, Borge OJ, Bryder D, et al. Upregulation of Flt3 expression within the bone marrow Lin(-)Sca1(+)c-kit(+) stem cell compartment is accompanied by loss of self-renewal capacity. *Immunity*. 2001;15(4):659-669.

59. Chu SH, Heiser D, Li L, et al. FLT3-ITD knockin impairs hematopoietic stem cell quiescence/homeostasis, leading to myeloproliferative neoplasm. *Cell Stem Cell*. 2012;11(3):346-358.

60. Kikushige Y, Yoshimoto G, Miyamoto T, et al. Human Flt3 is expressed at the hematopoietic stem cell and the granulocyte/macrophage progenitor stages to maintain cell survival. *J Immunol*. 2008;180(11):7358-7367.

61. Sitnicka E, Buza-Vidas N, Larsson S, Nygren JM, Liuba K, Jacobsen SE. Human CD34+ hematopoietic stem cells capable of multilineage engrafting NOD/SCID mice express flt3: distinct flt3 and c-kit expression and response patterns on mouse and candidate human hematopoietic stem cells. *Blood*. 2003;102(3):881-886.

62. Karsunky H, Merad M, Cozzio A, Weissman IL, Manz MG. Flt3 ligand regulates dendritic cell development from Flt3+ lymphoid and myeloid-committed progenitors to Flt3+ dendritic cells in vivo. *J Exp Med*. 2003;198(2):305-313.

63. Sambandam A, Maillard I, Zediak VP, et al. Notch signaling controls the generation and differentiation of early T lineage progenitors. *Nat Immunol*. 2005;6(7):663-670.

64. Boiers C, Buza-Vidas N, Jensen CT, et al. Expression and role of FLT3 in regulation of the earliest stage of normal granulocyte-monocyte progenitor development. *Blood*. 2010;115(24):5061-5068.

65. Sitnicka E, Bryder D, Theilgaard-Monch K, Buza-Vidas N, Adolfsson J, Jacobsen SE. Key role of flt3 ligand in regulation of the common lymphoid progenitor but not in maintenance of the hematopoietic stem cell pool. *Immunity*. 2002;17(4):463-472.

66. Mackarehtschian K, Hardin JD, Moore KA, Boast S, Goff SP, Lemischka IR. Targeted Disruption of the Flk2/Flt3 Gene Leads to Deficiencies in Primitive Hematopoietic Progenitors. *Immunity*. 1995;3(1):147-161.

67. Liu K, Nussenzweig MC. Origin and development of dendritic cells. *Immunological Reviews*. 2010;234:45-54.

68. Waskow C, Liu K, Darrasse-Jeze G, et al. The receptor tyrosine kinase Flt3 is required for dendritic cell development in peripheral lymphoid tissues. *Nature Immunology*. 2008;9(6):676-683.

69. Maraskovsky E, Brasel K, Teepe M, et al. Dramatic increase in the numbers of functionally mature dendritic cells in Flt3 ligand-treated mice: Multiple dendritic cell subpopulations identified. *Journal of Experimental Medicine*. 1996;184(5):1953-1962.

70. Maraskovsky E, Daro E, Roux E, et al. In vivo generation of human dendritic cell subsets by Flt3 ligand. *Blood*. 2000;96(3):878-884.

71. Lynch DH, Andreasen A, Maraskovsky E, Whitmore J, Miller RE, Schuh JCL. Flt3 ligand induces tumor regression and antitumor immune responses in vivo. *Nature Medicine*. 1997;3(6):625-631.

72. Pulendran B, Smith JL, Jenkins M, Schoenborn M, Maraskovsky E, Maliszewski CR. Prevention of peripheral tolerance by a dendritic cell growth factor: flt3 ligand as an adjuvant. *J Exp Med*. 1998;188(11):2075-2082.

73. Vollstedt S, Franchini M, Hefti HP, et al. Flt3 ligand-treated neonatal mice have increased innate immunity against intracellular pathogens and efficiently control virus infections. *J Exp Med*. 2003;197(5):575-584.

74. Kurts C, Kosaka H, Carbone FR, Miller JF, Heath WR. Class I-restricted cross-presentation of exogenous self-antigens leads to deletion of autoreactive CD8(+) T cells. *J Exp Med*. 1997;186(2):239-245.

75. Brocker T, Riedinger M, Karjalainen K. Targeted expression of major histocompatibility complex (MHC) class II molecules demonstrates that dendritic cells can induce negative but not positive selection of thymocytes in vivo. *J Exp Med*. 1997;185(3):541-550.

76. Hawiger D, Inaba K, Dorsett Y, et al. Dendritic cells induce peripheral T cell unresponsiveness under steady state conditions in vivo. *J Exp Med*. 2001;194(6):769-779.

77. Probst HC, McCoy K, Okazaki T, Honjo T, van den Broek M. Resting dendritic cells induce peripheral CD8+ T cell tolerance through PD-1 and CTLA-4. *Nat Immunol*. 2005;6(3):280-286.

78. Schildknecht A, Brauer S, Brenner C, et al. FoxP3+ regulatory T cells essentially contribute to peripheral CD8+ T-cell tolerance induced by steady-state dendritic cells. *Proc Natl Acad Sci U S A*. 2010;107(1):199-203.

79. Collins CB, Aherne CM, McNamee EN, et al. Flt3 ligand expands CD103(+) dendritic cells and FoxP3(+) T regulatory cells, and attenuates Crohn's-like murine ileitis. *Gut*. 2012;61(8):1154-1162.

80. Darrasse-Jeze G, Deroubaix S, Mouquet H, et al. Feedback control of regulatory T cell homeostasis by dendritic cells in vivo. *J Exp Med*. 2009;206(9):1853-1862.

81. Choi JH, Cheong C, Dandamudi DB, et al. Flt3 signaling-dependent dendritic cells protect against atherosclerosis. *Immunity*. 2011;35(5):819-831.

82. Chilton PM, Rezzoug F, Fugier-Vivier I, et al. Flt3-ligand treatment prevents diabetes in NOD mice. *Diabetes*. 2004;53(8):1995-2002.

83. Swee LK, Bosco N, Malissen B, Ceredig R, Rolink A. Expansion of peripheral naturally occurring T regulatory cells by Fms-like tyrosine kinase 3 ligand treatment. *Blood*. 2009;113(25):6277-6287.

84. Kim JM, Rasmussen JP, Rudensky AY. Regulatory T cells prevent catastrophic autoimmunity throughout the lifespan of mice. *Nat Immunol*. 2007;8(2):191-197.

85. Nakao M, Yokota S, Iwai T, et al. Internal tandem duplication of the flt3 gene found in acute myeloid leukemia. *Leukemia*. 1996;10(12):1911-1918.

86. Levis M. FLT3 mutations in acute myeloid leukemia: what is the best approach in 2013? *Hematology Am Soc Hematol Educ Program*. 2013;2013:220-226.

87. Rombouts WJ, Blokland I, Lowenberg B, Ploemacher RE. Biological characteristics and prognosis of adult acute myeloid leukemia with internal tandem duplications in the Flt3 gene. *Leukemia*. 2000;14(4):675-683.

88. Kottaridis PD, Gale RE, Frew ME, et al. The presence of a FLT3 internal tandem duplication in patients with acute myeloid leukemia (AML) adds important prognostic information to cytogenetic risk group and response to the first cycle of chemotherapy: analysis of 854 patients from the United Kingdom Medical Research Council AML 10 and 12 trials. *Blood*. 2001;98(6):1752-1759.

89. Frohling S, Schlenk RF, Breitruck J, et al. Prognostic significance of activating FLT3 mutations in younger adults (16 to 60 years) with acute myeloid leukemia and normal cytogenetics: a study of the AML Study Group Ulm. *Blood*. 2002;100(13):4372-4380.

90. Roboz GJ. Novel approaches to the treatment of acute myeloid leukemia. *Hematology Am Soc Hematol Educ Program*. 2011;2011:43-50.

91. Wander SA, Levis MJ, Fathi AT. The evolving role of FLT3 inhibitors in acute myeloid leukemia: quizartinib and beyond. *Ther Adv Hematol*. 2014;5(3):65-77.

92. Smith CC, Wang Q, Chin CS, et al. Validation of ITD mutations in FLT3 as a therapeutic target in human acute myeloid leukaemia. *Nature*. 2012;485(7397):260-U153.

93. Schnittger S, Schoch C, Dugas M, et al. Analysis of FLT3 length mutations in 1003 patients with acute myeloid leukemia: correlation to cytogenetics, FAB subtype, and prognosis in the AMLCG study and usefulness as a marker for the detection of minimal residual disease. *Blood*. 2002;100(1):59-66.

94. Breitenbuecher F, Schnittger S, Grundler R, et al. Identification of a novel type of ITD mutations located in nonjuxtamembrane domains of the FLT3 tyrosine kinase receptor. *Blood*. 2009;113(17):4074-4077.

95. Lee BH, Tothova Z, Levine RL, et al. FLT3 mutations confer enhanced proliferation and survival properties to multipotent progenitors in a murine model of chronic myelomonocytic leukemia. *Cancer Cell*. 2007;12(4):367-380.

96. Li L, Piloto O, Nguyen HB, et al. Knock-in of an internal tandem duplication mutation into murine FLT3 confers myeloproliferative disease in a mouse model. *Blood*. 2008;111(7):3849-3858.

97. Kelly LM, Kutok JL, Williams IR, et al. PML/RARalpha and FLT3-ITD induce an APL-like disease in a mouse model. *Proc Natl Acad Sci U S A*. 2002;99(12):8283-8288.

98. Stubbs MC, Kim YM, Krivtsov AV, et al. MLL-AF9 and FLT3 cooperation in acute myelogenous leukemia: development of a model for rapid therapeutic assessment. *Leukemia*. 2008;22(1):66-77.

99. Greenblatt S, Li L, Slape C, et al. Knock-in of a FLT3/ITD mutation cooperates with a NUP98-HOXD13 fusion to generate acute myeloid leukemia in a mouse model. *Blood*. 2012;119(12):2883-2894.

100. Vesely MD, Kershaw MH, Schreiber RD, Smyth MJ. Natural Innate and Adaptive Immunity to Cancer. *Annual Review of Immunology, Vol 29*. 2011;29:235-271.

101. Hanahan D, Weinberg RA. Hallmarks of Cancer: The Next Generation. *Cell*. 2011;144(5):646-674.

102. Dunn GP, Bruce AT, Ikeda H, Old LJ, Schreiber RD. Cancer immunoediting: from immunosurveillance to tumor escape. *Nat Immunol*. 2002;3(11):991-998.

103. Diamond MS, Kinder M, Matsushita H, et al. Type I interferon is selectively required by dendritic cells for immune rejection of tumors. *Journal of Experimental Medicine*. 2011;208(10):1989-2003.

104. Smyth MJ, Crowe NY, Godfrey DI. NK cells and NKT cells collaborate in host protection from methylcholanthrene-induced fibrosarcoma. *Int Immunol*. 2001;13(4):459-463.

105. Shankaran V, Ikeda H, Bruce AT, et al. IFNgamma and lymphocytes prevent primary tumour development and shape tumour immunogenicity. *Nature*. 2001;410(6832):1107-1111.

106. O'Sullivan T, Saddawi-Konefka R, Vermi W, et al. Cancer immunoediting by the innate immune system in the absence of adaptive immunity. *J Exp Med*. 2012;209(10):1869-1882.

107. Smyth MJ, Thia KY, Street SE, MacGregor D, Godfrey DI, Trapani JA. Perforin-mediated cytotoxicity is critical for surveillance of spontaneous lymphoma. *J Exp Med*. 2000;192(5):755-760.

108. Gabrilovich DI, Chen HL, Cunningham HT, et al. Production of vascular endothelial growth factor by human tumors inhibits the functional maturation of dendritic cells. *Nature Medicine*. 1996;2(10):1096-1103.

109. Villablanca EJ, Raccosta L, Zhou D, et al. Tumor-mediated liver X receptor-alpha activation inhibits CC chemokine receptor-7 expression on dendritic cells and dampens antitumor responses. *Nat Med*. 2010;16(1):98-105.

110. Krempski J, Karyampudi L, Behrens MD, et al. Tumor-infiltrating programmed death receptor-1+ dendritic cells mediate immune suppression in ovarian cancer. *J Immunol*. 2011;186(12):6905-6913.

111. Conrad C, Gregorio J, Wang YH, et al. Plasmacytoid dendritic cells promote immunosuppression in ovarian cancer via ICOS costimulation of Foxp3(+) T-regulatory cells. *Cancer Res*. 2012;72(20):5240-5249.

112. Barrett AJ, Le Blanc K. Immunotherapy prospects for acute myeloid leukaemia. *Clinical and Experimental Immunology*. 2010;161(2):223-232.

113. Mohty M, Jarrossay D, Lafage-Pochitaloff M, et al. Circulating blood dendritic cells from myeloid leukemia patients display quantitative and cytogenetic abnormalities as well as functional impairment. *Blood*. 2001;98(13):3750-3756.

114. Narita M, Takahashi M, Liu A, et al. Leukemia blast-induced T-cell anergy demonstrated by leukemia-derived dendritic cells in acute myelogenous leukemia. *Exp Hematol*. 2001;29(6):709-719.

115. Ge W, Ma X, Li X, et al. B7-H1 up-regulation on dendritic-like leukemia cells suppresses T cell immune function through modulation of IL-10/IL-12 production and generation of Treg cells. *Leuk Res*. 2009;33(7):948-957.

116. Teague RM, Kline J. Immune evasion in acute myeloid leukemia: current concepts and future directions. *J Immunother Cancer*. 2013;1(13).

117. Jung S, Aliberti J, Graemmel P, et al. Analysis of fractalkine receptor CX(3)CR1 function by targeted deletion and green fluorescent protein reporter gene insertion. *Mol Cell Biol*. 2000;20(11):4106-4114.

118. Li L, Bailey E, Greenblatt S, Huso D, Small D. Loss of the wild-type allele contributes to myeloid expansion and disease aggressiveness in FLT3/ITD knockin mice. *Blood*. 2011;118(18):4935-4945.

119. Mead AJ, Kharazi S, Atkinson D, et al. FLT3-ITDs instruct a myeloid differentiation and transformation bias in lymphomyeloid multipotent progenitors. *Cell Rep*. 2013;3(6):1766-1776.

120. Edelson BT, Bradstreet TR, Hildner K, et al. CD8alpha(+) dendritic cells are an obligate cellular entry point for productive infection by Listeria monocytogenes. *Immunity*. 2011;35(2):236-248.

121. Kharazi S, Mead AJ, Mansour A, et al. Impact of gene dosage, loss of wild-type allele, and FLT3 ligand on Flt3-ITD-induced myeloproliferation. *Blood*. 2011;118(13):3613-3621.

122. Rickmann M, Macke L, Sundarasetty BS, et al. Monitoring dendritic cell and cytokine biomarkers during remission prior to relapse in patients with FLT3-ITD acute myeloid leukemia. *Ann Hematol*. 2013.

123. Kamath AT, Pooley J, O'Keeffe MA, et al. The development, maturation, and turnover rate of mouse spleen dendritic cell populations. *J Immunol*. 2000;165(12):6762-6770.

124. Jan M, Snyder TM, Corces-Zimmerman MR, et al. Clonal evolution of preleukemic hematopoietic stem cells precedes human acute myeloid leukemia. *Sci Transl Med*. 2012;4(149):149ra118.

125. Shlush LI, Zandi S, Mitchell A, et al. Identification of pre-leukaemic haematopoietic stem cells in acute leukaemia. *Nature*. 2014;506(7488):328-333.

126. Rickmann M, Krauter J, Stamer K, et al. Elevated frequencies of leukemic myeloid and plasmacytoid dendritic cells in acute myeloid leukemia with the FLT3 internal tandem duplication. *Ann Hematol*. 2011;90(9):1047-1058.

127. Ustun C, Miller JS, Munn DH, Weisdorf DJ, Blazar BR. Regulatory T cells in acute myelogenous leukemia: is it time for immunomodulation? *Blood*. 2011;118(19):5084-5095.

128. Brunet S, Labopin M, Esteve J, et al. Impact of FLT3 internal tandem duplication on the outcome of related and unrelated hematopoietic transplantation for adult acute myeloid leukemia in first remission: a retrospective analysis. *J Clin Oncol*. 2012;30(7):735-741.

129. Mombaerts P, Iacomini J, Johnson RS, Herrup K, Tonegawa S, Papaioannou VE. RAG-1-deficient mice have no mature B and T lymphocytes. *Cell*. 1992;68(5):869-877.

130. Fontenot JD, Rasmussen JP, Williams LM, Dooley JL, Farr AG, Rudensky AY. Regulatory T cell lineage specification by the forkhead transcription factor foxp3. *Immunity*. 2005;22(3):329-341.

131. Ivanov, II, McKenzie BS, Zhou L, et al. The orphan nuclear receptor RORgammat directs the differentiation program of proinflammatory IL-17+ T helper cells. *Cell*. 2006;126(6):1121-1133.

132. Heng TS, Painter MW, Immunological Genome Project C. The Immunological Genome Project: networks of gene expression in immune cells. *Nat Immunol*. 2008;9(10):1091-1094.

133. Ghosh HS, Ceribelli M, Matos I, et al. ETO family protein Mtg16 regulates the balance of dendritic cell subsets by repressing Id2. *J Exp Med*. 2014;211(8):1623-1635.

134. Wu L, Nichogiannopoulou A, Shortman K, Georgopoulos K. Cell-autonomous defects in dendritic cell populations of Ikaros mutant mice point to a developmental relationship with the lymphoid lineage. *Immunity*. 1997;7(4):483-492.

135. Allman D, Dalod M, Asselin-Paturel C, et al. Ikaros is required for plasmacytoid dendritic cell differentiation. *Blood*. 2006;108(13):4025-4034.

136. Carotta S, Dakic A, D'Amico A, et al. The transcription factor PU.1 controls dendritic cell development and Flt3 cytokine receptor expression in a dose-dependent manner. *Immunity*. 2010;32(5):628-641.

137. Rathinam C, Geffers R, Yucel R, et al. The transcriptional repressor Gfi1 controls STAT3-dependent dendritic cell development and function. *Immunity*. 2005;22(6):717-728.

138. Laouar Y, Welte T, Fu XY, Flavell RA. STAT3 is required for Flt3L-dependent dendritic cell differentiation. *Immunity*. 2003;19(6):903-912.

139. Burkly L, Hession C, Ogata L, et al. Expression of relB is required for the development of thymic medulla and dendritic cells. *Nature*. 1995;373(6514):531-536.

140. Wu L, D'Amico A, Winkel KD, Suter M, Lo D, Shortman K. RelB is essential for the development of myeloid-related CD8alpha- dendritic cells but not of lymphoid-related CD8alpha+ dendritic cells. *Immunity*. 1998;9(6):839-847.

141. Le Bon A, Montoya M, Edwards MJ, et al. A role for the transcription factor RelB in IFN-alpha production and in IFN-alpha-stimulated cross-priming. *Eur J Immunol*. 2006;36(8):2085-2093.

142. Suzuki S, Honma K, Matsuyama T, et al. Critical roles of interferon regulatory factor 4 in CD11bhighCD8alpha- dendritic cell development. *Proc Natl Acad Sci U S A*. 2004;101(24):8981-8986.

143. Caton ML, Smith-Raska MR, Reizis B. Notch-RBP-J signaling controls the homeostasis of CD8-dendritic cells in the spleen. *J Exp Med*. 2007;204(7):1653-1664.

144. Jackson JT, Hu Y, Liu R, et al. Id2 expression delineates differential checkpoints in the genetic program of CD8alpha+ and CD103+ dendritic cell lineages. *EMBO J*. 2011;30(13):2690-2704.

145. Spits H, Couwenberg F, Bakker AQ, Weijer K, Uittenbogaart CH. Id2 and Id3 inhibit development of CD34(+) stem cells into predendritic cell (pre-DC)2 but not into pre-DC1. Evidence for a lymphoid origin of pre-DC2. *J Exp Med*. 2000;192(12):1775-1784.

146. Tamura T, Tailor P, Yamaoka K, et al. IFN regulatory factor-4 and -8 govern dendritic cell subset development and their functional diversity. *J Immunol*. 2005;174(5):2573-2581.

147. Schiavoni G, Mattei F, Sestili P, et al. ICSBP is essential for the development of mouse type I interferon-producing cells and for the generation and activation of CD8alpha(+) dendritic cells. *J Exp Med*. 2002;196(11):1415-1425.

148. Ghosh HS, Cisse B, Bunin A, Lewis KL, Reizis B. Continuous expression of the transcription factor e2-2 maintains the cell fate of mature plasmacytoid dendritic cells. *Immunity*. 2010;33(6):905-916.

149. Ippolito GC, Dekker JD, Wang YH, et al. Dendritic cell fate is determined by BCL11A. *Proc Natl Acad Sci U S A*. 2014;111(11):E998-1006.

150. Schotte R, Nagasawa M, Weijer K, Spits H, Blom B. The ETS transcription factor Spi-B is required for human plasmacytoid dendritic cell development. *J Exp Med*. 2004;200(11):1503-1509.

151. Sasaki I, Hoshino K, Sugiyama T, et al. Spi-B is critical for plasmacytoid dendritic cell function and development. *Blood*. 2012;120(24):4733-4743.

152. Meredith MM, Liu K, Darrasse-Jeze G, et al. Expression of the zinc finger transcription factor zDC (Zbtb46, Btbd4) defines the classical dendritic cell lineage. *J Exp Med*. 2012;209(6):1153-1165.

153. Satpathy AT, Kc W, Albring JC, et al. Zbtb46 expression distinguishes classical dendritic cells and their committed progenitors from other immune lineages. *J Exp Med*. 2012;209(6):1135-1152.

154. Meredith MM, Liu K, Kamphorst AO, et al. Zinc finger transcription factor zDC is a negative regulator required to prevent activation of classical dendritic cells in the steady state. *J Exp Med*. 2012;209(9):1583-1593.

155. Nau MM, Brooks BJ, Battey J, et al. L-myc, a new myc-related gene amplified and expressed in human small cell lung cancer. *Nature*. 1985;318(6041):69-73.

156. Dang CV. MYC on the path to cancer. *Cell*. 2012;149(1):22-35.

157. Barrett J, Birrer MJ, Kato GJ, Dosaka-Akita H, Dang CV. Activation domains of L-Myc and c-Myc determine their transforming potencies in rat embryo cells. *Mol Cell Biol*. 1992;12(7):3130-3137.

158. Moroy T, Verbeek S, Ma A, Achacoso P, Berns A, Alt F. E mu N- and E mu L-myc cooperate with E mu pim-1 to generate lymphoid tumors at high frequency in double-transgenic mice. *Oncogene*. 1991;6(11):1941-1948.

159. Hatton KS, Mahon K, Chin L, et al. Expression and activity of L-Myc in normal mouse development. *Mol Cell Biol*. 1996;16(4):1794-1804.

160. Zimmerman KA, Yancopoulos GD, Collum RG, et al. Differential expression of myc family genes during murine development. *Nature*. 1986;319(6056):780-783.

161. Su AI, Wiltshire T, Batalov S, et al. A gene atlas of the mouse and human protein-encoding transcriptomes. *Proc Natl Acad Sci U S A*. 2004;101(16):6062-6067.

162. Wu C, Orozco C, Boyer J, et al. BioGPS: an extensible and customizable portal for querying and organizing gene annotation resources. *Genome Biol*. 2009;10(11):R130.

163. Tussiwand R, Lee WL, Murphy TL, et al. Compensatory dendritic cell development mediated by BATF-IRF interactions. *Nature*. 2012;490(7421):502-507.

164. Kc W, Satpathy AT, Rapaport AS, et al. L-Myc expression by dendritic cells is required for optimal T-cell priming. *Nature*. 2014;507(7491):243-247.

165. Marcu KB, Bossone SA, Patel AJ. myc function and regulation. *Annu Rev Biochem*. 1992;61:809-860.

166. Gahan CG, Collins JK. Non-dystrophic 129 REJ mice are susceptible to i.p. infection with Listeria monocytogenes despite an ability to recruit inflammatory neutrophils to the peritoneal cavity. *Microb Pathog*. 1995;18(5):355-364.

167. Eilers M, Eisenman RN. Myc's broad reach. *Genes Dev*. 2008;22(20):2755-2766.

168. O'Gorman S, Dagenais NA, Qian M, Marchuk Y. Protamine-Cre recombinase transgenes efficiently recombine target sequences in the male germ line of mice, but not in embryonic stem cells. *Proc Natl Acad Sci U S A*. 1997;94(26):14602-14607.

169. Sharov AA, Dudekula DB, Ko MS. A web-based tool for principal component and significance analysis of microarray data. *Bioinformatics*. 2005;21(10):2548-2549.

170. Yona S, Kim KW, Wolf Y, et al. Fate mapping reveals origins and dynamics of monocytes and tissue macrophages under homeostasis. *Immunity*. 2013;38(1):79-91.

171. Varol C, Landsman L, Fogg DK, et al. Monocytes give rise to mucosal, but not splenic, conventional dendritic cells. *J Exp Med*. 2007;204(1):171-180.

172. van Furth R, Cohn ZA. The origin and kinetics of mononuclear phagocytes. *J Exp Med*. 1968;128(3):415-435.

173. van Furth R, Hirsch JG, Fedorko ME. Morphology and peroxidase cytochemistry of mouse promonocytes, monocytes, and macrophages. *J Exp Med*. 1970;132(4):794-812.

174. Goud TJ, Schotte C, van Furth R. Identification and characterization of the monoblast in mononuclear phagocyte colonies grown in vitro. *J Exp Med*. 1975;142(5):1180-1199.

175. Fogg DK, Sibon C, Miled C, et al. A clonogenic bone marrow progenitor specific for macrophages and dendritic cells. *Science*. 2006;311(5757):83-87.

176. Hettinger J, Richards DM, Hansson J, et al. Origin of monocytes and macrophages in a committed progenitor. *Nat Immunol*. 2013;14(8):821-830.

177. Ginhoux F, Jung S. Monocytes and macrophages: developmental pathways and tissue homeostasis. *Nat Rev Immunol*. 2014;14(6):392-404.

178. Dai XM, Ryan GR, Hapel AJ, et al. Targeted disruption of the mouse colony-stimulating factor 1 receptor gene results in osteopetrosis, mononuclear phagocyte deficiency, increased primitive progenitor cell frequencies, and reproductive defects. *Blood*. 2002;99(1):111-120.

179. Wiktor-Jedrzejczak W, Gordon S. Cytokine regulation of the macrophage (M phi) system studied using the colony stimulating factor-1-deficient op/op mouse. *Physiol Rev*. 1996;76(4):927-947.

180. Cecchini MG, Dominguez MG, Mocci S, et al. Role of colony stimulating factor-1 in the establishment and regulation of tissue macrophages during postnatal development of the mouse. *Development*. 1994;120(6):1357-1372.

181. Geissmann F, Jung S, Littman DR. Blood monocytes consist of two principal subsets with distinct migratory properties. *Immunity*. 2003;19(1):71-82.

182. Serbina NV, Pamer EG. Monocyte emigration from bone marrow during bacterial infection requires signals mediated by chemokine receptor CCR2. *Nat Immunol*. 2006;7(3):311-317.

183. Sunderkotter C, Nikolic T, Dillon MJ, et al. Subpopulations of mouse blood monocytes differ in maturation stage and inflammatory response. *J Immunol*. 2004;172(7):4410-4417.

184. Passlick B, Flieger D, Ziegler-Heitbrock HW. Identification and characterization of a novel monocyte subpopulation in human peripheral blood. *Blood*. 1989;74(7):2527-2534.

185. Weber C, Belge KU, von Hundelshausen P, et al. Differential chemokine receptor expression and function in human monocyte subpopulations. *J Leukoc Biol*. 2000;67(5):699-704.

186. Serbina NV, Salazar-Mather TP, Biron CA, Kuziel WA, Pamer EG. TNF/iNOS-producing dendritic cells mediate innate immune defense against bacterial infection. *Immunity*. 2003;19(1):59-70.

187. Mordue DG, Sibley LD. A novel population of Gr-1(+)-activated macrophages induced during acute toxoplasmosis. *Journal of Leukocyte Biology*. 2003;74(6):1015-1025.

188. Auffray C, Fogg D, Garfa M, et al. Monitoring of blood vessels and tissues by a population of monocytes with patrolling behavior. *Science*. 2007;317(5838):666-670.

189. Arnold L, Henry A, Poron F, et al. Inflammatory monocytes recruited after skeletal muscle injury switch into antiinflammatory macrophages to support myogenesis. *J Exp Med*. 2007;204(5):1057-1069.

190. Auffray C, Sieweke MH, Geissmann F. Blood monocytes: development, heterogeneity, and relationship with dendritic cells. *Annu Rev Immunol*. 2009;27:669-692.

191. Findlay VJ, LaRue AC, Turner DP, Watson PM, Watson DK. Understanding the role of ETS-mediated gene regulation in complex biological processes. *Adv Cancer Res*. 2013;119:1-61.

192. Coyne HJ, 3rd, De S, Okon M, et al. Autoinhibition of ETV6 (TEL) DNA binding: appended helices sterically block the ETS domain. *J Mol Biol*. 2012;421(1):67-84.

193. Mavrothalassitis G, Ghysdael J. Proteins of the ETS family with transcriptional repressor activity. *Oncogene*. 2000;19(55):6524-6532.

194. Golub TR, Barker GF, Lovett M, Gilliland DG. Fusion of PDGF receptor beta to a novel ets-like gene, tel, in chronic myelomonocytic leukemia with t(5;12) chromosomal translocation. *Cell*. 1994;77(2):307-316.

195. Bohlander SK. ETV6: a versatile player in leukemogenesis. *Semin Cancer Biol*. 2005;15(3):162-174.

196. Petrella T, Herve G, Bonnotte B, et al. Alpha-interferon secreting blastic plasmacytoid dendritic cells neoplasm: a case report with histological, molecular genetics and long-term tumor cells culture studies. *Am J Dermatopathol*. 2012;34(6):626-631.

197. Zhang MY, Churpek JE, Keel SB, et al. Germline ETV6 mutations in familial thrombocytopenia and hematologic malignancy. *Nat Genet*. 2015;47(2):180-185.

198. Wang LC, Kuo F, Fujiwara Y, Gilliland DG, Golub TR, Orkin SH. Yolk sac angiogenic defect and intra-embryonic apoptosis in mice lacking the Ets-related factor TEL. *EMBO J*. 1997;16(14):4374-4383.

199. Hock H, Meade E, Medeiros S, et al. Tel/Etv6 is an essential and selective regulator of adult hematopoietic stem cell survival. *Genes Dev*. 2004;18(19):2336-2341.

200. Lai ZC, Rubin GM. Negative control of photoreceptor development in Drosophila by the product of the yan gene, an ETS domain protein. *Cell*. 1992;70(4):609-620.

201. Rebay I, Rubin GM. Yan functions as a general inhibitor of differentiation and is negatively regulated by activation of the Ras1/MAPK pathway. *Cell*. 1995;81(6):857-866.

202. Maroulakou IG, Bowe DB. Expression and function of Ets transcription factors in mammalian development: a regulatory network. *Oncogene*. 2000;19(55):6432-6442.

203. Ciofani M, Madar A, Galan C, et al. A validated regulatory network for Th17 cell specification. *Cell*. 2012;151(2):289-303.

204. Dumont FJ, Coker LZ. Interferon-alpha/beta enhances the expression of Ly-6 antigens on T cells in vivo and in vitro. *Eur J Immunol*. 1986;16(7):735-740.

205. Meraro D, Gleit-Kielmanowicz M, Hauser H, Levi BZ. IFN-stimulated gene 15 is synergistically activated through interactions between the myelocyte/lymphocyte-specific transcription factors, PU.1, IFN regulatory factor-8/IFN consensus sequence binding protein, and IFN regulatory factor-4: characterization of a new subtype of IFN-stimulated response element. *J Immunol*. 2002;168(12):6224-6231.

206. Kuwata T, Gongora C, Kanno Y, et al. Gamma interferon triggers interaction between ICSBP (IRF-8) and TEL, recruiting the histone deacetylase HDAC3 to the interferon-responsive element. *Mol Cell Biol*. 2002;22(21):7439-7448.

207. de Luca C, Kowalski TJ, Zhang Y, et al. Complete rescue of obesity, diabetes, and infertility in db/db mice by neuron-specific LEPR-B transgenes. *J Clin Invest*. 2005;115(12):3484-3493.

208. Parkhurst CN, Yang G, Ninan I, et al. Microglia promote learning-dependent synapse formation through brain-derived neurotrophic factor. *Cell*. 2013;155(7):1596-1609.

209. Dighe AS, Richards E, Old LJ, Schreiber RD. Enhanced in vivo growth and resistance to rejection of tumor cells expressing dominant negative IFN gamma receptors. *Immunity*. 1994;1(6):447-456.

210. Kaplan DH, Shankaran V, Dighe AS, et al. Demonstration of an interferon gamma-dependent tumor surveillance system in immunocompetent mice. *Proceedings of the National Academy of Sciences of the United States of America*. 1998;95(13):7556-7561.

211. Vago L, Perna SK, Zanussi M, et al. Loss of mismatched HLA in leukemia after stem-cell transplantation. *N Engl J Med*. 2009;361(5):478-488.

212. Verheyden S, Bernier M, Demanet C. Identification of natural killer cell receptor phenotypes associated with leukemia. *Leukemia*. 2004;18(12):2002-2007.

213. Cancer Genome Atlas Research N. Genomic and epigenomic landscapes of adult de novo acute myeloid leukemia. *N Engl J Med*. 2013;368(22):2059-2074.

214. Ohtsuka H, Sakamoto A, Pan J, et al. Bcl6 is required for the development of mouse CD4+ and CD8alpha+ dendritic cells. *J Immunol*. 2011;186(1):255-263.